

**OPTIMAL COVARIANCE STEERING: THEORY AND ITS APPLICATION TO
AUTONOMOUS DRIVING**

A Dissertation
Presented to
The Academic Faculty

By

Kazuhide Okamoto

In Partial Fulfillment
of the Requirements for the Degree
Doctor of Philosophy in Aerospace Engineering

School of Aerospace Engineering
Georgia Institute of Technology

December 2019

Copyright © Kazuhide Okamoto 2019

OPTIMAL COVARIANCE STEERING: THEORY AND ITS APPLICATION TO AUTONOMOUS DRIVING

Approved by:

Dr. Panagiotis Tsiotras, Advisor
School of Aerospace Engineering
Georgia Institute of Technology

Dr. John-Paul Clarke
School of Aerospace Engineering
Georgia Institute of Technology

Dr. Sonia Chernova
School of Interactive Computing
Georgia Institute of Technology

Dr. Jonathan Rogers
School of Aerospace Engineering
Georgia Institute of Technology

Dr. Yongxin Chen
School of Aerospace Engineering
Georgia Institute of Technology

Date Approved: October 25, 2019

The best way to predict the future is to invent it.

Alan Kay

ACKNOWLEDGEMENTS

Throughout my years at the Georgia Institute of Technology, I have received unconditional help and guidance from a great number of people. Without their support, I would not have been able to successfully complete this dissertation.

First and foremost, I would like to express my sincere gratitude to my advisor, Prof. Panagiotis Tsiotras. I would also like to thank to the members of my thesis committee, Prof. John-Paul Clarke, Prof. Sonia Chernova, Prof. Jonathan Rogers, and Prof. Yongxin Chen for their insightful and professional comments to improve this dissertation. In addition, I would like to thank to my former advisor Prof. Takeshi Tsuchiya at the University of Tokyo for his support, which guided me coming to Georgia Tech for my Ph.D. study.

I would like to express my gratitude to Dr. Stefano Di Cairano and Dr. Karl Berntorp for providing me with the chance to work as a research intern at Mitsubishi Electric Research Laboratories. I would also like to thank Dr. Nanxiang Li and Dr. Teruhisa Misu for the opportunity to work as a research intern at Honda Research Institute USA.

The support I received from the Funai Foundation for Information Technology was essential to the start of my Ph.D. study at Georgia Tech. I would like to express my sincere gratitude to Mr. Tetsuro Funai for founding the scholarship. I would also like to thank Prof. Takashi Masuda, Mr. Akira Funai, Prof. Kei Sakamoto, Prof. Yuichiro Kato, Prof. Kosuke Takahashi, Ms. Keiko Saito, Ms. Mikiko Kondo, and supporters of the foundation, for the continuous support over the last five years and the opportunities to interact with distinguished researchers and Ph.D. students in other top schools. The financial support from the Ito-Foundation USA-FUTI Scholarship was also imperative for the continuation of my studies. I would like to express my gratitude to Dr. Shigenori Matsushita and the committee members for electing me to a recipient of the scholarship.

I wish to thank all my roommates, Ethan Evans, Matthew Brewer, Manan Gandhi, Atom Watanabe, Nishant Shah, and Shani Genosar for sharing invaluable time with me and being

kind friends. I would also like to extend my thanks to all labmates, Dr. Wei Sun, Dr. Ioannis Exarchos, Dr. Florian Hauer, Dr. Alfredo Valverde, Dr. Changxi You, Dr. Georgios Kotsalis, Dr. Dipankar Maity, Su Yeon Choi, Maxim Goldshtein, Takehiko Hanada, Kelsey Hawkins, Jack Ridderhof, Mehregan Dor, Daniel Larsson, Venkata Ramana Makkapati, Matt King-Smith, Sagar Joshi, Dongliang Zheng, Jaein Lim, and Scott Guan, who have been my great colleagues and considerate friends at Georgia Tech.

Because of the limitation of this space, I have quite a number of people who have not been explicitly mentioned but have been important for me to complete this dissertation. I would like to greatly appreciate the support from every person I have met.

Finally, I would like to express my most sincere gratitude to my parents Tsuyoshi and Satomi, and to my siblings Sakura and Daiki for their unconditional love and support.

TABLE OF CONTENTS

Acknowledgments	v
List of Tables	xi
List of Figures	xii
Chapter 1: Introduction	1
1.1 Motivation and Previous Work	1
1.1.1 Covariance Control Theory	3
1.1.2 Vehicle Path Planning under Uncertainty	5
1.1.3 Input Hard Constrained Optimal Covariance Steering	8
1.1.4 Stochastic Model Predictive Control	9
1.2 Thesis Statement and Contributions	12
1.3 Thesis Organization	14
Chapter 2: Background and Preliminaries	16
2.1 Symbols and Acronyms	16
2.1.1 Notation	16
2.1.2 Acronyms	16
2.2 Convex Programming	20

2.2.1	Convexity	20
2.2.2	Optimization Problem Description	21
Chapter 3: Optimal Covariance Steering Theory		26
3.1	Problem Formulation	26
3.1.1	Preliminaries	30
3.2	No Chance Constraint Case	33
3.2.1	Separation of Mean and Covariance Problems	34
3.2.2	Optimal Mean Steering	36
3.2.3	Optimal Covariance Steering	38
3.3	Proposed Approach	38
3.4	Numerical Simulations	44
3.5	Summary	50
Chapter 4: Vehicle Path Planning using Optimal Covariance Steering		51
4.1	Problem Statement	51
4.2	Optimal Covariance Control with Obstacles	53
4.3	Numerical Simulations	56
4.3.1	ZigZag	57
4.3.2	Double-Slit Obstacle	62
4.3.3	Cluttered Environment	68
4.3.4	Multi-Vehicle Path Planning	71
4.4	Discussion and Summary	79

Chapter 5: Input Hard Constrained Optimal Covariance Steering	85
5.1 Problem Formulation	85
5.2 Proposed Approach	88
5.3 Numerical Simulation	97
5.4 Summary	98
 Chapter 6: Stochastic Model Predictive Control using Optimal Covariance Steering	 101
6.1 Problem Statement	101
6.1.1 Problem Formulation	102
6.1.2 SMPC Formulation	105
6.2 Mathematical Preliminaries of Optimal Covariance Steering	106
6.3 CS-SMPC Design	112
6.3.1 CS-SMPC Formulation	112
6.4 Numerical Simulation	127
6.4.1 Illustrative Example with 2D Dynamics	127
6.4.2 Self-Driving Vehicle Control	132
6.5 Discussion and Summary	143
 Chapter 7: Conclusions	 144
7.1 Contributions	144
7.2 Future Work and Open Problems	146
7.2.1 Optimal Risk Allocation for Optimal Covariance Steering	147
7.2.2 Variable Horizon Optimal Covariance Steering	147

7.2.3	Optimal Covariance Steering with Measurement Noise	148
7.2.4	Path Planning under Uncertainty using Optimal Covariance Steering	149
7.2.5	Swarm Control using Optimal Covariance Steering	149
7.2.6	Optimal Covariance Steering Theory for Linear Systems with Multiplicative Noise	149
7.2.7	Optimal Covariance Steering-based ADAS or Human Robot Interaction	150
7.2.8	Corrective Steering while Obstacle Avoidance	151
7.2.9	ADAS for Aggressive Driving	151
Appendix A: Author's Publications		154
A.1	Journals	154
A.2	Conferences	155
A.3	Patents	156
Appendix B: Supplementary Material for Chapter 5		157
Appendix C: MATLAB Code		162
References		186
Vita		187

LIST OF TABLES

2.1	Logic Operators.	16
2.2	Sets.	17
2.3	Algebraic Operators.	17
2.4	Set Operators.	18
2.5	Probability Operators.	18
2.6	Acronyms.	19
6.1	Vehicle parameters and values. (CoM: the center of mass of the vehicle). . .	139

LIST OF FIGURES

1.1	A schematic of the finite horizon optimal covariance control problem. . . .	4
1.2	An example of chance-constrained vehicle path planning with open-loop dynamics; from [50].	7
2.1	Relationship among the convex programming problems.	25
3.1	Optimal covariance steering problem under state chance constraints.	29
3.2	Problem Setup for the numerical simulation.	46
3.3	Results by a mean steering controller with various N settings.	47
3.4	Results by a OCS controller without state chance constraints with various N settings.	48
3.5	Results by the proposed OCS controller under state chance constraints with various N settings.	49
4.1	Problem Setup for the first scenario.	58
4.2	Results from open-loop stochastic path planning approach.	59
4.3	Results from the proposed approach.	60
4.4	Representation of the feasible state subsets.	61
4.5	Problem setup.	62
4.6	Mean steering trajectory with open-loop covariance dynamics.	64
4.7	Proposed approach with closed-loop covariance dynamics.	65

4.8	Representation of the feasible region.	66
4.9	Problem setup.	67
4.10	Solution of the proposed approach.	68
4.11	Representation of the feasible region.	69
4.12	Problem Setup.	70
4.13	Mean steering trajectory with open-loop covariance dynamics.	71
4.14	Proposed approach with closed-loop covariance dynamics.	72
4.15	Problem setup for two-vehicle path planning.	75
4.16	Representation of the feasible region.	76
4.17	Results of two-vehicle collision avoidance using covariance steering.	77
4.18	Problem setup for two-vehicle path planning.	80
4.19	Representation of the feasible region.	81
4.20	Results of two-vehicle collision avoidance using covariance steering.	82
4.21	Zoom up of the solution illustrated in Fig. 4.10.	83
5.1	Results when input is constraint free.	99
5.2	Results when input constraints are imposed.	100
6.1	A schematic describing the proposed CS-SMPC approach.	114
6.2	Uncontrolled system state trajectories.	128
6.3	System state trajectories controlled by an LQR controller	129
6.4	System state trajectories.	133
6.5	Mean and standard deviation of the computation time of each method. The time is normalized by the computation time of the disturbance feedback method.	134

6.6	Comparison of MPC approaches for vehicle control example. Each figure shows a planned trajectory for a race car using different MPC approaches. The bold lines indicate the mean trajectories, and the shaded areas represent $1-\epsilon$ confidence regions. By directly controlling the covariance, it is possible to design more aggressive controllers that operate closer to the constraints.	135
6.7	Bicycle model. (x_I, y_I) is the inertial frame, and (x_B, y_B) is the body frame.	136
6.8	Geometry of the road circuit.	140
6.9	Result of Deterministic MPC without noise.	141
6.10	100 sample trajectories controlled by CS-SMPC approach.	142

SUMMARY

Optimal control under uncertainty has been one of the central research topics in the control community for decades. While a number of theories have been developed to control a single state from an initial state to a target state, in some situations, it is preferable to simultaneously compute control commands for multiple states that start from an initial distribution and converge to a target distribution. This dissertation aims to develop a stochastic optimal control theory that, in addition to the mean, explicitly steers the state covariance. Specifically, we focus on the control of linear time-varying (LTV) systems with additive Gaussian noise. The task is to steer a Gaussian-distributed initial system state distribution to a target Gaussian distribution, while minimizing a state and control expectation-dependent quadratic cost under probabilistic state constraints. Notice that, in such systems, the system state keeps being Gaussian distributed. Because Gaussian distributions can be fully described by the first two moments, the proposed optimal covariance steering (OCS) theory allows us to control the whole distribution of the state and quantify the effect of uncertainty without conducting Monte-Carlo simulations. We propose to use a control policy that is an affine function of filtered disturbances, which utilizes the results of convex optimization theory and efficiently finds the solution.

After the OCS theory for LTV systems is introduced, we extend the theory to vehicle path planning problems. While several path planning algorithms have been proposed, many of them have dealt with deterministic dynamics or stochastic dynamics with open-loop uncertainty, i.e., the uncertainty of the system state is not controlled and, typically, increases with time due to exogenous disturbances, which may lead to the design of potentially conservative nominal paths. A typical approach to deal with disturbances is to use a lower-level local feedback controller *after* the nominal path is computed. This unidirectional dependence of the feedback controller on the path planner makes the nominal path unnecessarily conservative. The path-planning approach we develop based on the OCS theory computes

the nominal path based on the closed-loop evolution of the system uncertainty by simultaneously optimizing the feedforward and feedback control commands. We validate the performance using numerical simulations with single and multiple vehicle path planning problems.

Furthermore, we introduce an optimal covariance steering controller for linear systems with input hard constraints. As many real-world systems have input constraints (e.g., aircraft and spacecraft have minimum/maximum thrust), this problem formulation will allow us to deal with realistic scenarios. In order to incorporate input hard constraints in the OCS theory framework, we use element-wise saturation functions and limit the effect of disturbance to the control commands. We prove that this problem formulation leads to a convex programming problem and demonstrate the effectiveness using simple numerical examples.

Finally, we develop the OCS-based stochastic model predictive control (CS-SMPC) theory for stochastic linear time-invariant (LTI) systems with additive Gaussian noise subject to state and control constraints. In addition to the conventional terminal cost and terminal mean constraints, we introduce terminal covariance constraints in the stochastic model predictive control theory. The OCS theory efficiently computes the control commands that satisfy the terminal covariance constraints. The key benefit of the CS-SMPC algorithm is its ability to ensure stability and recursive feasibility of the controlled system. In addition, thanks to the efficient OCS theory, the proposed CS-SMPC theory is computationally less demanding than previous SMPC approaches. In order to verify the effectiveness, the CS-SMPC approach is also applied to the problem of self-driving vehicle control under uncertainty.

CHAPTER 1

INTRODUCTION

1.1 Motivation and Previous Work

Optimal control under uncertainty has been one of the central research topics in the control community for decades. While a number of theories have been developed to control a single state from an initial state to a target state while minimizing a cost or objective function [1, 2], in some situations, it is preferable to simultaneously compute control commands for multiple states that start from an initial distribution to a target distribution. One typical example is the spacecraft powered descent guidance (PDG) problem, in which one needs to compute the sequence of the control command to guide the spacecraft, which finished its entry maneuver, to the landing point of the surface of the planet. While the original PDG problem is a non-convex programming problem, the approach in [3, 4] converted it to a convex programming problem and demonstrated that one can minimize the fuel consumption and compute fuel-optimal trajectories. While this approach is powerful and can be computationally efficient thanks to the convex programming formulation, the approach uses a deterministic spacecraft dynamics with fixed initial state and fixed terminal state. In reality, however, the initial state of the spacecraft at the descent maneuver is the state after the entry maneuver has ended, which is affected by the disturbance from the atmosphere and localization error. Therefore, it is hard to know a priori the exact initial state of the spacecraft starting its PDG maneuver. In addition, the PDG maneuver is also affected by noise such as the atmospheric disturbance and the model mismatch of the real and simulation vehicle dynamics. One way of dealing with these problems, similarly to other real-world systems, is to “close the loop” by using feedback from measurements. Unfortunately, because this additional feedback control is not incorporated in the analy-

sis, this approach implies that the guaranteed satisfaction of the constraints based on the analysis with deterministic dynamics may not hold anymore. Instead of using deterministic dynamics, one can use stochastic dynamics and take into account the system uncertainty a priori. In addition, the initial and terminal states can be modeled using probabilistic distributions instead of single deterministic values [5]. The resulting problem is a stochastic probability distribution control problem, in which one computes the control commands to steer the system state density distribution from a given initial distribution to a target distribution. This stochastic control problem of steering the probability density function (PDF) can be regarded as a dynamic formulation of the optimal mass transport problem [6, 7]. It is worth noticing that the evolution of the state PDFs follow either Liouville or Fokker-Planck-Kolmogorov partial differential equation (PDE), and the optimal control of these PDEs have been investigated by recent research works [8, 9, 10, 11].

The problem of steering the system state distribution is related to a wide variety of control and path-planning applications. In robotics, the problem of moving a swarm of robots from a initial spatial configuration to a target configuration in finite time can be formulated as a density control problem [12, 13, 14]. Another example is a closed-loop cooling system for the gravitational wave detector [15, 16]. Both of these applications are more natural to specify state distributions rather than fixed values.

While stochastic optimal control theory is a vast and active area of research, in this work, we focus on the optimal control problem of state variable under linear (possibly) time-varying dynamics with additive Gaussian noise. The optimal covariance steering theory steers the system state, which is a random variable sampled from a Gaussian distribution, to a prescribed target Gaussian distribution, while minimizing a state and control expectation-dependent cost. In addition to the boundary condition, we consider chance constraints, which restricts the maximum probability of violating the constraints to be less than a pre-specified threshold. This chance-constrained optimal covariance control problem is relevant to a wide range of control and planning task [17]. Although this problem set up

seems simple, we are able to derive a number of theoretically interesting properties of the control algorithm. Notice that, because a Gaussian distributed state governed by such systems remains Gaussian distributed, and because a Gaussian distribution is fully described by the mean and the covariance, we can regard our controller as a density controller that steers a initial Gaussian distribution to a target Gaussian distribution. This problem formulation is clearly different from classical optimal controllers such as linear quadratic control of a linear system under additive Gaussian noise [18, 19], in which the final state covariance is obtained as a by-product of the solution and usually not controlled to a pre-specified value. In our problem setting, our objective is to more actively control the state covariance to a target value, and we simultaneously control the mean of the system state to a target value, implying that we are steering the system state PDF.

1.1.1 Covariance Control Theory

The problem of controlling the state covariance of control systems dates back to the late 1980s [20, 21]. The authors of [20, 21] identified the state feedback gains of a linear time-invariant system such that the state covariance converges to a pre-specified value. In this thesis, we refer to this infinite-horizon covariance control theory as the covariance *assignment* theory. Notice that the original covariance assignment theory does not consider any optimality of the control action. The covariance assignment theory has been extensively studied both for continuous and discrete time systems [22, 23, 24, 25]. In [26], the optimality of control actions was first introduced to the covariance assignment controllers, and the minimum effort controller was designed both for continuous and discrete linear systems. Notice that these works dealt with only infinite-horizon case.

The finite-horizon version of the covariance assignment control problem has recently been investigated in [27, 28, 29], relating to the problems of Schrödinger bridges [30] and the optimal mass transport [31]. These works showed that, if the control input channels are disrupted by the diffusion term, with some mild assumptions, it is always possible to

achieve the target probability in finite time, and the minimum effort solution is given in a state feedback form. When the control input and the diffusion channels are different, the solution exists when a Schrödinger nonlinear system is solvable, but to find the solution, one needs to use a soft constraint on the target distribution, e.g., using the Wasserstein distance [32] or to use numerical optimization methods [33]. Notice that these works discussed the covariance control of continuous-time systems.

Figure 1.1 illustrates the finite-horizon case of optimal covariance control problem, where the control commands to steer the initial Gaussian distribution $\mathcal{N}(\mu_0, \Sigma_0)$ to the target Gaussian distribution $\mathcal{N}(\mu_f, \Sigma_f)$ are computed.

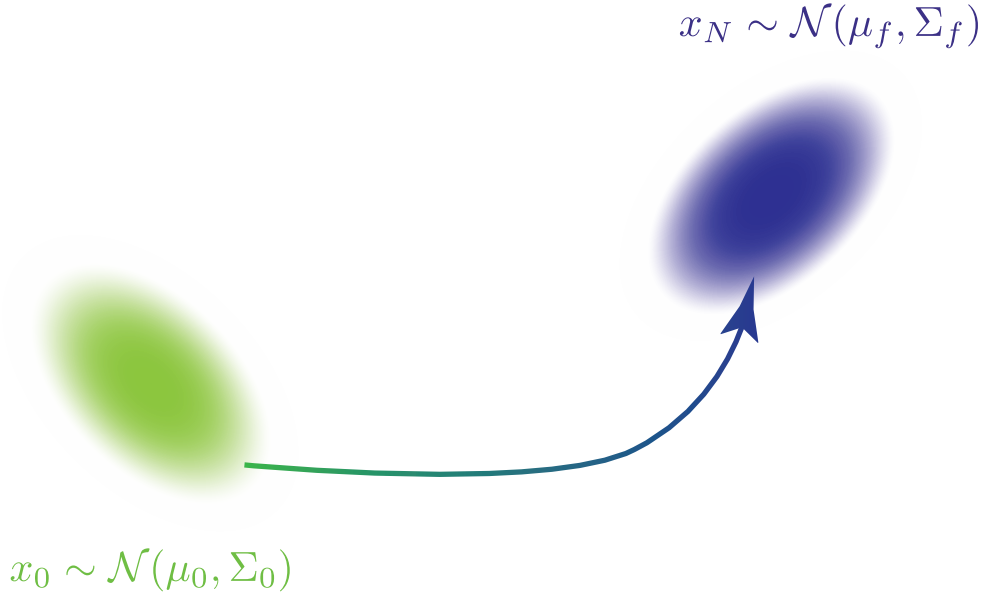


Figure 1.1: A schematic of the finite horizon optimal covariance control problem.

For discrete-time systems, the authors of [34, 35] developed covariance control theories that dealt with fixed reciprocal dynamics [36] and connected two prescribed probability densities at the endpoints of a prescribed finite time. In addition, the authors of [37] characterized the noise process that steers the state of a discrete-time stochastic linear system

from a given initial Gaussian distribution to another given terminal Gaussian distribution at a pre-specified time step. The approach proposed in [38] computes the control commands by showing that the finite covariance control problem solution can be seen as a linear quadratic controller with a particular terminal weight, which can be computed using a backward-propagated discrete-time dynamic Riccati equation. An interesting approach was proposed by the author of [39, 40], where instead of steering the covariance to the exact target value, one can steer the system state covariance to a value that is smaller than the target. In fact, this operation is a convex relaxation of the terminal covariance constraint [41]. By doing so, one can utilize a convex programming solver and efficiently compute the control commands. The approach we propose in this thesis follows a similar approach and incorporates some constraints. For example, we use chance constraints [42] to impose the maximum probability of state/control constraint violations, which can be reformulated as convex second-order cone constraints with mild technical assumptions. The more detailed descriptions about the description of this thesis is provided later in Section 1.2 in this chapter.

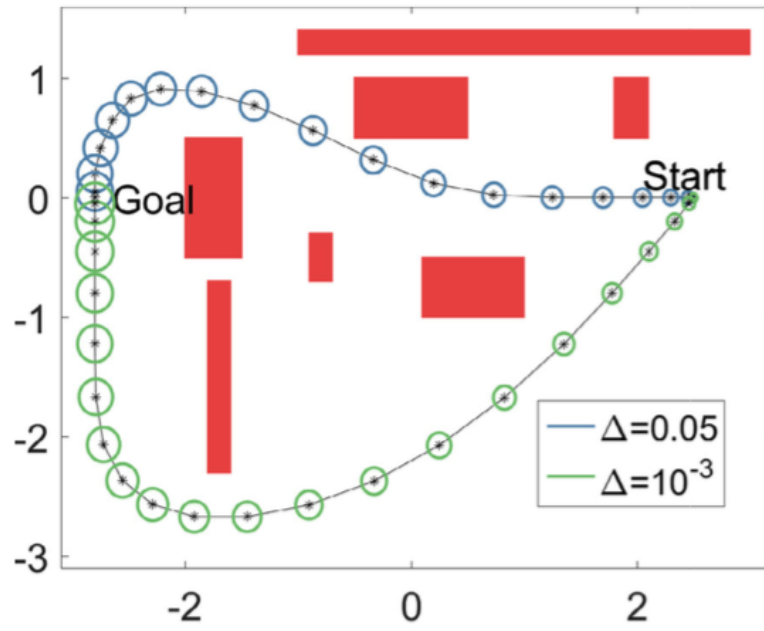
1.1.2 Vehicle Path Planning under Uncertainty

Vehicle path planning problems have been an active research topic for decades [43]. Among the existing literature, sampling-based algorithms, such as the rapidly-exploring random trees (RRT) [44], have been popular for solving motion planning problems subject to constraints. Variants of RRT ([45, 46]) have been proposed that offer asymptotic optimality guarantees. However, in general, these approaches deal with deterministic dynamics and cannot directly address uncertain systems.

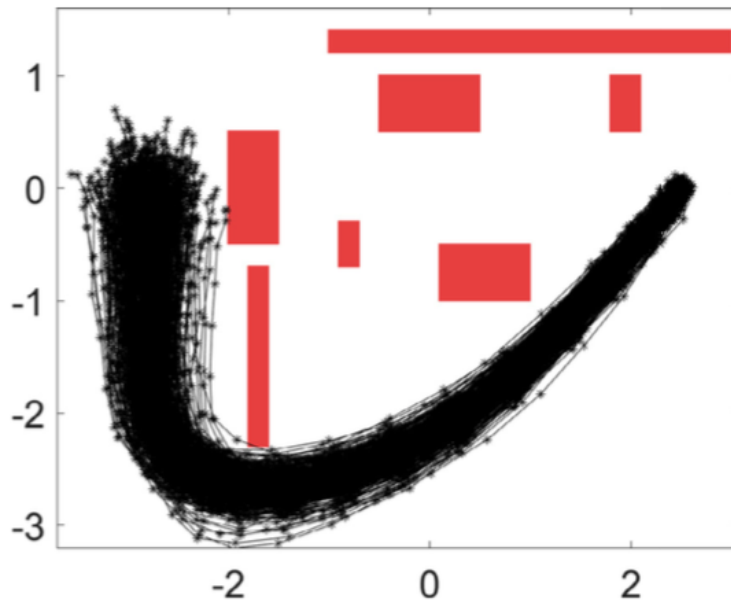
In order to solve path planning problems under uncertainty, several approaches have been proposed, such as finite cone cover method [47], chance-constrained rapidly exploring random trees (RRT) methods [48, 49], mixed-integer programming approaches [42, 50], and chance-constrained dynamic programming [51]. The authors of [50] used mixed

integer linear programming (MILP) for their path planning [52] under non-convex chance constraints, and the algorithm successfully changed the path depending on the allowed probability of collision. Figure 1.2 illustrates the results from [50]. While they changed the trajectory based on the allowed probabilistic threshold, as we steer the covariance, our approach will be able to pick the more aggressive trajectory with less variance. Locally convexifying the non-convex state constraints is another approach [53], and a stochastic MPC framework that uses this approach is proposed in [54]. These approaches consider only the *open-loop* dynamics of the covariance, i.e., the covariance of the system state is not controlled and, typically, increases with time due to the exogenous disturbances. In order to add robustness, state-feedback *closed-loop* feedback controllers are applied *after* the nominal path is computed. Alternatively, it is more natural to consider the closed-loop evolution of the covariance for path planning. Notice that there are several path planning algorithms that use the term “closed-loop” (see, e.g., [55, 56]). Those works are sampling-based methods, and instead of sampling in the control space, they take samples from the output space in order to handle differential constraints. It is worth noticing that their approach is dealing with deterministic dynamics and does not consider any uncertainty.

Recently, path-planning problems with closed-loop covariance dynamics have been addressed in the literature, such as [57, 58, 53, 59, 60]. Among these, the work of Vitus and Tomlin [59] is most closely related to our work, as it also uses mixed-integer programming (MIP) to deal with non-convex domains. MIP approaches have been actively investigated for path-planning problems in non-convex state constraint environments formulated as mixed-integer linear programming (MILP) [52, 61], mixed-integer quadratic programming (MIQP) [62], and mixed-integer semi-definite programming (MISDP) problems [63]. Vitus et al. [64] dealt with a path-planning problem with *closed-loop* dynamics of the covariance using the so-called Tunnel-MILP approach, which decomposes a non-convex environment into convex polygons and solves the optimal control problem through these convex polygons. In this formulation, integer variables indicate in which polygon the



(a) Path planning.



(b) Monte Carlo simulation.

Figure 1.2: An example of chance-constrained vehicle path planning with open-loop dynamics; from [50].

state variable belongs to at each time step. This is computationally more efficient than other MIP approaches, which typically use separate integer variables for each face of every obstacle. While the original Tunnel-MILP approach could not cope with constraint violations between time steps, the authors of [65] proposed a new constraint such that two consecutive system states have to belong to the same convex polygon in order for the system state to remain in the same polygon between consecutive time steps, implying no collision with obstacles.

The approach proposed in this thesis extends these previous works by adding the element of actively controlling the state covariance to achieve less conservative paths. In addition, unlike previous MIP-based approaches, the proposed approach has the control on the terminal state distribution. Specifically, in this paper we utilize the closed-loop dynamics of the covariance to compute a collision-free path under non-convex state chance constraints and steer the state to a pre-specified Gaussian distribution, and at the same time, minimize a quadratic cost that depends on the expectation of the state and control.

1.1.3 Input Hard Constrained Optimal Covariance Steering

It is worth noticing that, while a number of covariance controllers have been proposed, many of them do not consider any input constraints. In fact, they cannot deal with input hard constraints, because they are affine functions of the state or the disturbance, which are both unbounded, and the control commands become unbounded as well. Thus, they cannot satisfy input hard constraint specifications. Such a situation occurs in many real-world scenarios. For example, in aircraft [66] or spacecraft [67] control problems the control command values have physical restrictions such as minimum/maximum thrust.

To the best of our knowledge, input *hard* constraints have not been discussed in the framework of optimal covariance steering theory, while input *soft* constraints have been investigated by several prior works. For example, the controller proposed in [39, 40] can deal with input constraints that impose a maximum value of the expectation of quadratic

functions of the control inputs such as

$$\mathbb{E}[u_k^\top R_c u_k] \leq c,$$

where k is the time index, R_c is a positive definite matrix, and $c > 0$ is a scalar. In addition, the controller developed in [67] deals with the maximum probability of control constraint violation, namely, input chance constraints of the form

$$\Pr(u_k \notin \mathcal{U}) \leq c,$$

where $\mathcal{U} \subset \mathbb{R}^{n_u}$ is the feasible input set. Our formulation of the input constraint is different than these approaches, in the sense that we directly impose hard constraints on the input. Inspired by the approach in [68, 69], we propose to use a saturation function into our OCS controller [70] to impose input hard constraints.

1.1.4 Stochastic Model Predictive Control

Model predictive control (MPC), often also referred to as receding horizon control, has been an active research topic both in academia [71] and industry [72, 73], because of the ability to deal with complex constraints while yielding near-optimal performance. In the standard MPC framework, one solves a finite-horizon optimal control problem and executes the first element of the computed optimal control sequence. At the next time step, one solves another finite-horizon optimal control problem with the updated initial condition. By doing so, MPC implicitly closes the loop and achieves stability, assuming certain additional conditions hold [74]. Some variants of MPC such as the explicit MPC [75, 76, 77] and the hybrid MPC [78] have been developed, and the area of application has been extended.

The above mentioned MPC approaches have been developed for deterministic systems, and thus, they lack systematic approaches to deal with uncertainties that lie in the system. In order to overcome this difficulty, robust MPC (RMPC) and stochastic MPC (SMPC)

theories have been developed (see e.g., [79, 80, 81] for an extensive literature review.).

Robust MPC approaches assume deterministic uncertainties, which lie in a bounded set. For example, min-max MPC [82] computes the control command that can deal with the worst-case scenario from the system uncertainty. Another RMPC approach is the tube-MPC [83]. The control policy of the tube-MPC separates the controller to a mean controller and a feedback controller that is proportional to the deviation from the expected state value with stabilizing state feedback gain, and thus achieves asymptotic stability to a set [84].

RMPC approaches ignore the probabilistic nature of the disturbance. In order to explicitly deal with the probability distribution of the system uncertainty, SMPC has been developed. As open-loop controllers have difficulty in dealing with disturbances, generally, feedback *policies* are optimized instead of the control sequence alone for SMPC problems. Although there is no unique way to classify the numerous SMPC approaches [80], the most common approaches are the stochastic-tube and the affine-parameterization approaches. Other approaches such as the scenario-based approach [85] are outside the scope of this current manuscript.

In the stochastic-tube approach [86, 87, 88, 89, 90, 91], the system state is decomposed to the deterministic and random components. The random component is controlled using a state feedback controller with a *pre-computed* stabilizing gain, and only the additional control command to steer the deterministic component, which is the offset to the feedback controller, is computed online. By doing so, the stochastic-tube approach succeeded in avoiding the optimization over arbitrary feedback policies for the SMPC. This approach was used for the control of an autonomous vehicle control problem [92]. Although this approach reduces computational complexity, it is difficult and requires some time-consuming trial-and-error to compute a-priori a state feedback gain that is not too conservative especially when some constraints have to be satisfied.

In order to overcome this problem of the off-line computation of the reasonable feedback gain, the affine parameterization approach has been investigated [69, 93]. In the affine

parameterization approach, both the feedback gain and the deterministic component are design variables and have to be simultaneously optimized online. Figure ?? illustrates the difference between the two approaches. The stochastic-tube MPC approach knows the future state uncertainty evolution apriori because the feedback gain is pre-computed, and it tries to control the mean state so that, until the end of the horizon, the predicted state satisfy the given constraints. On the other hand, the affine parameterization approach simultaneously computes the feedback gains and the open-loop control sequens so that solutions satisfy the constraints. As a result, the affine parameterization approach leads to less conservative controllers that tend to operate closer to the boundaries, thus increasing performance. It is known that the state feedback parameterization approach leads to a non-convex programming problem [94, 95, 96], and one needs a relaxation of the constraints to make the problem convex, which may make the result unnecessarily conservative. The SMPC approach in [93] employs the disturbance feedback parameterization control policy, which can be shown to be equivalent to the state feedback parameterization policy [97]. This disturbance feedback parameterization approach is later extended to accommodate input hard constraints [98, 99, 69, 68], which is difficult to satisfy for the stochastic tube and state feedback parameterization approaches.

It is worth noticing that SMPC uses chance constraints and imposes a maximum probability of state/output constraint violation [100, 101]. When using the stochastic-tube approach, because the feedback gain is pre-computed, the chance constraints can be converted to linear inequality constraints, while when using the affine parameterization approach, because of the online computation of the feedback gains, the chance constraints can be converted to second-order cone constraints. Some applications of SMPC include building climate control [102], autonomous vehicle control [92], and bacterial fermentation control [68].

Many research works on SMPC achieve recursive feasibility and convergence by assuming a bounded probability distribution of the disturbance, e.g., a truncated Gaussian

distribution. SMPC approaches dealing with unbounded disturbance distributions have been proposed by several researchers [68, 95, 103]. For example, the approach proposed in [95] uses a state-feedback parameterization approach, which leads to the need to solve a non-convex programming problem. Specifically, the system state covariance dynamics with state feedback controller becomes non-convex and needs convex relaxation techniques [94]. Thus, this approach may have difficulty in computing the system covariance at each time step. The approach we propose in this article overcomes this difficulty by utilizing the results from the newly developed finite horizon optimal covariance steering control theory [66, 70].

1.2 Thesis Statement and Contributions

In this dissertation, we aim to develop an optimal covariance steering theory which simultaneously steers the mean and the covariance of the LTV system state to pre-scribed target values. It has been known that, if the dynamics is linear and no constraints exist, one can decouple the mean and the covariance dynamics and independently optimize the control commands to each mean and covariance steering subproblems. However, we show that if some constraints exist, the mean and the covariance trajectories couple, and one needs to simultaneously optimize the mean and the covariance trajectories to obtain the best performance. The key ingredients of the proposed optimal covariance controller is the convex relaxation of the terminal covariance constraint and the incorporation of the probabilistic state chance constraints. By doing so, we can formulate a convex programming problem. Specifically, the terminal covariance constraint is formulated as a linear matrix inequality (LMI), and the state chance constraints are formulated as second-order cone constraints. One can solve further formulate the problem as a semidefinite programming (SDP) problem, which can be efficiently solved using primal-dual interior point methods.

The contributions of this dissertation are as the following.

- With respect to the state-of-the-art covariance steering theories: Many preceding al-

gorithms separated the mean and the covariance steering problems and focused on the development of system state covariance controls. This problem setup holds only when there exists no state constraints. If a state constraint becomes active, the mean and the covariance trajectories couple, and thus, the theories that only considers covariance dynamics does not work well. The approach we propose in this dissertation has the ability to consider such scenarios. By introducing the chance constraints, the proposed approach is able to compute the optimal mean and covariance trajectories that minimize the cost function while satisfying the state constraints. Specifically, we assume that the feasible state space can be represented as a combination of the linear inequalities and is convex. Then, we are able to convert the chance constraint to second-order cone constraints, which allows us to simultaneously compute the mean and covariance steering commands using a convex programming solver. To our knowledge, this work is the first to incorporate state chance constraints into the covariance steering theory framework.

- With respect to the state-of-the-art vehicle path-planning algorithms: Over the years, several vehicle path-planning algorithms have been proposed, but many of them deal with deterministic dynamics or with open-loop stochastic dynamics, i.e., the uncertainty of the system state is not controlled and, typically, increases with time due to exogenous disturbances. This approach may lead to potentially conservative nominal paths. The vehicle path-planning algorithm based on the optimal covariance steering theory is a computationally efficient method that simultaneously optimizes the feedforward and feedback control actions, and thus, allows us to compute the closed-loop evolution of the system state. Therefore, the nominal paths computed from the proposed approach is expected to be less conservative than open-loop stochastic path planning approaches.
- The input hard constraint is incorporated in the optimal covariance steering theory

for the first time. Inspired by recent research works on stochastic model predictive approaches that deal with input-hard constraints, we propose to incorporate input-hard constraints to the optimal covariance steering theory.

- With respect to the previous stochastic MPC methods; The proposed covariance-steering-based stochastic model predictive control (CS-SMPC) assures the recursive feasibility and stability by imposing the maximum terminal covariance along with properly designing terminal cost and constraints. These properties of the CS-SMPC hold even when the noise is additive Gaussian, which previous SMPC algorithms had difficulty to deal with and avoided the problem by assuming the noise was truncated Gaussian and proved the properties. In addition, the proposed CS-SMPC algorithm develops a new approach to compute the system state covariance dynamics, which is computationally more efficient than previous SMPC approaches such as the state feedback or disturbance feedback affine parameterization approaches.

1.3 Thesis Organization

The remainder of this thesis is organized as follows.

- Chapter 2 introduces notation and definitions used throughout this dissertation. In addition, it provides a brief overview of the relevant theoretical background related to convex optimization theory.
- In Chapter 3 we introduce the optimal covariance steering problem under state chance constraints, and we propose an approach that conducts convex relaxation of the original non-convex programming problem and efficiently finds the solution.
- Chapter 4 extends the framework of the optimal covariance steering theory to vehicle path planning problems with stochastic dynamics. The approach proposed in Chapter 3 is modified so that it can deal with non-convex state chance constraints. In addition, we apply the algorithm to multiple vehicle path planning problems.

- Chapter 5 is devoted to the case when the system has input hard constraints. While the optimal covariance steering controller in chapter 3 was developed without any input constraints, many real-world scenarios have control constraints such as minimum/maximum thrust of aircraft and spacecraft. Thus, this extension will allow us to solve more realistic problems.
- Chapter 6 develops a new stochastic model predictive control algorithm for constrained linear time invariant systems based on the optimal covariance steering theory (CS-SMPC). Previous research works on SMPC assume that the additive noise is bounded and prove the recursive feasibility and stability of the closed-loop system. The proposed approach imposes the maximum system state covariance using the optimal covariance steering controller. Then, we are able to achieve the recursive feasibility and the guaranteed stability of the closed-loop system even when the noise is unbounded Gaussian. In addition, we apply the CS-SMPC algorithm to the control of an autonomous vehicle.
- Finally, in Chapter 7 we conclude the thesis with remarks and outline potential future research directions.

CHAPTER 2

BACKGROUND AND PRELIMINARIES

In this chapter we introduce the notation and acronyms used throughout this thesis. In addition, we briefly review the basics and important facts about the convex programming theory [41, 104, 105].

2.1 Symbols and Acronyms

In this thesis, we develop a stochastic optimal control theory, which we call the optimal covariance steering theory. Throughout this paper, we use the following terminology to distinguish our approach from others.

1. Optimal covariance steering: The proposed approach we develop in this thesis.
2. Optimal covariance control: Other optimal control methods that control the state covariance.
3. Covariance assignment: the method developed for infinite horizon case.

2.1.1 Notation

The notation we use in this thesis is quite standard as listed in Tables 2.1- 2.5.

Table 2.1: Logic Operators.

$A \Rightarrow B$	If A is true then B is true
$A \Leftrightarrow B$	If A is true if and only if B is true

2.1.2 Acronyms

The list of acronyms used throughout this thesis is provided in Table 2.6.

Table 2.2: Sets.

\mathbb{R}	Set of real numbers
\mathbb{R}^n	Set of real vectors with n elements
$\mathbb{R}^{n \times m}$	Set of real matrices with n rows and m columns

Table 2.3: Algebraic Operators.

A^\top	Transpose of a matrix A
A^{-1}	Inverse of matrix A
A^+	Moore-Penrose pseudo-inverse of a matrix A
$\text{tr} A$	Trace of a matrix A
$\det A$	Determinant of a matrix A
$A > 0$	Each element of A is positive
$A \geq 0$	Each element of A is non-negative
$A \succ 0$	Matrix A is symmetric and positive definite, i.e., $x^\top A x > 0, \forall x \neq 0$
$A \succeq 0$	Matrix A is symmetric and positive semidefinite, i.e., $x^\top A x \geq 0, \forall x \neq 0$
$ x $	Euclidian norm of vector $x \in \mathbb{R}^n$, $ x = \sqrt{x^\top x}$
$\ A\ _2$	Induced two norm of matrix A , $\ A\ _2 = \sup_{x \neq 0} \frac{ Ax }{ x }$
$\ A\ _F$	Frobenius norm of matrix A , $\ A\ _F = \sqrt{\text{tr}(AA^\top)}$
$0_{n,m}$	Zero matrix with n rows and m columns
I_n	Identity matrix with m rows and n columns
$\text{diag}(a_0, \dots, a_n)$	the diagonal matrix with diagonal elements $a_i, i \in \{0, n\}$ scalars
$\text{blkdiag}(A_0, \dots, A_n)$	the block diagonal matrix with diagonal elements $A_i, i \in \{0, n\}$ matrices

Table 2.4: Set Operators.

\emptyset	The empty set
:	“Such that”
$\mathcal{P} \setminus \mathcal{Q}$	Set difference, $\mathcal{P} \setminus \mathcal{Q} = \{x : x \in \mathcal{P} \text{ and } x \notin \mathcal{Q}\}$
$\mathcal{P} \subseteq \mathcal{Q}$	Set \mathcal{P} is a subset of \mathcal{Q} , $x \in \mathcal{P} \Rightarrow x \in \mathcal{Q}$
$\mathcal{P} \subset \mathcal{Q}$	Set \mathcal{P} is a strict subset of \mathcal{Q} , $x \in \mathcal{P} \Rightarrow x \in \mathcal{Q}$ and $\exists x \in (\mathcal{Q} \setminus \mathcal{P})$
$\mathcal{P} \cap \mathcal{Q}$	Set intersection, $\mathcal{P} \cap \mathcal{Q} = \{x : x \in \mathcal{P} \text{ and } x \in \mathcal{Q}\}$
$\mathcal{P} \cup \mathcal{Q}$	Set union, $\mathcal{P} \cup \mathcal{Q} = \{x : x \in \mathcal{P} \text{ or } x \in \mathcal{Q}\}$
$\bigcup_{r=0}^{R-1} \mathcal{P}_r$	Union of R sets \mathcal{P}_r , $\bigcup_{r=0}^R \mathcal{P}_r = \{x : x \in \mathcal{P}_0 \text{ or } \dots \text{ or } x \in \mathcal{P}_{R-1}\}$

Table 2.5: Probability Operators.

$\Pr(x)$	Probability of x
$\Pr(x y)$	Probability of x conditioned on y
$\mathbb{E}(x)$	Expectation of x
$\mathbb{E}(x y)$	Expectation of x conditioned on y
$\mathcal{N}(\mu, \Sigma)$	Gaussian distribution with mean μ and (co)variance Σ
\sim	“Has the probability distribution of”

Table 2.6: Acronyms.

CA	Covariance Assignment
CS-SMPC	Covariance-Steering-based Stochastic Model Predictive Control
DP	Dynamic Programming
LMI	Linear Matrix Inequality
LP	Linear Programming
LQR	Linear Quadratic Regulator
LTI	Linear Time Invariant
LTV	Linear Time Variant
MILP	Mixed Integer Linear Programming
MIQP	Mixed Integer Quadratic Programming
MPC	Model Predictive Control
OCS	Optimal Covariance Steering
QCQP	Quadratically Constrained Quadratic Programming
QP	Quadratic Programming
RMPC	Robust Model Predictive Control
SDP	Semi-definite Programming
SOCP	Second-order Cone Programming
SMPC	Stochastic Model Predictive Control

2.2 Convex Programming

2.2.1 Convexity

The proposed optimal covariance steering is based on the convex optimization theory [41].

In this section, we list some important facts on convexity [41, 104].

Definition 1. A set $S \in \mathbb{R}^s$ is *convex* if

$$\lambda x_1 + (1 - \lambda)x_2 \in S, \quad (2.1)$$

for all $x_1 \in S$, $x_2 \in S$, and $\lambda \in [0, 1]$.

Definition 2. A function $f : S \rightarrow \mathbb{R}$ is *convex* if

$$f(\lambda x_1 + (1 - \lambda)x_2) \leq \lambda f(x_1) + (1 - \lambda)f(x_2), \quad (2.2)$$

for all $x_1 \in S$, $x_2 \in S$, and $\lambda \in [0, 1]$.

Definition 3. A function $f : S \rightarrow \mathbb{R}$ is *strictly convex* if

$$f(\lambda x_1 + (1 - \lambda)x_2) < \lambda f(x_1) + (1 - \lambda)f(x_2), \quad (2.3)$$

for all $x_1 \in S$, $x_2 \in S$, and $\lambda \in [0, 1]$.

Definition 4. A function $f : S \rightarrow \mathbb{R}$ is *concave* if S is convex and $-f$ is convex.

Fact. If the Hessian of a twice differentiable function $f : S \rightarrow \mathbb{R}$ satisfies, for all $x \in S$,

$$\nabla^2 f(x) \succ 0, \quad (2.4)$$

then the function f is strongly convex.

Fact. If $f(x)$ is convex, then $S_\alpha = \{x \in S : f(x) \leq \alpha\}$ is convex $\forall \alpha \in \mathbb{R}$.

Fact. If f_1, \dots, f_N are convex functions, then, $\sum_{i=1}^N \alpha_i f_i$ is a convex function $\forall \alpha_i \geq 0$, $i = 1, \dots, N$.

Fact. If $f(x)$ is convex, then $f(Ax + b)$ is convex on $\{x : Ax + b \in \text{dom}(f)\}$

Fact. A linear function $f(x) = \alpha^\top x + \beta$ is both convex and concave.

Fact. A quadratic function $f(x) = x^\top Qx + \alpha^\top x + \beta$ is convex if and only if $Q \succeq 0$.

Fact. Let x^* be the local optimal solution of a convex programming problem. Then x^* is also a global optimal solution.

2.2.2 Optimization Problem Description

In this thesis, an optimization problem is formulated as follows. Let $x \in \mathbb{R}^s$ be the vector collecting the decision variables.

$$\min \quad f(x), \tag{2.5}$$

$$\text{subject to} \quad g_i(x) \leq 0, \quad i = 1, \dots, m, \tag{2.6}$$

$$h_j(x) = 0, \quad j = 1, \dots, n, \tag{2.7}$$

where $f : \mathbb{R}^s \rightarrow \mathbb{R}$, $g_i : \mathbb{R}^s \rightarrow \mathbb{R}$, and $h_j : \mathbb{R}^s \rightarrow \mathbb{R}$ are real-valued functions. Specifically, we refer to f , g_i , and h_j as the cost function, inequality constraints, and equality constraints, respectively. The remainder of this section introduces some of the most major convex programming problems [41, 105].

Linear Programming

A standard form linear programming (LP) problem has an equality constraint and an element-wise non-negativity constraint on $x \in \mathbb{R}^s$:

$$\min \quad c^\top x, \quad (2.8)$$

$$\text{subject to} \quad Ax = b, \quad (2.9)$$

$$x \geq 0, \quad (2.10)$$

where $c \in \mathbb{R}^s$ and $A \in \mathbb{R}^{n \times s}$, and $b \in \mathbb{R}^n$.

Quadratic Programming

A quadratic programming (LP) problem can be formulated with a convex quadratic cost function and affine constraints. Specifically, with the design variable $x \in \mathbb{R}^s$,

$$\min \quad \frac{1}{2}x^\top Px + q^\top x + r, \quad (2.11)$$

$$\text{subject to} \quad Gx \leq h, \quad (2.12)$$

$$Ax = b, \quad (2.13)$$

where $P \in \mathbb{R}^{s \times s}$ is positive and symmetric definite, $G \in \mathbb{R}^{m \times n}$, $h \in \mathbb{R}^m$, $A \in \mathbb{R}^{n \times s}$, and $b \in \mathbb{R}^n$.

Second-order Cone Programming

A second-order cone programming (SOCP) problem is formulated as follows,

$$\min \quad f^\top x, \quad (2.14)$$

$$\text{subject to} \quad |A_i x + b| \leq c_i^\top x + d_i, \quad i = 1, \dots, m \quad (2.15)$$

$$Fx = g, \quad (2.16)$$

where $x \in \mathbb{R}^s$ is the design variable while $f \in \mathbb{R}^s$, $A_i \in \mathbb{R}^{m_i \times s}$, $b_i \in \mathbb{R}^{m_i}$, $c_i \in \mathbb{R}^s$, $d_i \in \mathbb{R}$, $F \in \mathbb{R}^{n \times s}$, and $g \in \mathbb{R}^n$ are constant. The constraint (2.15) is called a second-order cone constraint.

Quadratically Constrained Quadratic Programming

A quadratically constrained quadratic programming (QCQP) problem is formulated as follows,

$$\min \quad \frac{1}{2}x^\top P_0 x + q_0^\top x, \quad (2.17)$$

$$\text{subject to} \quad \frac{1}{2}x^\top P_i x + q_i^\top x + r_i \leq 0, \quad i = 1, \dots, m \quad (2.18)$$

$$Fx = g, \quad (2.19)$$

where $x \in \mathbb{R}^s$ is the design variable while $P_i \in \mathbb{R}^{s \times s}$, $q_i \in \mathbb{R}^s$, $F \in \mathbb{R}^{n \times s}$, and $g \in \mathbb{R}^n$ are constant for $i = 0, \dots, m$. Notice that in order for a QCQP problem to be convex, all P_0, \dots, P_m have to be symmetric and positive definite.

Semidefinite Programming

A standard form semidefinite programming (SDP) has linear equality constraints and a matrix non-negativity constraint on the symmetric matrix variable $X \in \mathbb{R}^n$ as the following.

$$\min \quad \text{tr } CX, \tag{2.20}$$

$$\text{subject to} \quad \text{tr } A_i X = 0, \quad i = 1, \dots, m, \tag{2.21}$$

$$X \succeq 0, \tag{2.22}$$

where $C, A_1, \dots, A_m \in \mathbb{R}^{n \times n}$ are symmetric.

Remark

Among the approaches introduced above, SDP is the most general and LP is the most specific problem formulation [41, 105]. The relationship among the approaches is illustrated in Fig. 2.1.

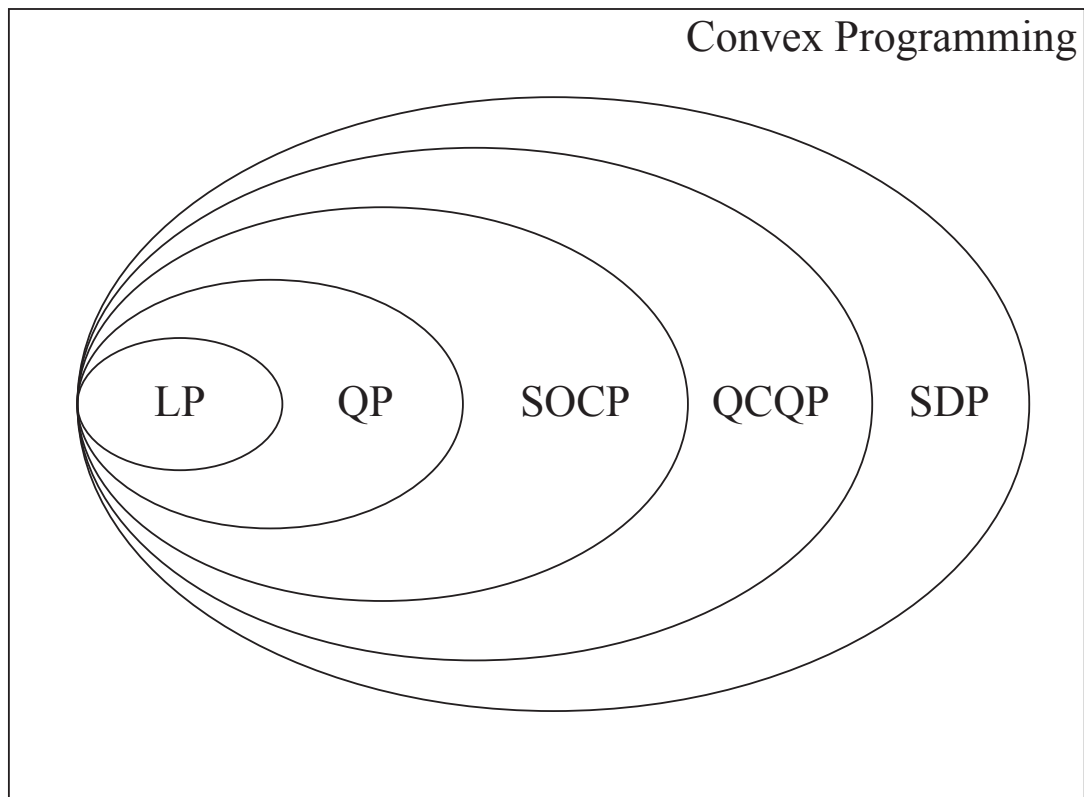


Figure 2.1: Relationship among the convex programming problems.

CHAPTER 3

OPTIMAL COVARIANCE STEERING THEORY

In this chapter we formulate the finite-horizon optimal covariance control problem for a stochastic, linear, and time-varying system in discrete-time subject to state chance constraints. This problem setup is the basis for the other problem setups discussed later in this thesis.

Specifically, Section 3.1 formulates the optimal covariance steering problem under state chance constraints with the introduction of the assumptions and the mathematical preliminaries we utilize throughout this thesis. After formulating the problem, in Section 3.2, we first discuss the case when there does not exist any state constraints. Through this discussion, we aim at demonstrating the need for simultaneously optimizing the mean and the covariance steering trajectories. The main result of this chapter is provided in Section 3.3, where we introduce a novel optimal covariance steering controller that utilizes the convex relaxation of the original problem and is computationally efficient. The effectiveness of the proposed controller is verified through numerical examples in Section 3.4. Finally, Section 3.5 provides a brief summary of this chapter.

3.1 Problem Formulation

In this chapter, we deal with the following discrete-time stochastic linear system with (possibly time-varying) additive Gaussian noise

$$x_{k+1} = A_k x_k + B_k u_k + D_k w_k, \quad (3.1)$$

where $k = 0, 1, \dots, N - 1$ denotes the time step, $x \in \mathbb{R}^{n_x}$ is the state, $u \in \mathbb{R}^{n_u}$ is the control input, and $w \in \mathbb{R}^{n_w}$ is a zero-mean independently and identically distributed (i.i.d.)

Gaussian noise with unit covariance. Namely,

$$\mathbb{E}[w_k] = 0, \quad \mathbb{E}[w_{k_1} w_{k_2}^\top] = I_{n_w} \delta_{k_1, k_2}, \quad (3.2)$$

where δ_{k_1, k_2} is the Kronecker's delta function. In addition, the following condition holds

$$\mathbb{E}[x_{k_1} w_{k_2}^\top] = 0, \quad 0 \leq k_1 \leq k_2 \leq N - 1. \quad (3.3)$$

The initial state x_0 is a random vector that is drawn from the multi-variate normal distribution

$$x_0 \sim \mathcal{N}(\mu_0, \Sigma_0), \quad (3.4)$$

where $\mu_0 \in \mathbb{R}^{n_x}$ is the initial state mean and $\Sigma_0 \in \mathbb{R}^{n_x \times n_x}$ is the initial state covariance. In this work, we assume that $\Sigma_0 \succeq 0$. Our objective is to steer the trajectories of the system (3.1) from this initial distribution to a target Gaussian distribution

$$x_N \sim \mathcal{N}(\mu_f, \Sigma_f), \quad (3.5)$$

where $\mu_f \in \mathbb{R}^{n_x}$ and $\Sigma_f \in \mathbb{R}^{n_x \times n_x}$ at a given time step N , while minimizing the cost function

$$J(x_0, u_0, \dots, u_{N-1}, x_N) = \mathbb{E} \left[\sum_{k=0}^{N-1} x_k^\top Q_k x_k + u_k^\top R_k u_k \right], \quad (3.6)$$

where $Q_k \succeq 0$ and $R_k \succ 0$ for all $k = 0, \dots, N - 1$. In this work, we assume that $\Sigma_f \succ 0$.

The state is subject to some constraints

$$x_k \in \mathcal{X}, \quad k = 0, \dots, N, \quad (3.7)$$

where $\mathcal{X} \subseteq \mathbb{R}^{n_x}$ is a feasible state set. Throughout this work, we assume that the set \mathcal{X} is convex and represented as the intersection of a finite number of linear inequality constraints as

$$\mathcal{X} \triangleq \bigcap_{i=0}^{N_s-1} \{x : \alpha_{x,i}^\top x \leq \beta_{x,i}\}, \quad (3.8)$$

where $\alpha_{x,i} \in \mathbb{R}^{n_x}$ and $\beta_{x,i} \in \mathbb{R}$. In addition, N_s is the number of state constraints. Notice that, since the system noise w_k in (3.1) is possibly unbounded, the state may be unbounded as well. Therefore, we probabilistically formulate the state constraints (3.7) as chance constraints

$$\Pr(x_k \in \mathcal{X}) \geq 1 - \epsilon_x, \quad k = 0, \dots, N-1, \quad (3.9)$$

where, as we explain later, this work sets $\epsilon_x \in (0, 0.5)$.

In summary, the optimal covariance steering problem is formulated as follows.

Problem 1 (Optimal Covariance Steering under State Chance Constraints).

$$\begin{aligned} \min J(x_0, u_0, \dots, u_{N-1}, x_N) &= \mathbb{E} \left[\sum_{k=0}^{N-1} x_k^\top Q_k x_k + u_k^\top R_k u_k \right], \\ \text{subject to} \\ x_{k+1} &= A_k x_k + B_k u_k + D_k w_k, \quad x_0 \sim \mathcal{N}(\mu_0, \Sigma_0), \\ x_N &\sim \mathcal{N}(\mu_f, \Sigma_f), \\ \Pr(x_k \in \mathcal{X}) &\geq 1 - \epsilon_x. \end{aligned}$$

In addition, the optimal covariance steering problem is illustrated in Fig. 3.1.

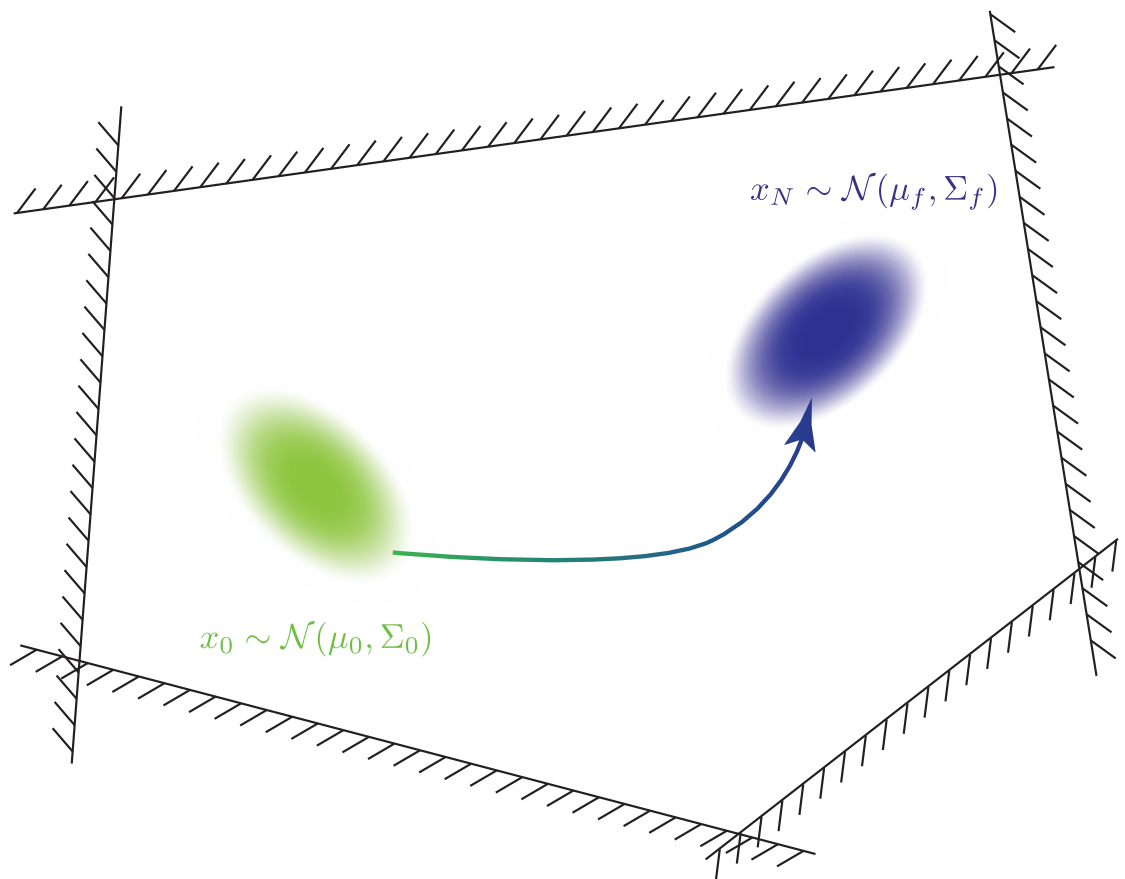


Figure 3.1: Optimal covariance steering problem under state chance constraints.

3.1.1 Preliminaries

In order to solve Problem 1, we provide the alternative description, which will be instrumental to solve the problem. It follows from the system dynamics (3.1) that, at each time step k , we explicitly represent the system state x_k as a function of the initial state x_0 , control sequence, and disturbance sequence, as follows. Let A_{k_1, k_0} , B_{k_1, k_0} , and D_{k_1, k_0} , where $k_1 > k_0$, denote the transition matrices of the state, input, and the disturbance from step k_0 to step $k_1 + 1$, respectively, as follows

$$A_{k_1, k_0} = A_{k_1} A_{k_1-1} \cdots A_{k_0}, \quad (3.11a)$$

$$B_{k_1, k_0} = A_{k_1, k_0+1} B_{k_0}, \quad (3.11b)$$

$$D_{k_1, k_0} = A_{k_1, k_0+1} D_{k_0}. \quad (3.11c)$$

We define the concatenated vectors $U_k \in \mathbb{R}^{(k+1)n_u}$ and $W_k \in \mathbb{R}^{(k+1)n_w}$ as

$$U_k = \begin{bmatrix} u_0 \\ u_1 \\ \vdots \\ u_k \end{bmatrix}, \quad W_k = \begin{bmatrix} w_0 \\ w_1 \\ \vdots \\ w_k \end{bmatrix}. \quad (3.12)$$

Then x_k can be equivalently computed from

$$x_k = \bar{A}_k x_0 + \bar{B}_k U_{k-1} + \bar{D}_k W_{k-1}, \quad (3.13)$$

where

$$\bar{A}_k = A_{k-1,0}, \quad (3.14a)$$

$$\bar{B}_k = \begin{bmatrix} B_{k-1,0} & B_{k-1,1} & \cdots & B_{k-1} \end{bmatrix}, \quad (3.14b)$$

$$\bar{D}_k = \begin{bmatrix} D_{k-1,0} & D_{k-1,1} & \cdots & D_{k-1} \end{bmatrix}. \quad (3.14c)$$

Furthermore, we introduce the concatenated state vector $X_k \in \mathbb{R}^{(k+1)n_x}$ as the following.

$$X_k = \begin{bmatrix} x_0 \\ x_1 \\ \vdots \\ x_k \end{bmatrix}. \quad (3.15)$$

Then, it is straightforward to derive the following form of the concatenated state vector

$$X = X_N \in \mathbb{R}^{(N+1)n_x}$$

$$X = \mathcal{A}x_0 + \mathcal{B}U + \mathcal{D}W, \quad (3.16)$$

where $U = U_{N-1} \in \mathbb{R}^{Nn_u}$, $W = W_{N-1} \in \mathbb{R}^{Nn_w}$, and the matrices $\mathcal{A} \in \mathbb{R}^{(N+1)n_x \times n_x}$,

$\mathcal{B} \in \mathbb{R}^{(N+1)n_x \times Nn_u}$, and $\mathcal{D} \in \mathbb{R}^{(N+1)n_x \times Nn_w}$ are defined as

$$\mathcal{A} = \begin{bmatrix} I \\ \bar{A}_1 \\ \bar{A}_2 \\ \vdots \\ \bar{A}_N \end{bmatrix}, \quad \mathcal{B} = \begin{bmatrix} 0 & 0 & \cdots & 0 \\ B_0 & 0 & \cdots & 0 \\ B_{1,0} & B_1 & \cdots & 0 \\ \vdots & \vdots & \vdots & \vdots \\ B_{N-1,0} & B_{N-1,1} & \cdots & B_{N-1} \end{bmatrix}, \quad (3.17a)$$

and

$$\mathcal{D} = \begin{bmatrix} 0 & 0 & \cdots & 0 \\ D_0 & 0 & \cdots & 0 \\ D_{1,0} & D_1 & \cdots & 0 \\ \vdots & \vdots & \vdots & \vdots \\ D_{N-1,0} & D_{N-1,1} & \cdots & D_{N-1} \end{bmatrix}. \quad (3.17b)$$

Note that the following properties hold.

$$\mathbb{E}[x_0 x_0^\top] = \Sigma_0 + \mu_0 \mu_0^\top, \quad (3.18a)$$

$$\mathbb{E}[x_0 W^\top] = 0, \quad (3.18b)$$

$$\mathbb{E}[W W^\top] = I_{N n_w}. \quad (3.18c)$$

Using the previous expressions for X and U , we rewrite the cost (3.6) as follows

$$J(X, U) = \mathbb{E} [X^\top \bar{Q} X + U^\top \bar{R} U], \quad (3.19)$$

where

$$\bar{Q} = \text{blkdiag}(Q_0, Q_1, \dots, Q_{N-1}, 0) \in \mathbb{R}^{(N+1)n_x \times (N+1)n_x}, \quad (3.20)$$

$$\bar{R} = \text{blkdiag}(R_0, R_1, \dots, R_{N-1}) \in \mathbb{R}^{N n_u \times N n_u}. \quad (3.21)$$

Since $Q_k \succeq 0$ and $R_k \succ 0$ for all $k = 0, 1, \dots, N-1$, it follows that $\bar{Q} \succeq 0$ and $\bar{R} \succ 0$.

We can rewrite the terminal target Gaussian distribution constraint (3.5) as

$$\mu_f = E_N \mathbb{E}[X], \quad (3.22a)$$

$$\Sigma_f = E_N (\mathbb{E}[X X^\top] - \mathbb{E}[X] \mathbb{E}[X]^\top) E_N^\top, \quad (3.22b)$$

where $E_N \in \mathbb{R}^{n_x \times (N+1)n_x}$ is introduced such that $x_N = E_N X$. Specifically, for all $k =$

$0, \dots, N,$

$$E_k = [0_{n_x, kn_x}, I_{n_x}, 0_{n_x, (N-k)n_x}] \in \mathbb{R}^{n_x \times (N+1)n_x}, \quad (3.23)$$

and thus $x_k = E_k X$. Using this notation, we can also rewrite the state chance constraints (3.9) as

$$\Pr(E_k X \in \mathcal{X}) \geq 1 - \epsilon_x. \quad (3.24)$$

So far, we have introduced the following equivalent form of Problem 1

Problem 2 (Optimal Covariance Steering under State Chance Constraints (Converted)).

$$\begin{aligned} \min J(X, U) &= \mathbb{E} [X^\top \bar{Q} X + U^\top \bar{R} U], \\ \text{subject to} \\ X &= \mathcal{A}x_0 + \mathcal{B}U + \mathcal{D}W, \quad x_0 \sim \mathcal{N}(\mu_0, \Sigma_0), \\ \mu_f &= E_N \mathbb{E}[X], \\ \Sigma_f &= E_N (\mathbb{E}[X X^\top] - \mathbb{E}[X] \mathbb{E}[X]^\top) E_N^\top. \\ \Pr(E_k X \in \mathcal{X}) &\geq 1 - \epsilon_x. \end{aligned}$$

Notice that, in general, Problem 1 (and equivalently, Problem 2) is difficult to solve for an optimal infinite dimensional control policy. In this thesis, in order to make the problem tractable, we use an affine feedback control policy and convert the Problem 2 to a convex programming problem. This approach makes the solution sub-optimal, and thus, finding a computationally more efficient control approach is a possible future research topic.

3.2 No Chance Constraint Case

Before discussing the optimal covariance steering theory with chance constraints, we introduce the case without chance constraints. In such cases, it is possible to decouple the mean

and the covariance steering optimization problems.

3.2.1 Separation of Mean and Covariance Problems

First, it follows immediately from an equivalent form of x_k in (3.13) that

$$\mu_k \triangleq \mathbb{E}[x_k] = \bar{A}_k \mu_0 + \bar{B}_k \bar{U}_k, \quad (3.26)$$

where $\bar{U}_k = \mathbb{E}[U_k]$. Furthermore, by defining

$$\tilde{U}_k \triangleq U_k - \bar{U}_k, \quad \tilde{x}_k \triangleq x_k - \mu_k, \quad (3.27)$$

and using (3.13), the following equation holds for \tilde{x}_k

$$\tilde{x}_k = \bar{A}_k \tilde{x}_0 + \bar{B}_k \tilde{U}_k + \bar{D}_k W_k. \quad (3.28)$$

Furthermore,

$$\begin{aligned} \Sigma_k &\triangleq \mathbb{E}[\tilde{x}_k \tilde{x}_k^\top], \\ &= \mathbb{E} \left[\left(\bar{A}_k \tilde{x}_0 + \bar{B}_k \tilde{U}_k + \bar{D}_k W_k \right) \left(\bar{A}_k \tilde{x}_0 + \bar{B}_k \tilde{U}_k + \bar{D}_k W_k \right)^\top \right], \\ &= \bar{A}_k \mathbb{E}[\tilde{x}_0 \tilde{x}_0^\top] \bar{A}_k^\top + \bar{A}_k \mathbb{E}[\tilde{x}_0 \tilde{U}_k^\top] \bar{B}_k^\top + \bar{B}_k \mathbb{E}[\tilde{U}_k \tilde{x}_0^\top] \bar{A}_k^\top + \bar{B}_k \mathbb{E}[\tilde{U}_k \tilde{U}_k^\top] \bar{B}_k^\top \\ &\quad + \bar{D}_k \mathbb{E}[W_k W_k^\top] \bar{D}_k^\top + \bar{D}_{k-1} \mathbb{E}[W_{k-1} \tilde{U}_k^\top] \bar{B}_k^\top + \bar{B}_k \mathbb{E}[\tilde{U}_k W_{k-1}^\top] \bar{D}_{k-1}^\top. \end{aligned}$$

Note that the evolution of the mean μ_k from (3.26) depends only on \bar{U}_k , whereas the evolution of \tilde{x}_k and Σ_k depend solely on \tilde{U}_k and W_k . This separation of the state variable from x_k to μ_k and Σ_k can be applied to every time step k .

Similarly, it follows from (3.16) and (3.26) that

$$\bar{X} \triangleq \mathbb{E}[X] = \mathcal{A} \mu_0 + \mathcal{B} \bar{U}, \quad (3.29)$$

and from (3.28) that

$$\tilde{X} \triangleq X - \mathbb{E}[X] = \mathcal{A}\tilde{x}_0 + \mathcal{B}\tilde{U} + \mathcal{D}W. \quad (3.30)$$

The objective function (3.19) can also be rewritten as follows

$$J(X, U) = \mathbb{E} [X^\top \bar{Q} X + U^\top \bar{R} U] \quad (3.31a)$$

$$= \text{tr}(\bar{Q} \mathbb{E}[\tilde{X} \tilde{X}^\top]) + \bar{X}^\top \bar{Q} \bar{X} + \text{tr}(\bar{R} \mathbb{E}[\tilde{U} \tilde{U}^\top]) + \bar{U}^\top \bar{R} \bar{U}, \quad (3.31b)$$

$$= J_\mu(\bar{X}, \bar{U}) + J_\Sigma(\tilde{X}, \tilde{U}), \quad (3.31c)$$

where

$$J_\mu(\bar{X}, \bar{U}) = \bar{X}^\top \bar{Q} \bar{X} + \bar{U}^\top \bar{R} \bar{U}, \quad (3.32)$$

and

$$J_\Sigma(\tilde{X}, \tilde{U}) = \text{tr}(\bar{Q} \mathbb{E}[\tilde{X} \tilde{X}^\top]) + \text{tr}(\bar{R} \mathbb{E}[\tilde{U} \tilde{U}^\top]). \quad (3.33)$$

It follows that the original optimization problem in terms of (X, U) is equivalent to two separate optimization problems in terms of (\bar{X}, \bar{U}) and (\tilde{X}, \tilde{U}) with optimization costs (3.32) and (3.33), respectively.

We have therefore shown the following result.

Proposition 1. *Let the system (3.16), the initial and terminal state constraints (3.4) and (3.5), and the objective function (3.6). The control sequence U^* that solves this optimization problem is given by $U^* = \bar{U}^* + \tilde{U}^*$, where \bar{U}^* is the solution of the optimization problem*

$$\text{Mean Steering} \left\{ \begin{array}{l} \min J_\mu(\bar{X}, \bar{U}) = \bar{X}^\top \bar{Q} \bar{X} + \bar{U}^\top \bar{R} \bar{U} \\ \text{subject to } \bar{X} = \mathcal{A}\mu_0 + \mathcal{B}\bar{U}, \\ E_0 \bar{X} = \mu_0, \quad E_N \bar{X} = \mu_f, \end{array} \right. \quad (3.34)$$

and \tilde{U}^* is the solution of the optimization problem

$$\text{Covariance Steering} \left\{ \begin{array}{l} \min J_{\Sigma}(\tilde{X}, \tilde{U}) = \text{tr}(\bar{Q}\mathbb{E}[\tilde{X}\tilde{X}^{\top}]) + \text{tr}(\bar{R}\mathbb{E}[\tilde{U}\tilde{U}^{\top}]), \\ \text{subject to } \tilde{X} = \mathcal{A}\tilde{x}_0 + \mathcal{B}\tilde{U} + \mathcal{D}W \\ E_0\mathbb{E}[\tilde{X}\tilde{X}^{\top}]E_0^{\top} = \Sigma_0, \quad E_N\mathbb{E}[\tilde{X}\tilde{X}^{\top}]E_N^{\top} = \Sigma_f. \end{array} \right. \quad (3.35)$$

The rest of this section introduces the methods to solve these two subproblems.

3.2.2 Optimal Mean Steering

The solution to the optimal mean steering subproblem (3.34) is summarized in the following proposition.

Proposition 2. *The optimal control sequence that solves the optimization problem (3.34) is given by*

$$\bar{U}^* = \mathcal{R}^{-1} (\mathcal{B}^{\top} \bar{Q} \mathcal{A} \mu_0 + \bar{B}_N^{\top} (\bar{B}_N \mathcal{R}^{-1} \bar{B}_N^{\top})^{-1} (\mu_N - \bar{A}_N \mu_0 - \bar{B}_N \mathcal{R}^{-1} \mathcal{B}^{\top} \bar{Q} \mathcal{A} \mu_0)), \quad (3.36)$$

where $\mathcal{R} = \mathcal{B}^{\top} \bar{Q} \mathcal{B} + \bar{R}$.

Proof. Since the terminal constraint is $\mu_f = E_N \bar{X} = \bar{A}_N \mu_0 + \bar{B}_N \bar{U}$ we can write the Lagrangian as

$$\mathcal{L}(\bar{U}, \lambda) = \bar{X}^{\top} \bar{Q} \bar{X} + \bar{U}^{\top} \bar{R} \bar{U} + \lambda^{\top} (\mu_N - \bar{A}_N \mu_0 - \bar{B}_N \bar{U}) \quad (3.37)$$

$$= (\mathcal{A} \mu_0 + \mathcal{B} \bar{U})^{\top} \bar{Q} (\mathcal{A} \mu_0 + \mathcal{B} \bar{U}) + \bar{U}^{\top} \bar{R} \bar{U} + \lambda^{\top} (\mu_N - \bar{A}_N \mu_0 - \bar{B}_N \bar{U}), \quad (3.38)$$

where $\lambda \in \mathbb{R}^{n_x}$. The first-order optimality condition yields

$$\nabla_{\bar{U}} \mathcal{L} = 2(\mathcal{B}^{\top} \bar{Q} \mathcal{B} + \bar{R}) \bar{U} + 2\mathcal{B}^{\top} \bar{Q} \mathcal{A} \mu_0 - \bar{B}_N^{\top} \lambda = 0. \quad (3.39)$$

Thus,

$$\bar{U}^* = \mathcal{R}^{-1}(\mathcal{B}^\top \bar{Q} \mathcal{A} \mu_0 + \frac{1}{2} \bar{B}_N^\top \lambda), \quad (3.40)$$

where $\mathcal{R} = \mathcal{B}^\top \bar{Q} \mathcal{B} + \bar{R}$ is invertible because of the second-order optimality condition

$$\nabla_{\bar{U}\bar{U}} \mathcal{L} = \mathcal{B}^\top \bar{Q} \mathcal{B} + \bar{R} \succ 0. \quad (3.41)$$

In order to find the optimal value of λ we substitute equation (3.40) into the terminal constraint to obtain

$$\mu_f = \bar{A}_N \mu_0 + \bar{B}_N \mathcal{R}^{-1}(\mathcal{B}^\top \bar{Q} \mathcal{A} \mu_0 + \frac{1}{2} \bar{B}_N^\top \lambda), \quad (3.42)$$

or

$$\frac{1}{2} \bar{B}_N \mathcal{R}^{-1} \bar{B}_N^\top \lambda = \mu_N - \bar{A}_N \mu_0 - \bar{B}_N \mathcal{R}^{-1} \mathcal{B}^\top \bar{Q} \mathcal{A} \mu_0. \quad (3.43)$$

Note that $\text{rank}(\bar{B}_N \mathcal{R}^{-1} \bar{B}_N^\top) = \text{rank}(\mathcal{R}^{-1/2} \bar{B}_N^\top)$. Also, since the system is controllable, it follows that $\text{rank}(\bar{B}_N)$ is full row rank, i.e., $\text{rank}(\bar{B}_N) = n_x$ [38]. In addition, since \mathcal{R} is invertible, $\text{rank}(\mathcal{R}^{-1/2}) = N n_u$. It follows from Corollary 2.5.10 in [106] that

$$\begin{aligned} \text{rank}(\mathcal{R}^{-1/2}) + \text{rank}(\bar{B}_N^\top) - N n_u &\leq \text{rank}(\mathcal{R}^{-1/2} \bar{B}_N^\top) \leq \min \{ \text{rank}(\mathcal{R}^{-1/2}), \text{rank}(\bar{B}_N^\top) \} \\ n_x &\leq \text{rank}(\bar{B}_N \mathcal{R}^{-1} \bar{B}_N^\top) \leq \min \{ N n_u, n_x \} = n_x \end{aligned}$$

Thus, the matrix $(\bar{B}_N \mathcal{R}^{-1} \bar{B}_N^\top)$ is full rank and invertible. Therefore,

$$\lambda = 2(\bar{B}_N \mathcal{R}^{-1} \bar{B}_N^\top)^{-1} (\mu_N - \bar{A}_N \mu_0 - \bar{B}_N \mathcal{R}^{-1} \mathcal{B}^\top \bar{Q} \mathcal{A} \mu_0). \quad (3.44)$$

By substituting in (3.40) the expression for the optimal mean steering controller, the expression (3.36) follows. \square

By comparing (3.36) with the corresponding controller in [38] we have the following immediate result.

Corollary 1. *The minimum-effort mean-steering optimal controller introduced in [38] is a special case of the optimal controller (3.36).*

Proof. The result directly follows by plugging $\bar{Q} = 0$, $\bar{R} = I$ into Eq. (3.36). \square

3.2.3 Optimal Covariance Steering

While many previous works have attempted to solve the optimal covariance-steering problem, the majority of them deals with a minimum effort cost function such as

$$J(u_0, \dots, u_{N-1}) = \mathbb{E} \left[\sum_{k=0}^{N-1} u_k^\top u_k \right], \quad (3.45)$$

Bakolas [39] addressed the case with the more general L_2 -norm cost function Eq. (3.6) by using a convex relaxation to change the terminal constraint to an inequality as follows

$$E_N \left(\mathbb{E}[XX^\top] - \mathbb{E}[X]\mathbb{E}[X]^\top \right) E_N^\top \preceq \Sigma_N. \quad (3.46)$$

By making the problem convex, it can be efficiently solved using standard convex programming solvers. At the same time, but independently, Halder and Wendel [32] solved a problem with a similar terminal covariance constraint using a soft constraint on the terminal state covariance under continuous-time dynamics.

3.3 Proposed Approach

In the previous section, we discussed the case when no state chance constraint exists. In this section, we propose a new optimal covariance steering controller that can deal with state chance constraints. Specifically, the proposed controller takes the form of affine parameterization approach, and we simultaneously optimize the mean and the covariance trajectories in order to deal with the coupling between the mean and the covariance. The main result of this chapter is summarized in the following theorem.

Theorem 1. *The following control policy*

$$u_k = v_k + K_k y_k, \quad (3.47)$$

where $v_k \in \mathbb{R}^{n_u}$, $K_k \in \mathbb{R}^{n_u \times n_x}$, and $y_k \in \mathbb{R}^{n_x}$ is given by

$$y_{k+1} = A_k y_k + D_k w_k, \quad (3.48a)$$

$$y_0 = x_0 - \mu_0, \quad (3.48b)$$

results in a convex programming formulation of Problem 2 (and equivalently, Problem 1).

Proof. The control sequence vector U can be represented as

$$U = V + KY, \quad (3.49)$$

where

$$V = \begin{bmatrix} v_0 \\ \vdots \\ v_{N-1} \end{bmatrix} \in \mathbb{R}^{Nn_u}, \quad Y = \begin{bmatrix} y_0 \\ \vdots \\ y_N \end{bmatrix} \in \mathbb{R}^{(N+1)n_x}, \quad (3.50a)$$

$$K = \begin{bmatrix} K_0 & & & 0 \\ & K_1 & & 0 \\ & & \ddots & 0 \\ & & & K_{N-1} & 0 \end{bmatrix} \in \mathbb{R}^{Nn_u \times (N+1)n_x}. \quad (3.50b)$$

Using the matrices in (3.17), it is straightforward to derive the following expression of the sequence vector for y

$$Y = \mathcal{A}y_0 + \mathcal{D}W, \quad (3.51)$$

and thus,

$$U = V + K (\mathcal{A}y_0 + \mathcal{D}W). \quad (3.52)$$

Because $\mathbb{E}[y_0] = 0$ and $\mathbb{E}[W] = 0$, it follows that $\mathbb{E}[U] = V$. Thus, it follows from (3.16) that

$$\bar{X} = \mathbb{E}[X] = \mathcal{A}\mu_0 + \mathcal{B}V, \quad (3.53)$$

$$\tilde{X} = X - \mathbb{E}[X] = (I + \mathcal{B}K) (\mathcal{A}y_0 + \mathcal{D}W). \quad (3.54)$$

The cost function may be rewritten as

$$J(\bar{X}, \tilde{X}, V, \tilde{U}) = \text{tr}(\bar{Q}\mathbb{E}[\tilde{X}\tilde{X}^\top]) + \text{tr}(\bar{R}\mathbb{E}[\tilde{U}\tilde{U}^\top]) + \bar{X}^\top \bar{Q} \bar{X} + V^\top \bar{R} V, \quad (3.55)$$

where $\tilde{U} = U - V$. Defining

$$\Sigma_Y = \mathcal{A}\Sigma_0\mathcal{A}^\top + \mathcal{D}\mathcal{D}^\top \quad (3.56)$$

we can further convert the cost function into

$$\begin{aligned} J(V, K) &= (\mathcal{A}\mu_0 + \mathcal{B}V)^\top \bar{Q} (\mathcal{A}\mu_0 + \mathcal{B}V) + V^\top \bar{R} V \\ &\quad + \text{tr} \left[((I + \mathcal{B}K)^\top \bar{Q} (I + \mathcal{B}K) + K^\top \bar{R} K) \Sigma_Y \right]. \end{aligned} \quad (3.57)$$

Note that we used the following facts: $\mathbb{E}[y_0 W^\top] = 0$, and $\mathbb{E}[WW^\top] = I_{Nn_w}$. In addition, we reformulate the terminal constraint as

$$\mu_f = E_N (\mathcal{A}\mu_0 + \mathcal{B}V), \quad (3.58a)$$

$$\Sigma_f = E_N (I + \mathcal{B}K) \Sigma_Y (I + \mathcal{B}K)^\top E_N^\top. \quad (3.58b)$$

Note that V steers the mean and K steers the covariance to the target values μ_f and Σ_f ,

respectively. Because the terminal covariance constraint is non-convex, similarly to [107], we relax the covariance equality constraint to the following inequality constraint.

$$\Sigma_f \succeq E_N(I + \mathcal{B}K)\Sigma_Y(I + \mathcal{B}K)^\top E_N^\top, \quad (3.59)$$

which, using the Schur complement, can be rewritten as

$$\begin{bmatrix} \Sigma_f & E_N(I + \mathcal{B}K)S \\ S^\top(I + \mathcal{B}K)^\top E_N^\top & I \end{bmatrix} \succeq 0, \quad (3.60)$$

where $SS^\top = \Sigma_Y$.

Finally, the chance constraint can be formulated as follows. As we discussed, we assume that the feasible state space \mathcal{X} can be represented as a convex polytope (3.8). As shown in [108], using Boole's inequality [109], under this assumption, we convert the chance constraint to

$$\Pr(\alpha_{x,i}^\top E_k X < \beta_{x,i}) \geq 1 - p_{x,i}, \quad (3.61)$$

$$\sum_{j=1}^M p_{x,i} \leq \epsilon_x. \quad (3.62)$$

Notice that $\alpha_{x,i}^\top E_k X$ is a scalar random variable sampled from univariate Gaussian distribution. Therefore, we can analytically write the probability of satisfying one state constraint

as

$$\begin{aligned}
\Pr(\alpha_{x,i}^\top E_k X < \beta_{x,i}) &= \frac{1}{\sqrt{2\pi\alpha_{x,i}^\top E_k (I + \mathcal{B}K)\Sigma_Y(I + \mathcal{B}K)^\top E_k^\top \alpha_{x,i}}} \times \\
&\int_{-\infty}^{\beta_{x,i}} \exp\left(-\frac{(\xi - \alpha_{x,i}^\top E_k \bar{X})^2}{2\alpha_{x,i}^\top E_k (I + \mathcal{B}K)\Sigma_Y(I + \mathcal{B}K)^\top E_k^\top \alpha_{x,i}}\right) d\xi, \quad (3.63) \\
&= \Phi\left(\frac{\beta_{x,i} - \alpha_{x,i}^\top E_k \bar{X}}{\sqrt{\alpha_{x,i}^\top E_k (I + \mathcal{B}K)\Sigma_Y(I + \mathcal{B}K)^\top E_k^\top \alpha_{x,i}}}\right) \geq 1 - p_{x,i}, \quad (3.64)
\end{aligned}$$

where Φ is the cumulative distribution function of the standard normal distribution, which is a monotonically increasing function, and thus its inverse function $\Phi^{-1}()$ exists. Therefore,

$$\frac{\beta_{x,i} - \alpha_{x,i}^\top E_k \bar{X}}{\sqrt{\alpha_{x,i}^\top E_k (I + \mathcal{B}K)\Sigma_Y(I + \mathcal{B}K)^\top E_k^\top \alpha_{x,i}}} \geq \Phi^{-1}(1 - p_{x,i}). \quad (3.65)$$

This inequality leads to the following form

$$\alpha_{x,i}^\top E_k \bar{X} - \beta_{x,i} + \sqrt{\alpha_{x,i}^\top E_k (I + \mathcal{B}K)\Sigma_Y(I + \mathcal{B}K)^\top E_k^\top \alpha_{x,i}} \Phi^{-1}(1 - p_{x,i}) \leq 0, \quad (3.66)$$

which is equivalent to the following

$$\alpha_{x,i}^\top E_k \bar{X} - \beta_{x,i} + |S^\top (I + \mathcal{B}K)^\top E_k^\top \alpha_{x,i}| \Phi^{-1}(1 - p_{x,i}) \leq 0. \quad (3.67)$$

Notice that if we set $p_{x,i}$ as a design variable, this constraint becomes a non-convex multiplicative constraint, and the entire problem becomes difficult to solve. Thus, in this work, we fix $p_{x,i} \in (0, 0.5)$ to keep $\Phi^{-1}(1 - p_{x,i}) > 0$. Then, (3.67) is a convex second-order cone constraint in terms of V and K .

In summary, we have converted Problems 1 and 2 to the following convex programming problem.

Problem 3 (OCS Problem under State Chance Constraints).

$$\begin{aligned} \min J(V, K) &= (\mathcal{A}\mu_0 + \mathcal{B}V)^\top \bar{Q}(\mathcal{A}\mu_0 + \mathcal{B}V) + V^\top \bar{R}V \\ &\quad + \text{tr} \left[((I + \mathcal{B}K)^\top \bar{Q}(I + \mathcal{B}K) + K^\top \bar{R}K) \Sigma_Y \right], \end{aligned}$$

subject to

$$\begin{aligned} \mu_f &= E_N(\mathcal{A}\mu_0 + \mathcal{B}V), \\ \begin{bmatrix} \Sigma_f & E_N(I + \mathcal{B}K)S \\ S^\top(I + \mathcal{B}K)^\top E_N^\top & I \end{bmatrix} &\succeq 0, \\ \alpha_{x,i}^\top E_k \bar{X} - \beta_{x,i} + |S^\top(I + \mathcal{B}K)^\top E_k^\top \alpha_{x,i}| \Phi^{-1}(1 - p_{x,i}) &\leq 0. \end{aligned}$$

□

Remark 1. Previous works on chance-constrained stochastic optimal control [110, 108, 92] assumed some prior knowledge about the covariance, which implies that the future state covariance is computed a priori, and thus, (3.67) is a linear inequality constraint. However, as we are interested in the covariance steering problem, the future state covariance is a function of our design variable K , and thus (3.67) becomes a second-order cone constraint.

Remark 2. Instead of (3.57), it is possible to separately design the cost functions for the mean and covariance steering as

$$J(V, K) = J_m(V) + J_v(K), \quad (3.69)$$

where $J_m(V) = (\mathcal{A}\mu_0 + \mathcal{B}V)^\top \bar{Q}_m(\mathcal{A}\mu_0 + \mathcal{B}V) + V^\top \bar{R}_m V$ and $J_v(K) = \text{tr}[(I + \mathcal{B}K)^\top \bar{Q}_v(I + \mathcal{B}K) + K^\top \bar{R}_v K] \Sigma_Y$.

3.4 Numerical Simulations

In this section we validate the proposed approach in Theorem 1 using simple numerical examples. We use YALMIP [111] with MOSEK [112] to solve the relevant optimization problems.

We consider the path-planning problem for a vehicle under the following time-invariant double integrator system dynamics with

$$x_k = \begin{bmatrix} x \\ y \\ v_x \\ v_y \end{bmatrix} \in \mathbb{R}^4, \quad u_k = \begin{bmatrix} a_x \\ a_y \end{bmatrix} \in \mathbb{R}^2, \quad w_k \in \mathbb{R}^4, \quad (3.70)$$

and

$$A = \begin{bmatrix} 1 & 0 & \Delta t & 0 \\ 0 & 1 & 0 & \Delta t \\ 0 & 0 & 1 & 0 \\ 0 & 0 & 0 & 1 \end{bmatrix}, \quad B = \begin{bmatrix} \frac{\Delta t^2}{2} & 0 \\ 0 & \frac{\Delta t^2}{2} \\ \Delta t & 0 \\ 0 & \Delta t \end{bmatrix}, \quad D = 0.01I_4, \quad (3.71)$$

where Δt is the time-step size, and we set $\Delta t = 0.2$. Figure 3.2 illustrates the problem setup. The red circle denotes the 3σ error of the initial state distribution of x and y coordinates. The magenta circle denotes the 3σ error of the terminal state distribution of x and y coordinates. Specifically, the initial condition is

$$\mu_0 = \begin{bmatrix} -10 & 1 & 0 & 0 \end{bmatrix}, \quad \Sigma_0 = \text{diag}(0.05, 0.05, 0.01, 0.01), \quad (3.72)$$

while the terminal constraint is

$$\mu_f = \begin{bmatrix} 0 & 0 & 0 & 0 \end{bmatrix}, \quad \Sigma_f = \text{diag}(0.01, 0.01, 0.001, 0.001). \quad (3.73)$$

The green dotted lines indicate the state constraints. Specifically,

$$0.2(x - 1) \leq y \leq -0.2(x - 1). \quad (3.74)$$

The vehicle has to remain in the region between the two lines while moving from the red to the magenta regions. Such a “cone”-shaped constraint is seen in many engineering applications, e.g., the instrument landing for aircraft, spacecraft rendezvous, and drone-landing on a moving platform. The probabilistic threshold for the violation of chance constraints was specified a priori, and we set $p_{x,i} = 5.0 \cdot 10^{-4}$ for $i = 0, 1$.

The cost matrices are set to

$$Q_k = \text{diag}(0.5, 4.0, 0.05, 0.05), \quad (3.75a)$$

$$R_k = \text{diag}(20, 20). \quad (3.75b)$$

Notice that this problem is infeasible if we do not control the state covariance. For instance, Figure 3.3 shows the results controlled only by an optimal mean steering controller. The blue ellipses are the predicted 3σ confidence region of the system state, and gray lines are the 100 sample trajectories. As the state covariance grows, it is impossible to find a feasible solution to this problem that will guarantee the satisfaction of chance constraints.

Before discussing the case with chance constraints, we discuss the case without chance constraints, which is illustrated in Fig. 3.4. By introducing the covariance steering, the uncertainty of the future trajectory successfully reduced.

Finally, Fig. 3.5 illustrates the results of the proposed state chance-constrained OCS approach. The error ellipses successfully change their shapes and avoid collision with the

constraints while maintaining the terminal covariance constraints to be less than the target state covariance. The difference from Fig. 3.4 indicate the coupling between the mean and covariance steering controls.

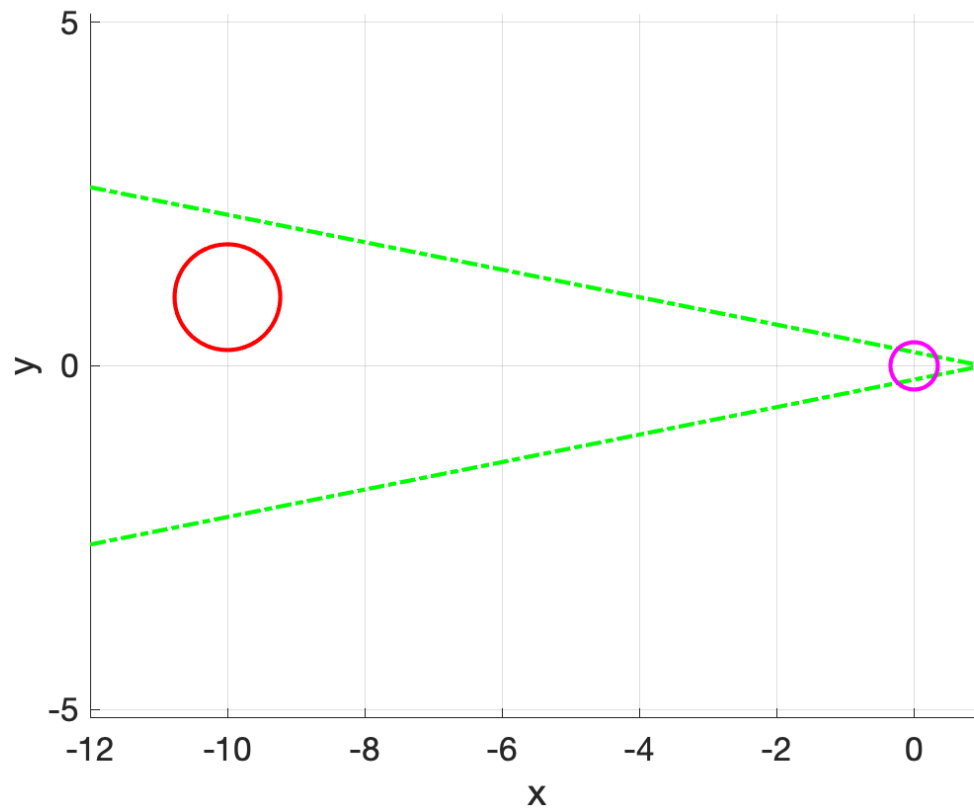
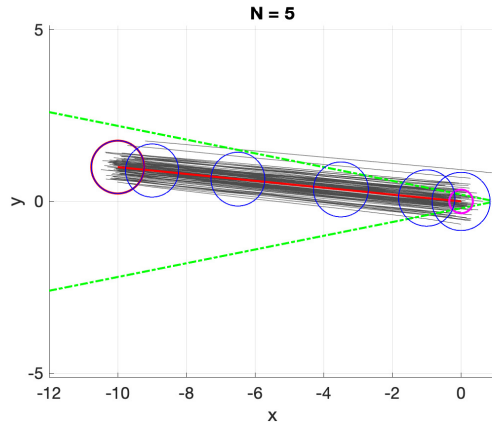
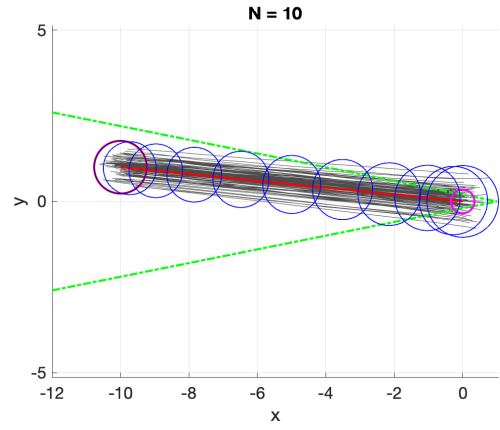


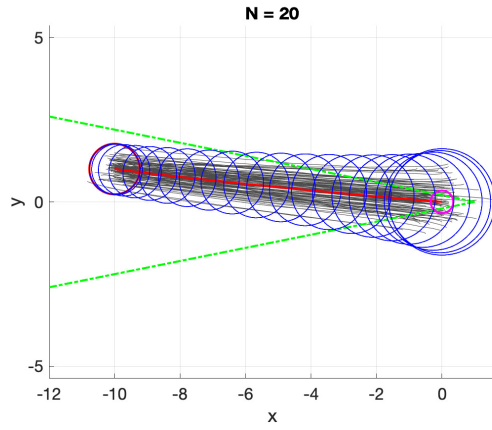
Figure 3.2: Problem Setup for the numerical simulation.



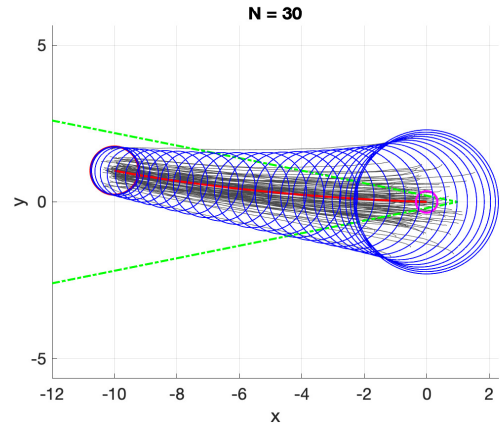
(a) $N = 5$ case.



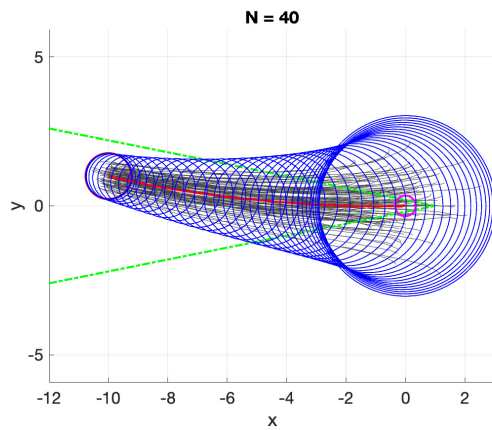
(b) $N = 10$ case.



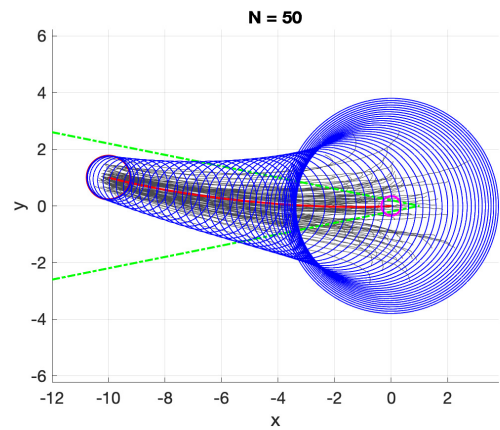
(c) $N = 20$ case.



(d) $N = 30$ case.



(e) $N = 40$ case.



(f) $N = 50$ case.

Figure 3.3: Results by a mean steering controller with various N settings.

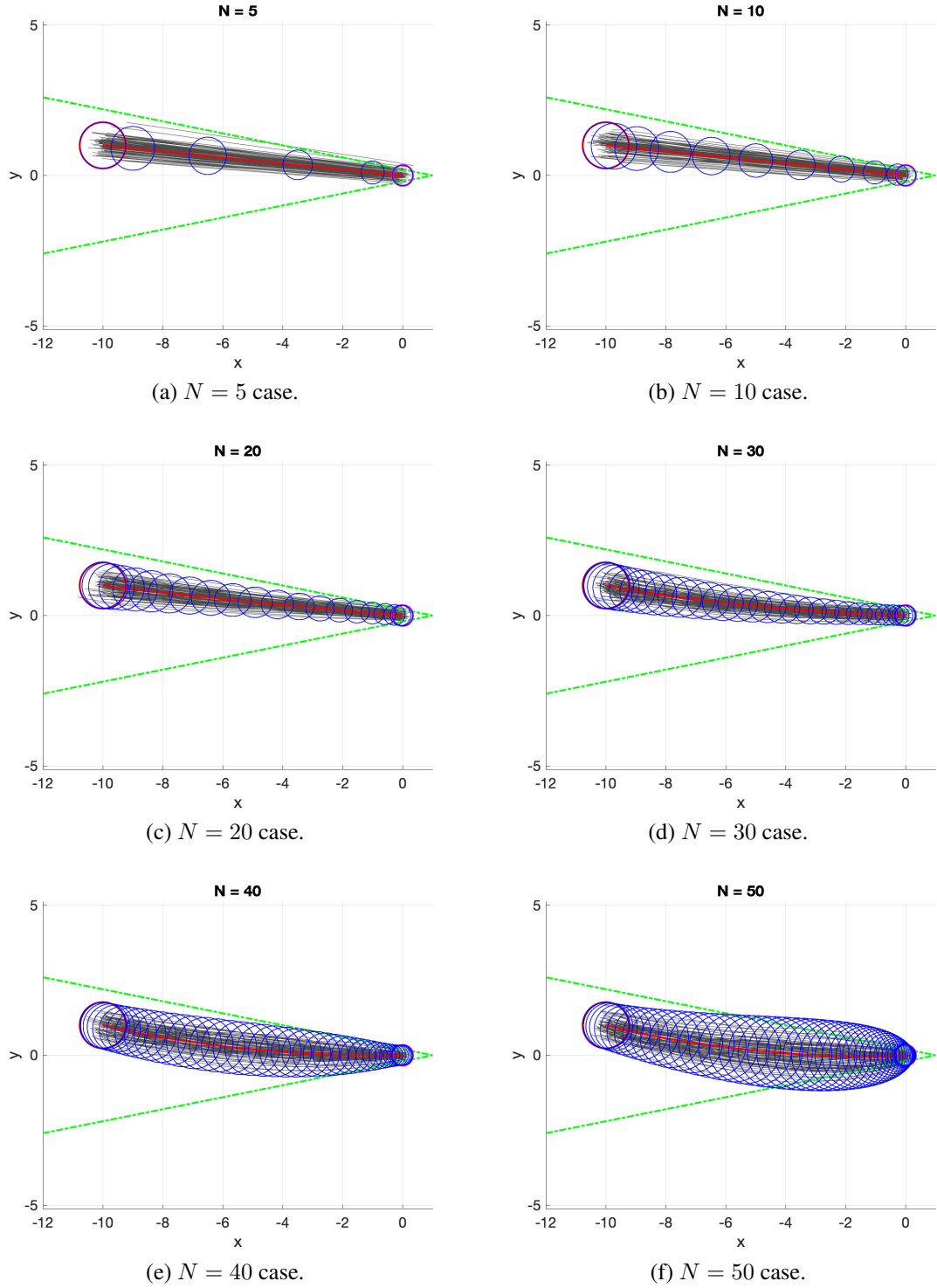


Figure 3.4: Results by a OCS controller without state chance constraints with various N settings.

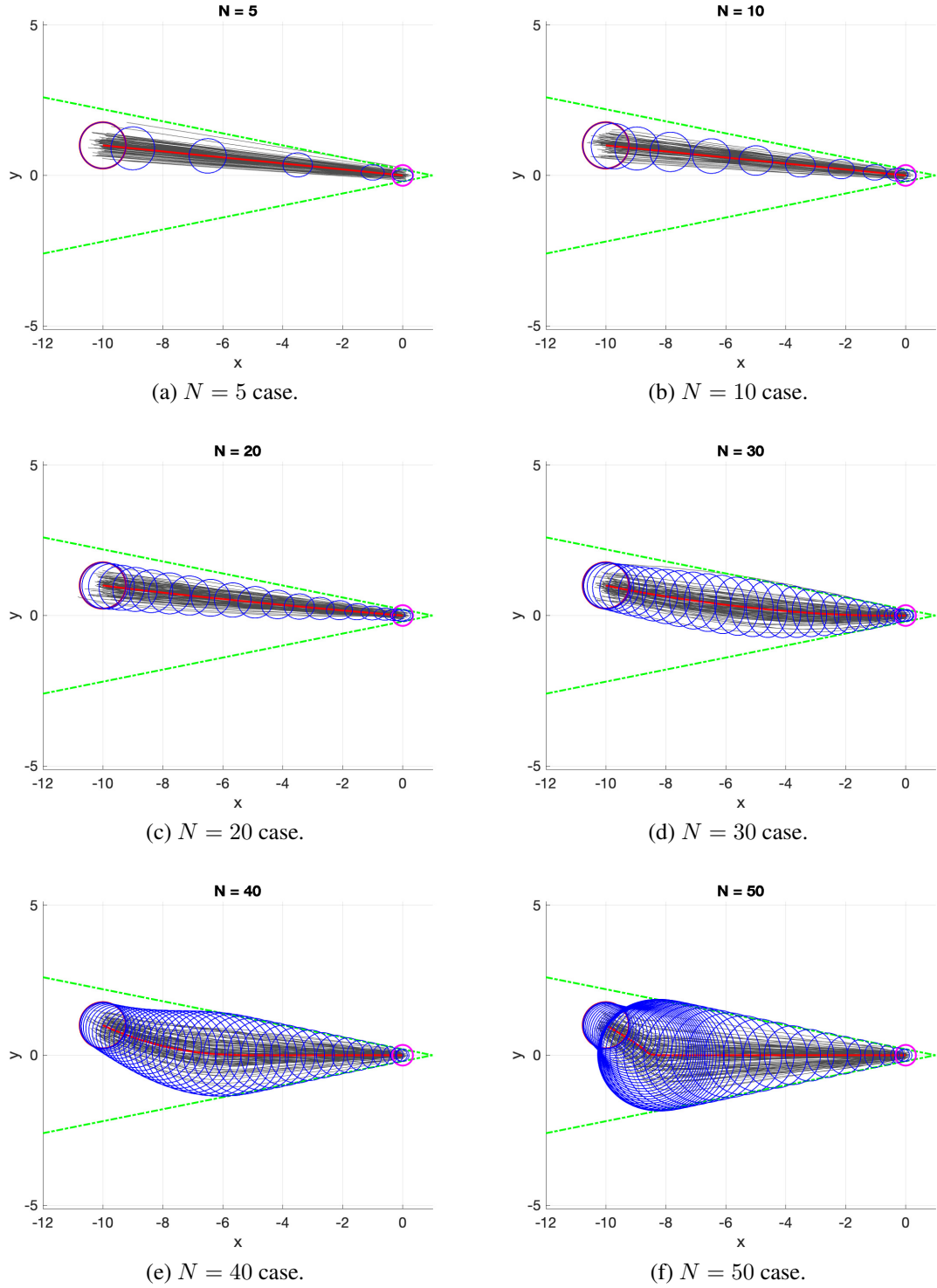


Figure 3.5: Results by the proposed OCS controller under state chance constraints with various N settings.

3.5 Summary

In this chapter we addressed the optimal covariance steering problem for stochastic discrete-time linear time-varying systems subject to chance constraints. Because the mean and the covariance trajectories couple when state constraints exist, we need to design a controller that simultaneously optimizes the state mean and covariance trajectories. We proposed a novel stochastic optimal control policy that can be categorized as an affine parameterization approach. The proposed controller is an affine function of a filtered disturbance, and the entire problem is converted to a convex programming problem. We demonstrated the effectiveness of the proposed approach using numerical simulations.

In the following sections, we start from Theorem 1 and deal with various situations, namely under non-convex state chance constraints (Chap. 4) and under input hard constraints (Chap. 5). In addition, we apply the proposed approach to stochastic model predictive control (Chap. 6).

CHAPTER 4

VEHICLE PATH PLANNING USING OPTIMAL COVARIANCE STEERING

In this chapter, we apply the optimal covariance steering controller developed in Theory 1 in Chapter 3 to the problem of vehicle path planning in the presence of obstacles and uncertainties. By steering the state covariance, we aim to mitigate the conservativeness of the ensuing path. To this end, we need to deal with non-convex state constraints. We represent the feasible state space as a union of overlapping convex feasible subspaces and formulate the entire problem as a mixed-integer convex programming problem.

Section 4.1 formulates the problem based on the discussions in Chapter 3. Then, we introduce the proposed path planning algorithm in Section 4.2. The effectiveness of the algorithm is verified using numerical simulations in Section 4.3. The proposed approach can also be applied to the multi-vehicle path planning. Finally, we discuss the proposed approach and provides a summary of this chapter in Section 4.4.

4.1 Problem Statement

We follow an identical problem set up to the one in Chapter 3, namely discrete-time stochastic linear time-varying system (3.1), with the i.i.d. additive Gaussian assumption (3.2), the Gaussian distributed initial state (3.4) and target state (3.5), and the quadratic cost function (3.6). In this chapter, we extend the problem setup in Chapter 3) and consider non-convex state chance constraints so that we can design nominal trajectories that avoid collisions with obstacles using the optimal covariance steering theory. This extension will allow us to apply the optimal covariance steering algorithm to more versatile scenarios.

Specifically, in this chapter, we consider the following state chance constraints

$$\Pr(x_k \in \mathcal{X}) \geq 1 - \epsilon_x, \quad k = 0, \dots, N - 1. \quad (4.1)$$

The feasible state set $\mathcal{X} \subset \mathbb{R}^{n_x}$, we discuss in this Chapter, is *non-convex* owing to the presence of several obstacles, i.e.,

$$\mathcal{X} = \mathcal{X}_\Omega \setminus \left(\bigcup_{j=1}^{N_{\text{obs}}} \mathcal{X}_j \right), \quad (4.2)$$

where $\mathcal{X}_\Omega, \mathcal{X}_1, \dots, \mathcal{X}_{N_{\text{obs}}} \subset \mathbb{R}^{n_x}$ are (typically) polytopes and N_{obs} is the number of obstacles.

In summary, we wish to solve the following stochastic optimal control problem.

Problem 4 (Vehicle Path Planning Problem).

$$\min J(x, u_0, \dots, x_{N-1}, u_{N-1}) = \mathbb{E} \left[\sum_{k=0}^{N-1} x_k^\top Q_k x_k + u_k^\top R_k u_k \right],$$

subject to

$$x_{k+1} = A_k x_k + B_k u_k + D_k w_k, \quad x_0 \sim \mathcal{N}(\mu_0, \Sigma_0),$$

$$x_N \sim \mathcal{N}(\mu_f, \Sigma_f),$$

$$\Pr(E_k X \in \mathcal{X}) \geq 1 - \epsilon_x,$$

$$\mathcal{X} = \mathcal{X}_\Omega \setminus \left(\bigcup_{j=1}^{N_{\text{obs}}} \mathcal{X}_j \right),$$

Similarly to the approach in Chapter 3, because Problem 4 is not instrumental to solve, we use an equivalent description and try to solve the following.

Problem 5 (Vehicle Path Planning Problem (Converted Form)).

$$\begin{aligned}
& \min J(X, U) = \mathbb{E} [X^\top \bar{Q} X + U^\top \bar{R} U], \\
& \text{subject to} \\
& X = \mathcal{A}x_0 + \mathcal{B}U + \mathcal{D}W, \quad x_0 \sim \mathcal{N}(\mu_0, \Sigma_0), \\
& \mu_f = E_N \mathbb{E}[X], \\
& \Sigma_f = E_N (\mathbb{E}[X X^\top] - \mathbb{E}[X] \mathbb{E}[X]^\top) E_N^\top. \\
& \Pr(E_k X \in \mathcal{X}) \geq 1 - \epsilon_x, \\
& \mathcal{X} = \mathcal{X}_\Omega \setminus \left(\bigcup_{j=1}^{N_{\text{obs}}} \mathcal{X}_j \right),
\end{aligned}$$

4.2 Optimal Covariance Control with Obstacles

In this section, we propose a novel approach to efficiently deal with non-convex state chance constraints in the optimal covariance control framework.

We start by representing the non-convex set of obstacle-free states as the union of a finite number of overlapping *convex* sub-regions \mathcal{R}_r . Specifically, we represent \mathcal{X} in (4.2) as

$$\mathcal{X} = \bigcup_{r=0}^{N_R-1} \mathcal{R}_r, \quad (4.5)$$

where N_R is the number of sub-regions. We assume that each \mathcal{R}_r can be represented as

$$\mathcal{R}_r = \bigcap_{i=0}^{M_r-1} \{x : \alpha_{r,i}^\top x \leq \beta_{r,i}\}, \quad (4.6)$$

where $\alpha_{r,i} \in \mathbb{R}^{n_x}$ and $\beta_{r,i} \in \mathbb{R}$. Let now the Boolean matrix $\mathcal{M} \in \{0, 1\}^{N_R \times (N-1)}$, where $\mathcal{M}_{r,k} = 1$ implies that the state at time steps k and $k+1$ belongs to \mathcal{R}_r with high probability. Note that, because of the noise, the state constraints need to be probabilistically formulated,

i.e., using chance constraints. Namely,

$$\mathcal{M}_{r,k} = 1 \Rightarrow \begin{cases} \Pr(x_k \in \mathcal{R}_r) \geq 1 - \epsilon, \\ \Pr(x_{k+1} \in \mathcal{R}_r) \geq 1 - \epsilon, \end{cases} \quad (4.7)$$

where $0 < \epsilon \ll 1$. By imposing the following constraint,

$$\sum_{r=0}^{N_R-1} \mathcal{M}_{r,k} = 1, \quad (4.8)$$

we ensure that, with high probability, the state is collision-free at time step k . As there can be overlaps between sub-regions, the state variables at steps k and $k + 1$ can belong to multiple regions. Thus, the implication is only one directional [63].

The main result of this chapter is summarized in the following lemma.

Lemma 1. *Using the controller in Theorem 1 and given \mathcal{R}_r in (4.6), the conditions*

$$\begin{cases} \Pr(x_k \in \mathcal{R}_r) \geq 1 - \epsilon, \\ \Pr(x_{k+1} \in \mathcal{R}_r) \geq 1 - \epsilon, \end{cases} \quad (4.9)$$

are converted to second-order cone constraints.

Proof. Because \mathcal{R}_r is as in (4.6), following a similar discussion to the proof of Theorem 1, one can convert

$$\Pr(x_\kappa \in \mathcal{R}_r) \geq 1 - \epsilon, \quad (4.10)$$

where $\kappa \in \{k, k + 1\}$, to the following

$$\alpha_{r,i}^\top E_\kappa (\mathcal{A}\mu_0 + \mathcal{B}V) - \beta_{r,i} + |S^\top (I + \mathcal{B}K)^\top E_\kappa^\top \alpha_{r,i}| \Phi^{-1}(1 - \epsilon) \leq 0. \quad (4.11)$$

where $i = 0, \dots, M_r - 1$. This inequality is a second-order cone constraint in terms of V

and K . □

Finally, we reformulate Problem 5 into the following mixed-integer convex programming problem summarized in Problem. The element-wise constraints on V and K were introduced to expedite the solution. Note that, although MIP problems are, in general, NP-hard, a number of tools have been recently developed in the literature to efficiently solve such problems. In the following section, using simple numerical examples, we demonstrate that our problem setup can be efficiently solved with current MIP solvers.

Problem 6 (Vehicle Path Planning using Optimal Covariance Steering Theory).

$$\begin{aligned} \min_{V,K} J(V, K) = & (\mathcal{A}\mu_0 + \mathcal{B}V)^\top \bar{Q}(\mathcal{A}\mu_0 + \mathcal{B}V) + V^\top \bar{R}V \\ & + \text{tr} \left[((I + \mathcal{B}K)^\top \bar{Q}(I + \mathcal{B}K) + K^\top \bar{R}K) \Sigma_Y \right], \end{aligned}$$

subject to

$$\mu_f = E_N (\mathcal{A}\mu_0 + \mathcal{B}V),$$

$$\begin{bmatrix} \Sigma_f & E_N(I + \mathcal{B}K)S \\ S^\top(I + \mathcal{B}K)^\top E_N^\top & I \end{bmatrix} \succeq 0,$$

$$V_{\min} \leq V \leq V_{\max},$$

$$K_{\min} \leq K \leq K_{\max},$$

$$\sum_{r=0}^{N_R-1} \mathcal{M}_{r,k} = 1,$$

$$\mathcal{M}_{r,k} = 1 \Rightarrow$$

$$\begin{cases} \alpha_{r,i}^\top E_k (\mathcal{A}\mu_0 + \mathcal{B}V) - \beta_{r,i} + |S^\top(I + \mathcal{B}K)^\top E_\kappa^\top \alpha_{r,i}| \Phi^{-1}(1 - \epsilon) \leq 0, \\ \alpha_{r,i}^\top E_{k+1} (\mathcal{A}\mu_0 + \mathcal{B}V) - \beta_{r,i} + |S^\top(I + \mathcal{B}K)^\top E_\kappa^\top \alpha_{r,i}| \Phi^{-1}(1 - \epsilon) \leq 0. \end{cases}$$

4.3 Numerical Simulations

In this section we validate the proposed algorithm using simple numerical examples. We consider the path-planning problem for a vehicle under the same dynamics and disturbance as the numerical simulations in Chap. 3. The vehicle dynamics is as in (3.71) with $\Delta t = 0.2$. In this section, we use the following cost function

$$J(V, K) = \text{tr} \left(((I + \mathcal{B}K)^\top \bar{Q}_{\text{cov}}(I + \mathcal{B}K) + K^\top \bar{R}_{\text{cov}}K) \Sigma_Y \right) \\ + (\mathcal{A}\mu_0 + \mathcal{B}V)^\top \bar{Q}_{\text{mean}} (\mathcal{A}\mu_0 + \mathcal{B}V) + V^\top \bar{R}_{\text{mean}} V, \quad (4.13)$$

where

$$\bar{Q}_{\text{mean}} = \text{blkdiag}(Q_{0,m}, Q_{1,m}, \dots, Q_{N-1,m}, 0), \quad (4.14a)$$

$$\bar{R}_{\text{mean}} = \text{blkdiag}(R_{0,m}, R_{1,m}, \dots, R_{N-1,m}), \quad (4.14b)$$

$$\bar{Q}_{\text{cov}} = \text{blkdiag}(Q_{0,v}, Q_{1,v}, \dots, Q_{N-1,v}, 0), \quad (4.14c)$$

$$\bar{R}_{\text{cov}} = \text{blkdiag}(R_{0,v}, R_{1,v}, \dots, R_{N-1,v}), \quad (4.14d)$$

with

$$Q_{k,m} = \text{diag}(0.5, 4.0, 0.05, 0.05), \quad (4.15a)$$

$$R_{k,m} = \text{diag}(20, 20), \quad (4.15b)$$

$$Q_{k,v} = 0_{4 \times 4}, \quad (4.15c)$$

$$R_{k,v} = \text{diag}(200, 200), \quad (4.15d)$$

for all $k = 0, \dots, N - 1$.

Similarly to Chapter 3, we use YALMIP [111] and MOSEK [112]. In order to reduce the search space and the computational time, we restricted the control vector and gain

matrix as

$$-100 \leq K \leq 100, \quad (4.16a)$$

$$-100 \leq V \leq 100. \quad (4.16b)$$

It is worth noticing that, although we manually divide and represent the entire feasible region as a union of convex polytopes, algorithms are available to automatically conduct the same job such as [113].

4.3.1 ZigZag

Here, we consider the case illustrated in Fig. 4.1, where the optimal paths go through between the two obstacles and draw zigzagging lines. The mean and the covariance of the initial Gaussian distribution of the system state are set to

$$\mu_0 = \begin{bmatrix} -10 \\ 0 \\ 0 \\ 0 \end{bmatrix}, \quad \Sigma_0 = \begin{bmatrix} 0.05 & & & \\ & 0.05 & & \\ & & 0.001 & \\ & & & 0.001 \end{bmatrix}, \quad (4.17)$$

and we are interested in steering the system state distribution to the target Gaussian distribution $\mathcal{N}(\mu_f, \Sigma_f)$, where

$$\mu_f = \begin{bmatrix} 0 \\ 0 \\ 0 \\ 0 \end{bmatrix}, \quad \Sigma_f = \begin{bmatrix} 0.01 & & & \\ & 0.01 & & \\ & & 0.001 & \\ & & & 0.001 \end{bmatrix}. \quad (4.18)$$

We set the number of time steps to $N = 10$ and the probability threshold to $\epsilon = 1e - 3$.

We first illustrate, in Fig. 4.2, the results generated by an open-loop stochastic path

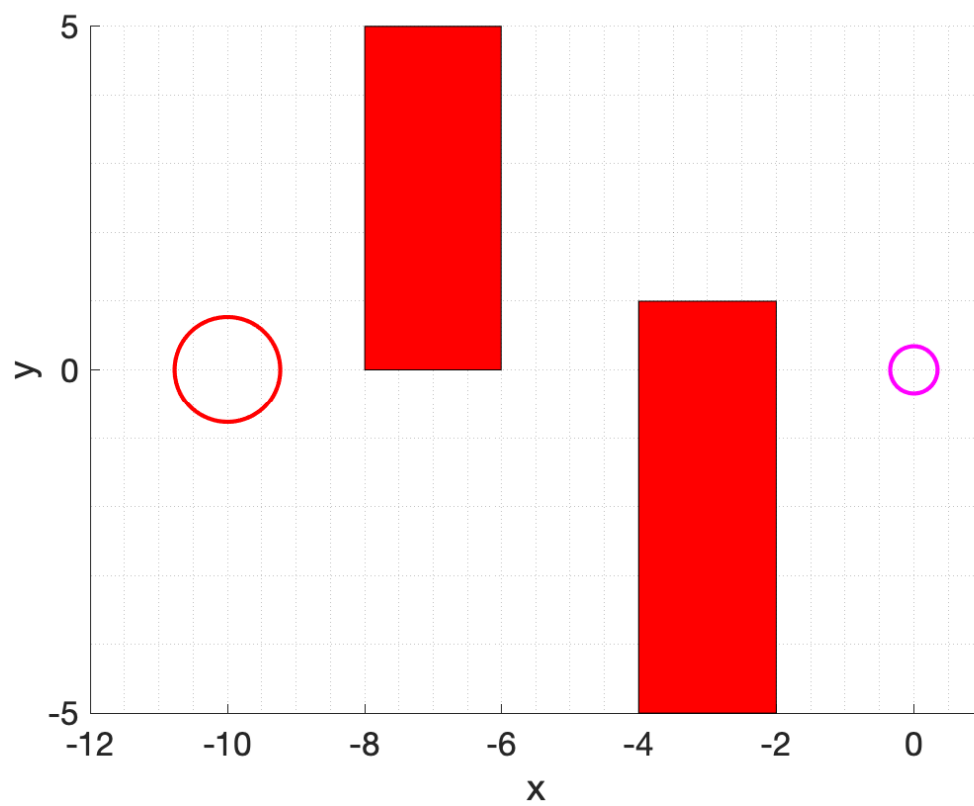


Figure 4.1: Problem Setup for the first scenario.

planner, which corresponds to the case with the feedback gain always zero, i.e., $K = 0$. In addition, this approach cannot impose the terminal covariance constraint. Each ellipse denotes the error ellipse corresponding to 3σ , and blue line indicates the mean trajectory, or the nominal path. Gray lines are trajectories starting from 100 randomly-picked different initial conditions. Because the path planner cannot shrink the covariance, or cannot consider the future feedback control, the future state covariance keeps increasing its size. Hence, the nominal path needs to obtain large margins to the obstacles and thus becomes conservative.

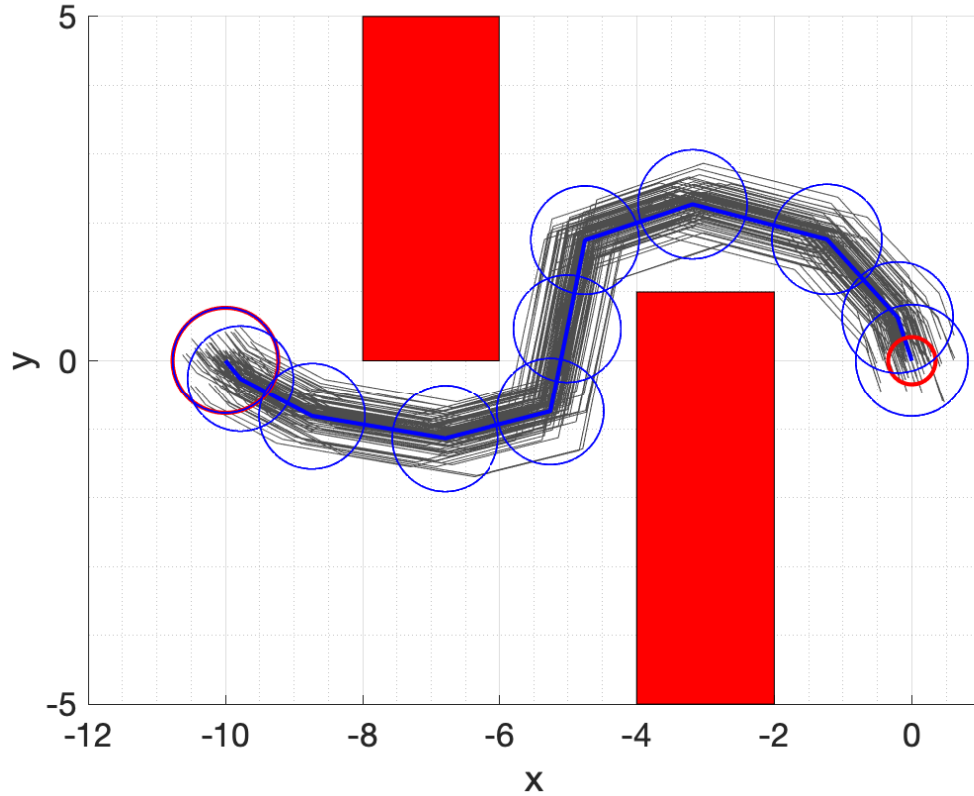


Figure 4.2: Results from open-loop stochastic path planning approach.

Figure 4.3 illustrates the solution generated by the proposed path planner based on the optimal covariance steering theory. Because the state covariance shrinks, the nominal path can take smaller margins to the obstacles than the ones in Fig. 4.2. In order to compute this solution, we used five rectangle sub-regions to represent the feasible region (see Fig. 4.4).

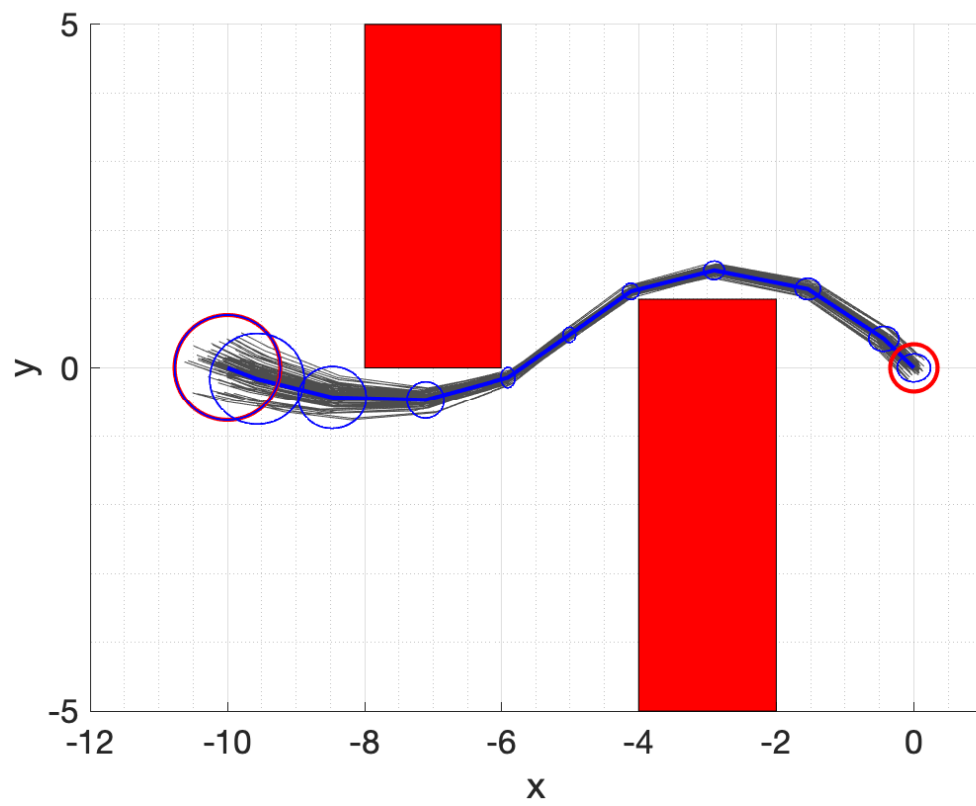


Figure 4.3: Results from the proposed approach.

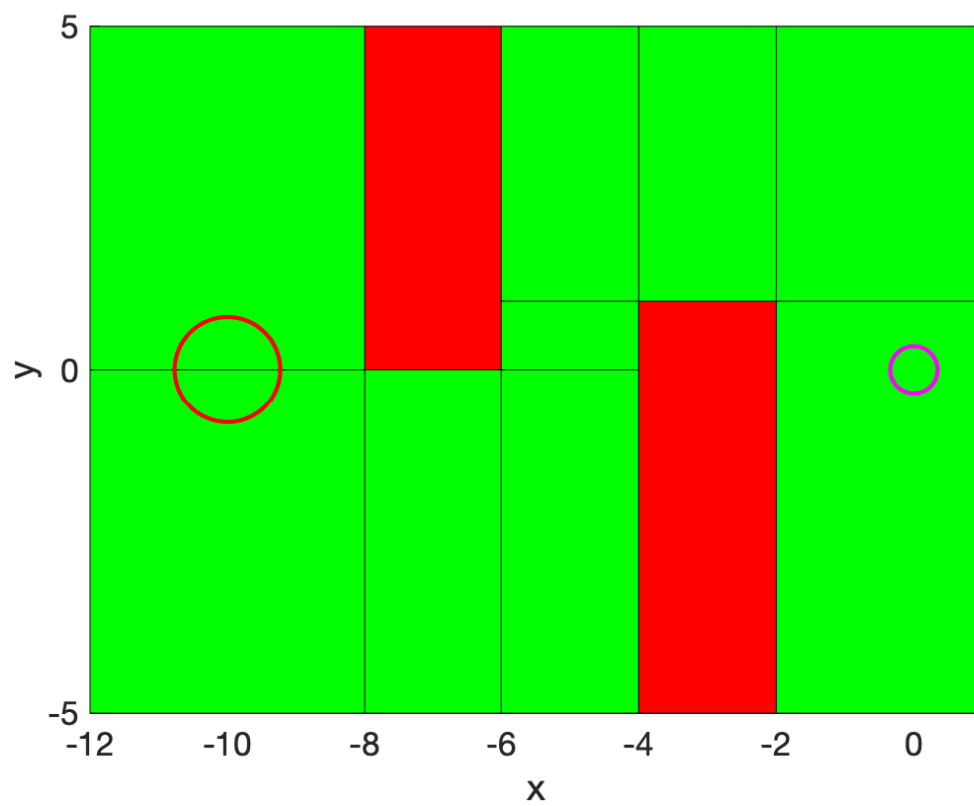


Figure 4.4: Representation of the feasible state subsets.

4.3.2 Double-Slit Obstacle

We consider the case illustrated in Fig. 4.5, where we need to find the trajectory to go from left to right through one of the two “slits.” Notice that going through the top slit takes smaller detour and costs less than going through the bottom slit. However, the top slit is narrower than the bottom one.

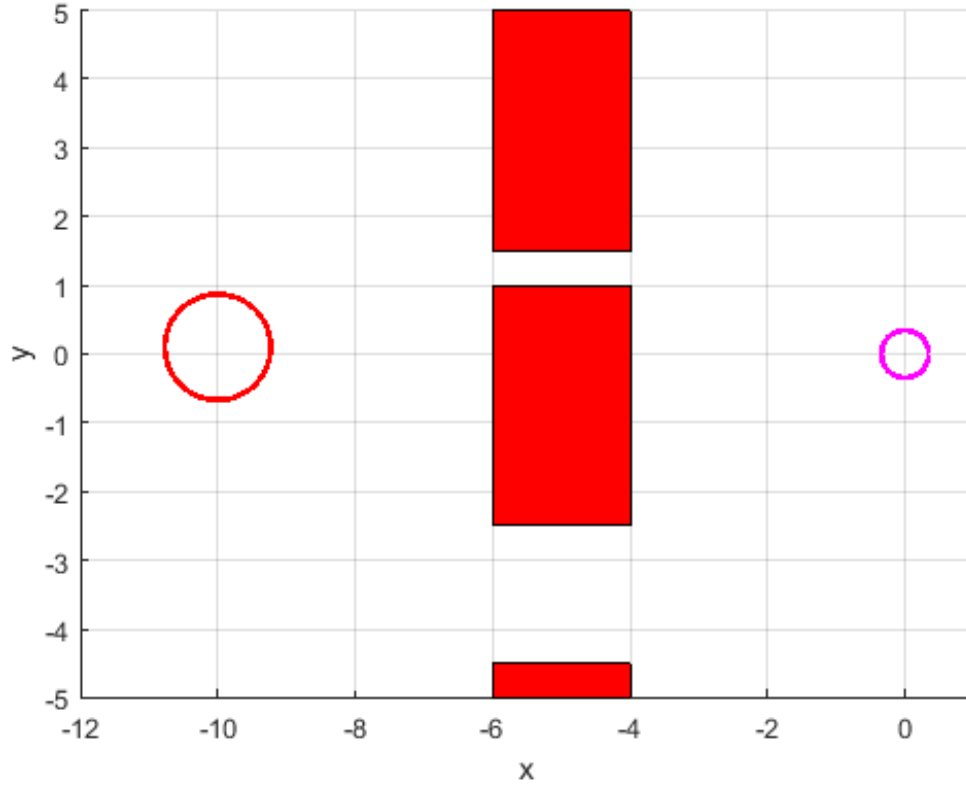


Figure 4.5: Problem setup.

The initial condition is

$$\mu_0 = [-10, 0.1, 0, 0], \quad \Sigma_0 = \begin{bmatrix} 0.05 & & & \\ & 0.05 & & \\ & & 0.001 & \\ & & & 0.001 \end{bmatrix}, \quad (4.19)$$

while the terminal constraint is

$$\mu_f = [0, 0, 0, 0], \quad \Sigma_f = \begin{bmatrix} 0.01 & & & \\ & 0.01 & & \\ & & 0.001 & \\ & & & 0.001 \end{bmatrix}. \quad (4.20)$$

We set $N = 20$.

First, for comparison, we conduct only mean steering as shown in Fig. 4.6. In this case, the covariance is not controlled, and thus, the terminal covariance constraint cannot be satisfied. Since the initial covariance is large and state covariance keeps growing due to the disturbance, the mean steering controller cannot find any feasible solutions that guide the trajectory through the top slit, and the path has to go through the larger but further away bottom slit as illustrated in Fig. 4.6.

The result of the proposed approach is illustrated in Fig. 4.7. The controller shrinks the state covariance and successfully computes an optimal path that goes through the narrow top slit. In order to compute this solution, we used the rectangular-shaped sub-regions shown in Fig. 4.8.

We also conducted another numerical simulation with slightly different setup as illustrated in Fig. 4.9, where the top slit is much narrower than the one in Fig. 4.5. As illustrated in Fig. 4.10, the algorithm found that the cost of shrinking the error ellipses and going through the top slit is higher than going through the lower slit. In order to compute this path, we used the rectangular-shaped sub-regions shown in Fig. 4.11.

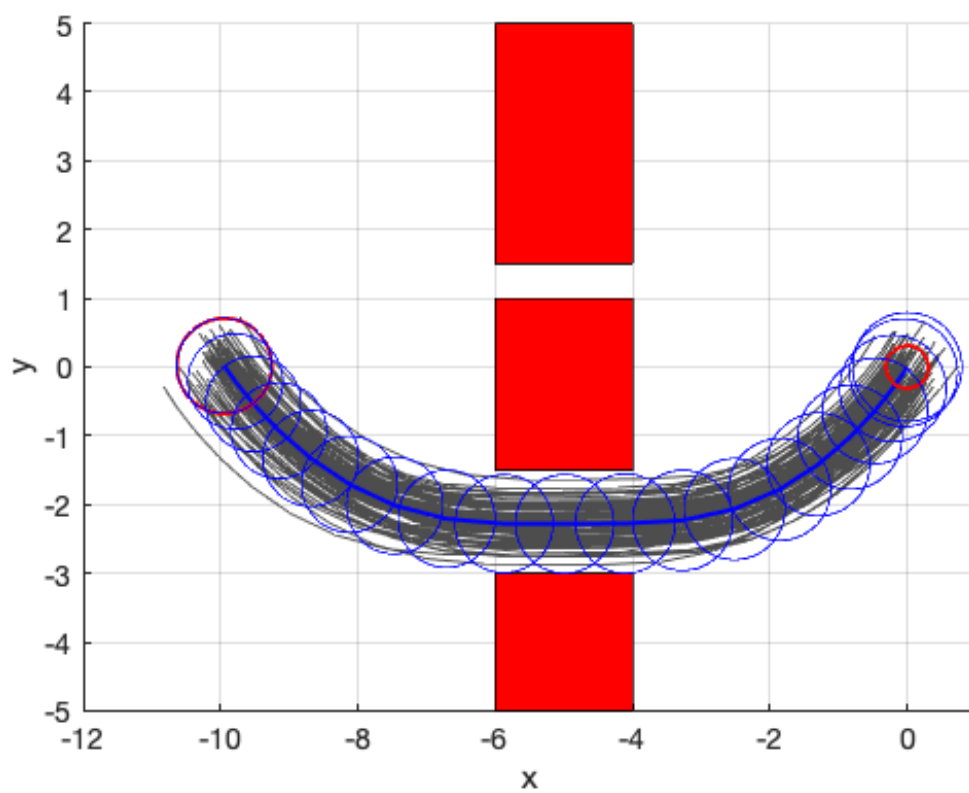


Figure 4.6: Mean steering trajectory with open-loop covariance dynamics.

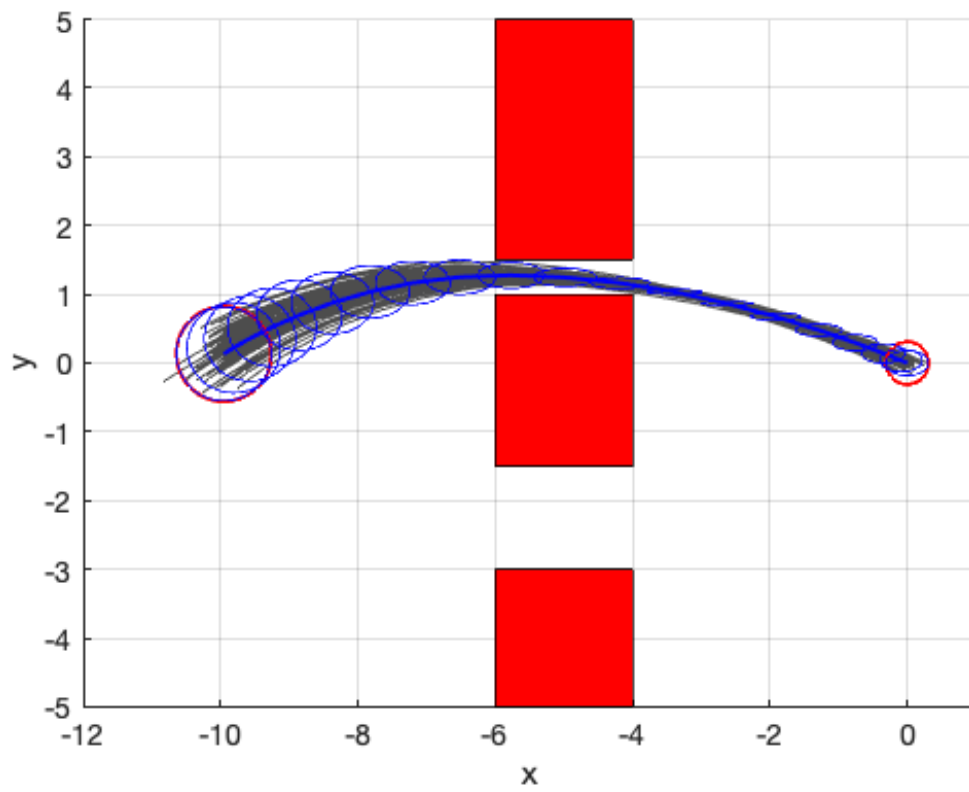
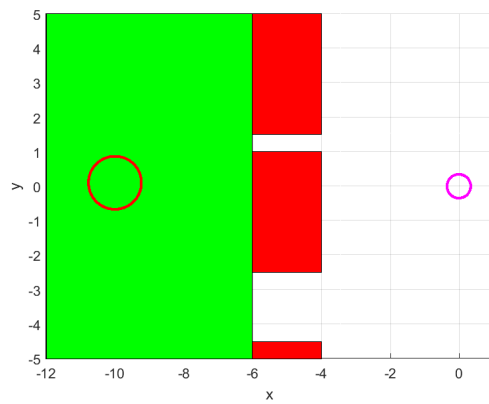
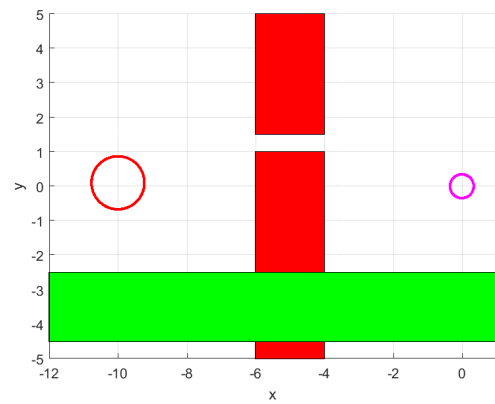


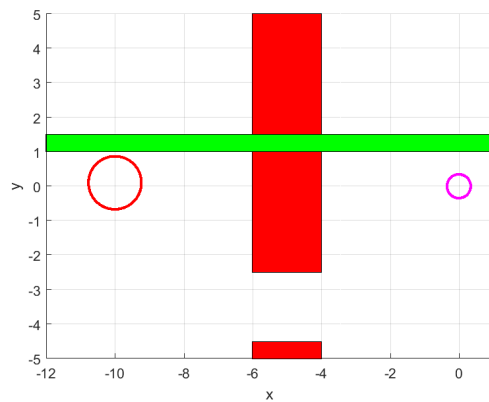
Figure 4.7: Proposed approach with closed-loop covariance dynamics.



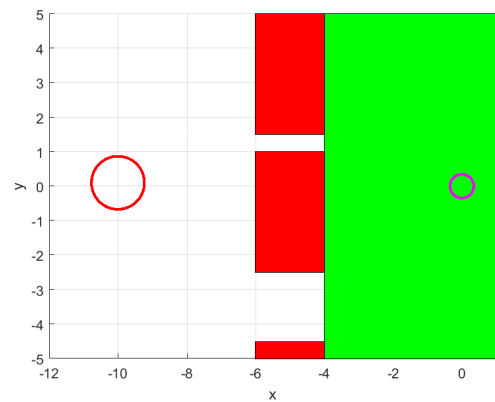
(a) Region 1



(b) Region 2



(c) Region 3



(d) Region 4

Figure 4.8: Representation of the feasible region.

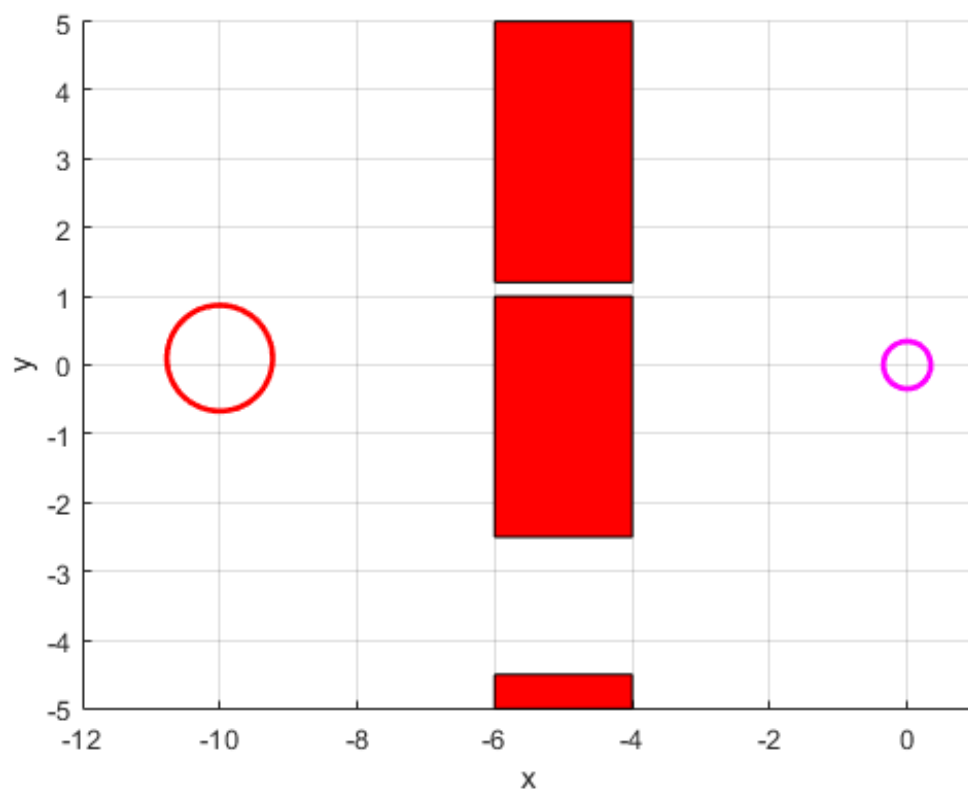


Figure 4.9: Problem setup.

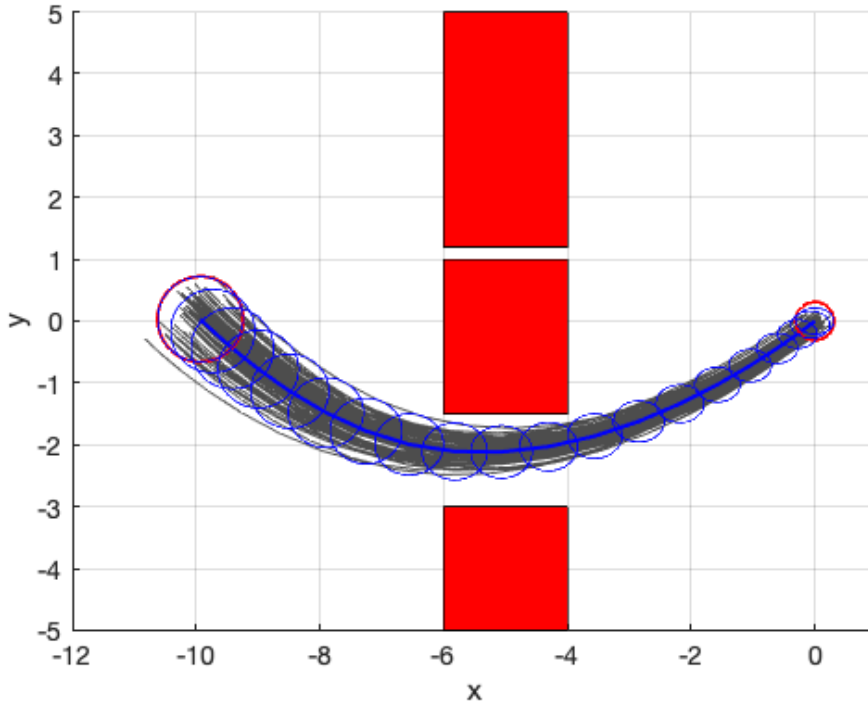


Figure 4.10: Solution of the proposed approach.

4.3.3 Cluttered Environment

Next, we consider the case illustrated in Fig. 4.12, where we compute the optimal collision-free trajectory in a somewhat cluttered environment. The initial condition is

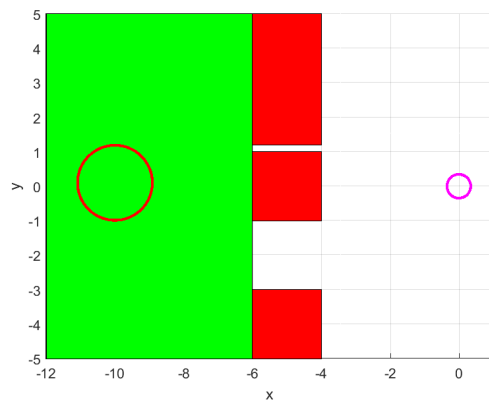
$$\mu_0 = [-10, 0.1, 0, 0], \quad \Sigma_0 = \text{diag}(0.05, 0.05, 0.001, 0.001), \quad (4.21)$$

while the terminal constraint is

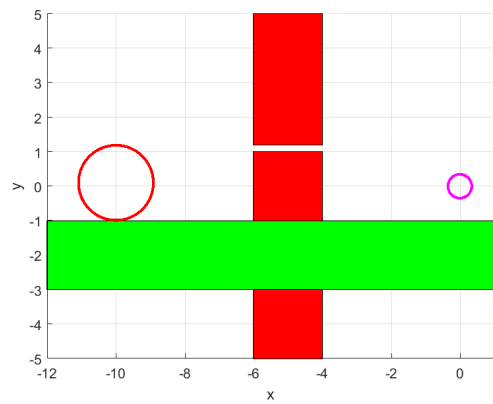
$$\mu_N = [0, 0, 0, 0], \quad \Sigma_N = \text{diag}(0.01, 0.01, 0.001, 0.001). \quad (4.22)$$

We set $N = 20$.

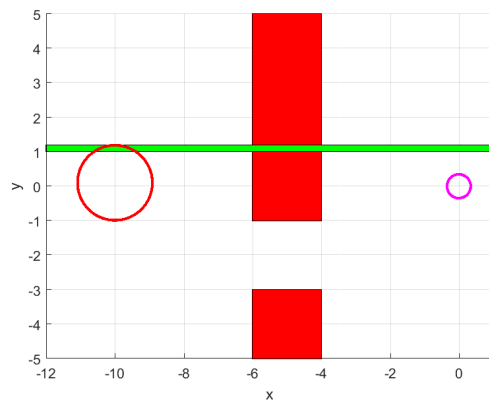
We first show the results of a mean steering controller in Fig. 4.13. The controller finds that the “corridor” between $y = 0$ and $y = 1$ is too narrow, and the path needs to detour to



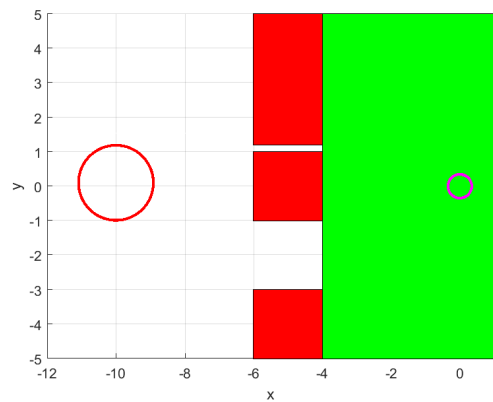
(a) Region 1



(b) Region 2



(c) Region 3



(d) Region 4

Figure 4.11: Representation of the feasible region.

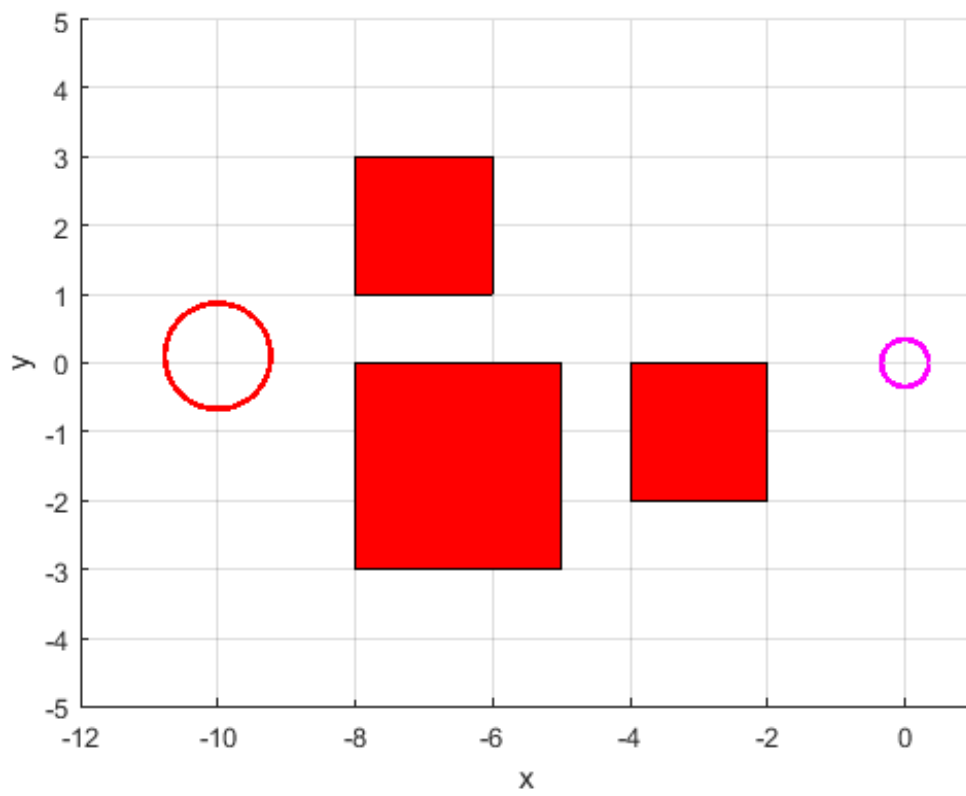


Figure 4.12: Problem Setup.

the top region. In contrast, the proposed approach shrinks the covariance and successfully follows the shortest corridor while satisfying the non-convex state constraints as shown in Fig. 4.14.

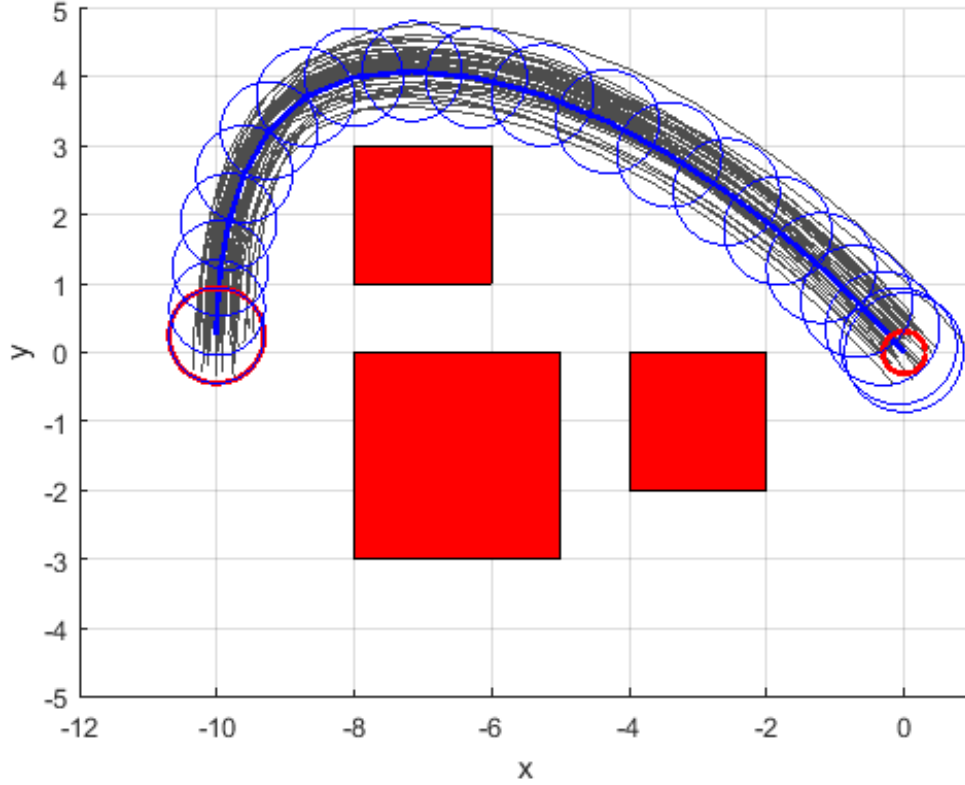


Figure 4.13: Mean steering trajectory with open-loop covariance dynamics.

4.3.4 Multi-Vehicle Path Planning

Here, we use multiple vehicles that are moving on a flat plane, and we compute the optimal path planning for each vehicle to reach a pre-specified goal region. As each vehicle has to avoid collisions with other vehicles, the feasible state space is non-convex. A number of research works such as [52, 61, 59] attempted to solve this problem, but to our knowledge, none of them have achieved the steering of covariance of the state variables to the pre-specified values.

We assume that the number of vehicles we steer is N_v . The vehicle dynamics of each

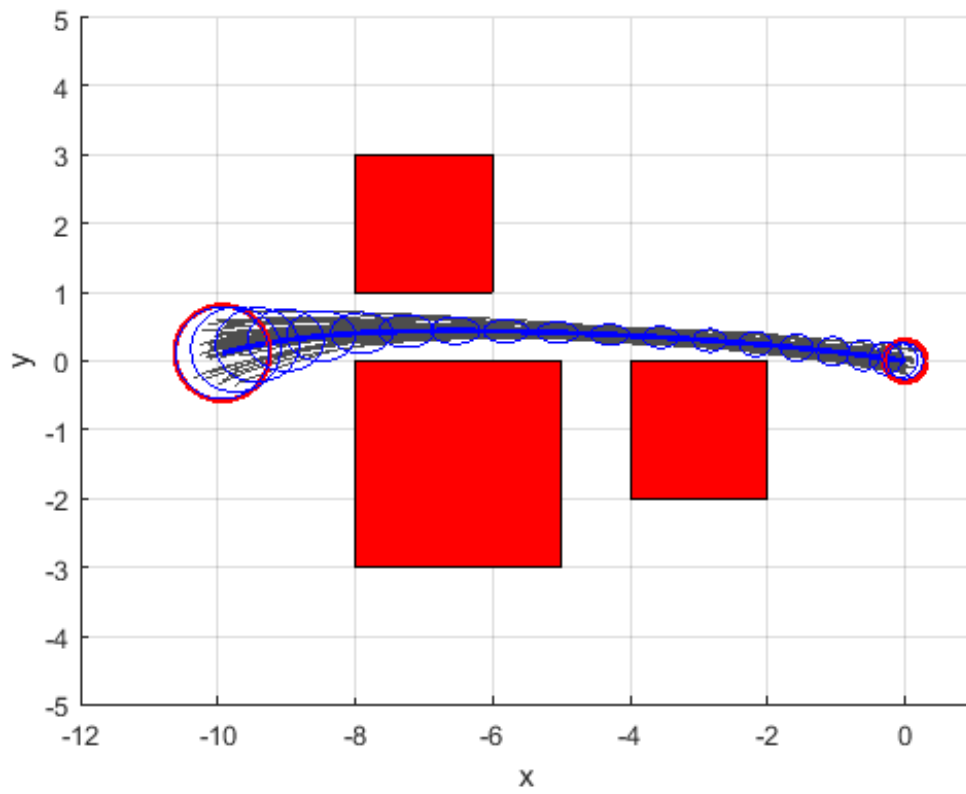


Figure 4.14: Proposed approach with closed-loop covariance dynamics.

vehicle is represented as a linear time invariant system

$$x_{k+1}^i = Ax_k^i + Bu_k^i + Dw_k^i, \quad (4.23)$$

where the matrices A , B , and D are the the same matrices as in (3.71) with $\Delta t = 0.2$. In addition, the superscript $i = 1, \dots, N_v$ denotes the vehicle index. We concatenate the state vector as

$$X = \begin{bmatrix} x_0^1 \\ x_1^1 \\ \vdots \\ x_{N-1}^{N_v} \\ x_N^{N_v} \end{bmatrix}, \quad U = \begin{bmatrix} u_0^1 \\ u_1^1 \\ \vdots \\ u_{N-2}^{N_v} \\ u_{N-1}^{N_v} \end{bmatrix}, \quad W = \begin{bmatrix} w_0^1 \\ w_1^1 \\ \vdots \\ w_{N-2}^{N_v} \\ w_{N-1}^{N_v} \end{bmatrix}. \quad (4.24)$$

Then we follow the same process described in Section 4.2. We use the cost function in (3.69) and the cost function weights are chosen as $\bar{Q}_{\text{mean}} = 0$, $\bar{Q}_{\text{cov}} = 0$, $\bar{R}_{\text{mean}} = \text{blkdiag}(R_0, R_1, \dots, R_{N-1})$ with $R_k = \text{blkdiag}(R_k^1, \dots, R_k^{N_v})$ and $R_k^i = \text{diag}(1, 1)$, and $\bar{R}_{\text{cov}} = \text{blkdiag}(R_{\text{cov},0}, R_{\text{cov},1}, \dots, R_{\text{cov},N-1})$ with $R_{\text{cov},k} = \text{blkdiag}(R_{\text{cov},k}^1, \dots, R_{\text{cov},k}^{N_v})$ and $R_{\text{cov},k}^i = \text{diag}(1, 1)$ for $k = 0, \dots, N-1$ and $i = 1, \dots, N_v$. We also set the horizon to $N = 20$ and the probability threshold to $\epsilon = 1.0 \times 10^{-3}$.

2-Vehicle Case

In this scenario, we steer two vehicles from a pre-specified initial distribution to a pre-specified goal distribution as illustrated in Fig. 4.15. Figure 4.15a denotes the initial distribution of the vehicles, and Figure 4.15b illustrates the target distributions. The task here is to steer Vehicle 1 from the left distribution in Fig. 4.15a to the right distribution in Fig. 4.15b while steering Vehicle 2 from the right distribution in Fig. 4.15a to the left distribution in Fig. 4.15b. Specifically, the initial state distributions of Vehicles 1 and 2 are

given as $\mathcal{N}(\mu_0^1, \Sigma_0^1)$ and $\mathcal{N}(\mu_0^2, \Sigma_0^2)$, where

$$\mu_0^1 = [-1, 0, 0, 0]^\top, \quad \Sigma_0^1 = \text{diag}(0.05, 0.05, 0.001, 0.001), \quad (4.25)$$

and

$$\mu_0^2 = [1, 0, 0, 0]^\top, \quad \Sigma_0^2 = \text{diag}(0.05, 0.05, 0.001, 0.001). \quad (4.26)$$

In addition, the target distributions for Vehicles 1 and 2 are $\mathcal{N}(\mu_f^1, \Sigma_f^1)$ and $\mathcal{N}(\mu_f^2, \Sigma_f^2)$, where

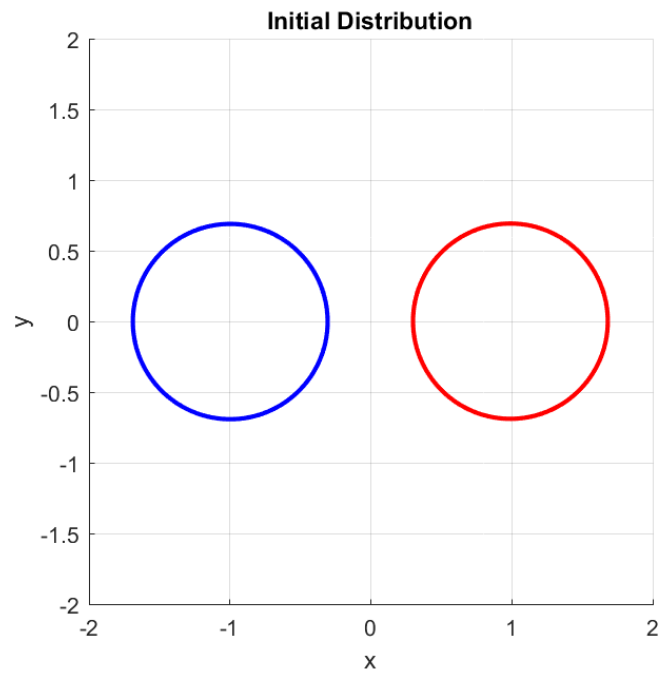
$$\mu_f^1 = [1, 0, 0, 0]^\top, \quad \Sigma_f^1 = \text{diag}(0.01, 0.01, 0.001, 0.001), \quad (4.27)$$

and

$$\mu_f^2 = [-1, 0, 0, 0]^\top, \quad \Sigma_f^2 = \text{diag}(0.01, 0.01, 0.001, 0.001). \quad (4.28)$$

As this scenario is symmetric, we denote the non-convex state space as the union of the feasible convex subspace as illustrated in Fig. 4.16. The feasible region of Vehicle 1 is blue, and the feasible region of Vehicle 2 is red. Informally speaking, Vehicle 1 drives the bottom part while Vehicle 2 drives the top part of the plane.

Figure 4.17(a) shows the results. The blue ellipses are the state covariance of Vehicle 1 and the red ones are the error ellipses of Vehicle 2. The covariance is minimal when they get very close to each other in the middle. After they pass the middle point, the collision avoidance does not need to be considered. Thus, the state covariance enlarged as far as the terminal covariance constraint is smaller than the pre-specified target values. Note that, if we only steer the mean and do not control the covariance of the state variable, we cannot shrink the covariance and the resulting trajectories become conservative as illustrated in Fig. 4.17(b).

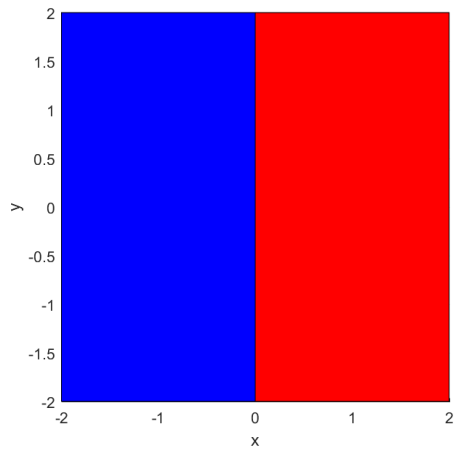


(a) Initial Distributions.

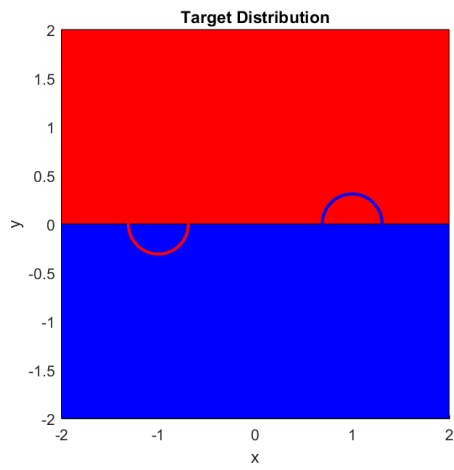


(b) Target Distributions.

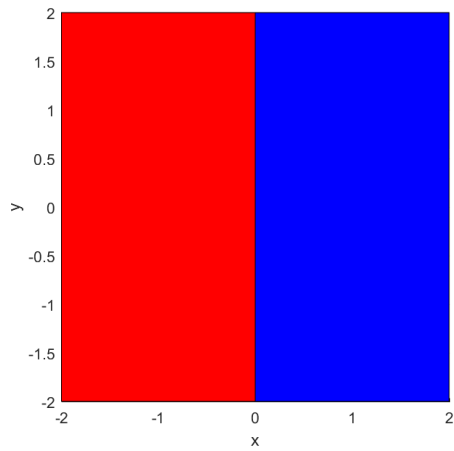
Figure 4.15: Problem setup for two-vehicle path planning.



(a) Regions 1

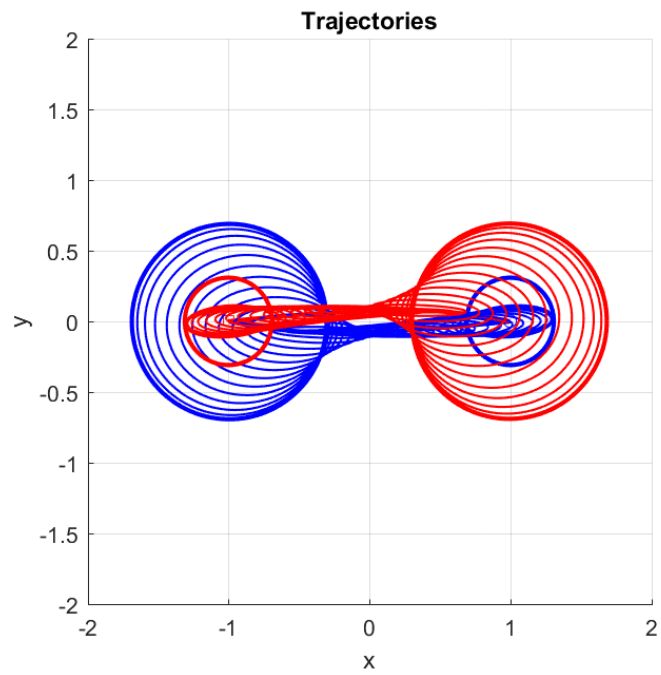


(b) Regions 2.

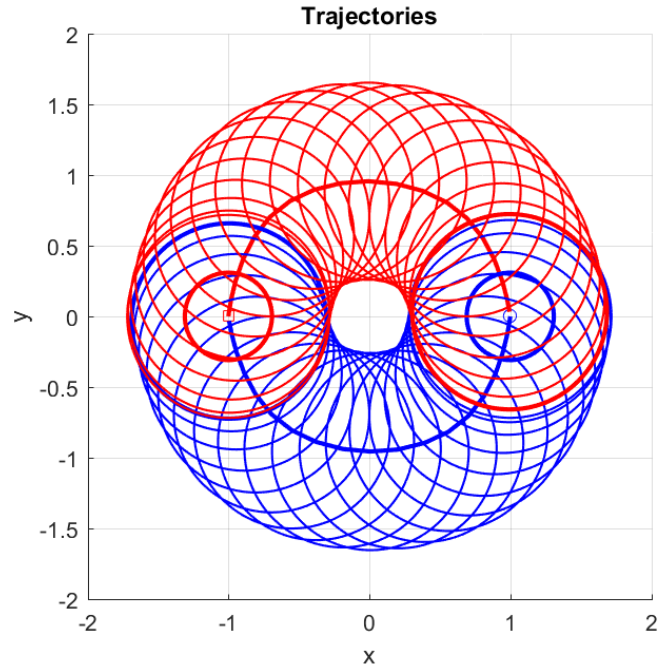


(c) Regions 3.

Figure 4.16: Representation of the feasible region.



(a) Closed loop.



(b) Open loop.

Figure 4.17: Results of two-vehicle collision avoidance using covariance steering.

3-Vehicle Case

Figure 4.18 illustrates the setup of this scenario. In this scenario, the initial distributions of Vehicles 1, 2, and 3 are $\mathcal{N}(\mu_0^1, \Sigma_0^1)$, $\mathcal{N}(\mu_0^2, \Sigma_0^2)$, and $\mathcal{N}(\mu_0^3, \Sigma_0^3)$, where

$$\mu_0^1 = [-1, 0, 0, 0]^\top, \quad \Sigma_0^1 = \text{diag}(0.005, 0.005, 0.001, 0.001), \quad (4.29)$$

$$\mu_0^2 = [1, 0, 0, 0]^\top, \quad \Sigma_0^2 = \text{diag}(0.005, 0.005, 0.001, 0.001), \quad (4.30)$$

$$\mu_0^3 = [0, 0.8, 0, 0]^\top, \quad \Sigma_0^3 = \text{diag}(0.005, 0.005, 0.001, 0.001). \quad (4.31)$$

Furthermore, the target distributions are $\mathcal{N}(\mu_f^1, \Sigma_f^1)$, $\mathcal{N}(\mu_f^2, \Sigma_f^2)$, and $\mathcal{N}(\mu_f^3, \Sigma_f^3)$, where

$$\mu_f^1 = [1, 0, 0, 0]^\top, \quad \Sigma_f^1 = \text{diag}(0.001, 0.001, 0.001, 0.001), \quad (4.32)$$

$$\mu_f^2 = [-1, 0, 0, 0]^\top, \quad \Sigma_f^2 = \text{diag}(0.001, 0.001, 0.001, 0.001), \quad (4.33)$$

$$\mu_f^3 = [0, -0.8, 0, 0]^\top, \quad \Sigma_f^3 = \text{diag}(0.001, 0.001, 0.001, 0.001). \quad (4.34)$$

In order to represent the non-convex state space with the union of convex state space, we first solve this problem with deterministic setting, i.e., no covariance dynamics and disturbances are concerned. Specifically, we use the mixed-integer programming-based approach proposed in [61] with safety margin 0.5 in both x and y directions. The results of this deterministic path programming is illustrated in Fig. 4.19(a). The blue, red, and cyan lines indicate the trajectories of Vehicles 1, 2, and 3, respectively. In addition, asterisk shows the vehicle positions at time steps $k = 0, N/2$, and N . Then, we compute the Voronoi diagram [114] from the vehicle positions at time steps $k = 0, N/2$, and N as illustrated in Fig. 4.19(b), 4.19(c), and 4.19(d).

Remark 3. As Voronoi cells are convex, we can extend this approach to scenarios that use more than 3 vehicles.

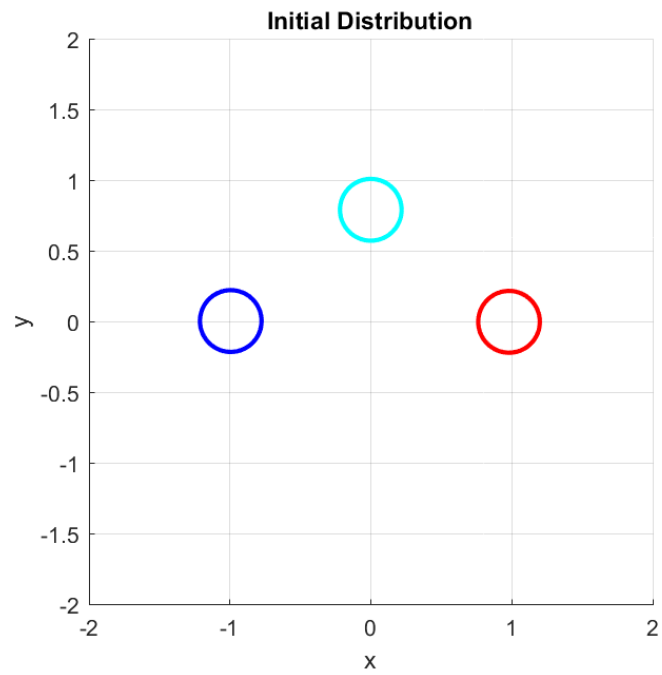
Figure 4.20(a) shows the results. The blue, red, and cyan ellipses are the error ellipses

of Vehicles 1, 2, and 3, respectively. Again, the error ellipses are minimal when they get close in the middle, and after they pass the middle point, the error ellipses enlarged, and the terminal covariance converged to values that are smaller than the target. The difference between the proposed approach and the one in [61] is that the proposed approach has a more systematic way of obtaining safety margins to other vehicles than only pre-specifying some constants to x - and y - directions. Note that, if we only steer the mean and do not control the covariance of the state variable, the resulting trajectories do not go into the middle portion of the space as illustrated in Fig. 4.20(b).

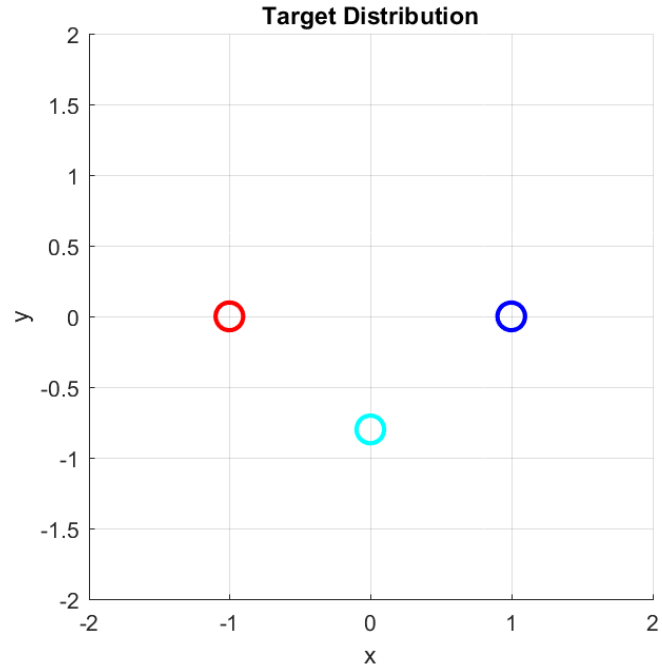
4.4 Discussion and Summary

The proposed approach is a non-trivial extension of Theorem 1, where we addressed the problem of optimal covariance steering under *convex* state chance constraints and cannot deal with *non-convex* state chance constraints. In order to apply covariance steering to path planning problems, a different approach was needed. Deterministic path-planning algorithms typically use Boolean variables to indicate collision with obstacles. As a result, the problem is converted to a mixed-integer programming problem [52]. It is known, however, that this approach typically needs separate integer variables for each face of each obstacle, which leads to a large computational overhead. Here, we employed instead an approach similar to [63, 64], in which integer variables indicate in which sub-region the state variable exists at each time step, leading to a much lower computational cost.

One point we need to stress is that, because we represent the feasible state space as the union of feasible convex sub-regions, the solution may become conservative. Figure 4.21 shows the solution in Fig. 4.9 around $(x, y) = (-6, -1)$ (close to the lower left corner of the middle obstacle). The green areas are the feasible regions, and the red area is the obstacle. The black lines indicate the edges of the sub-regions. The error ellipse touches these boundaries, but it does not touch the corner of the obstacle, which indicates that the path has unnecessarily large safety margin from the obstacle. This extra margin is

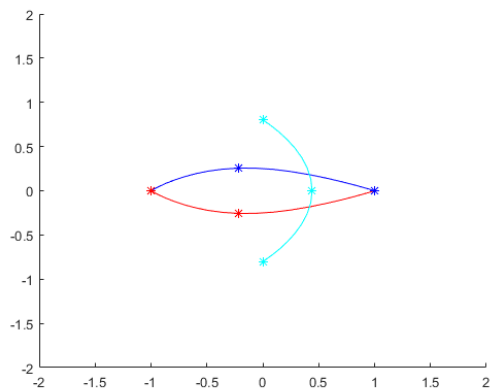


(a) Initial Distributions.

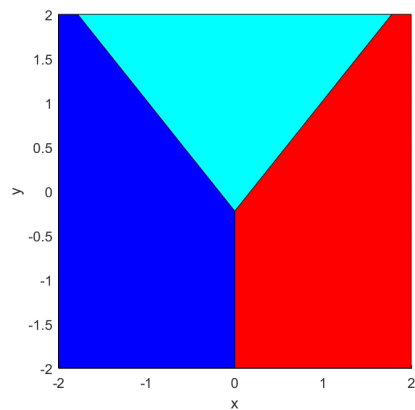


(b) Target Distributions.

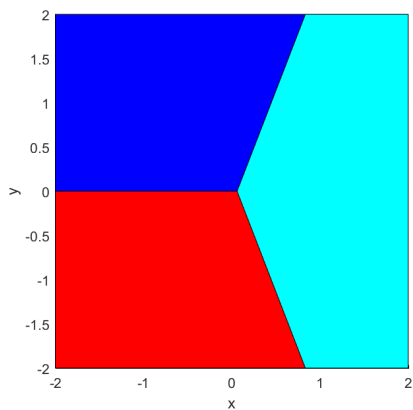
Figure 4.18: Problem setup for two-vehicle path planning.



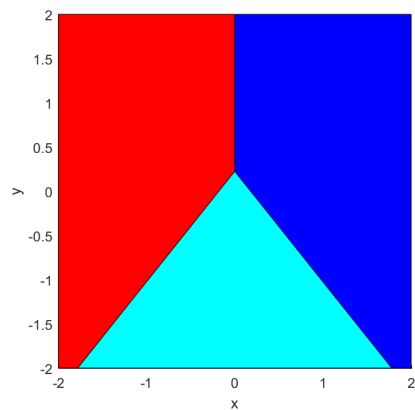
(a) Results of deterministic approach and vehicle positions at time steps $k = 0, N/2$ and N .



(b) Regions 1

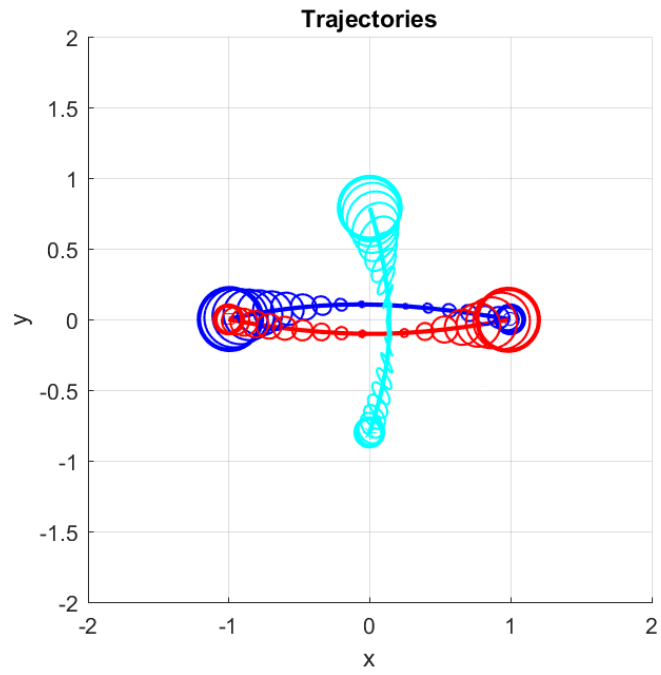


(c) Regions 2.

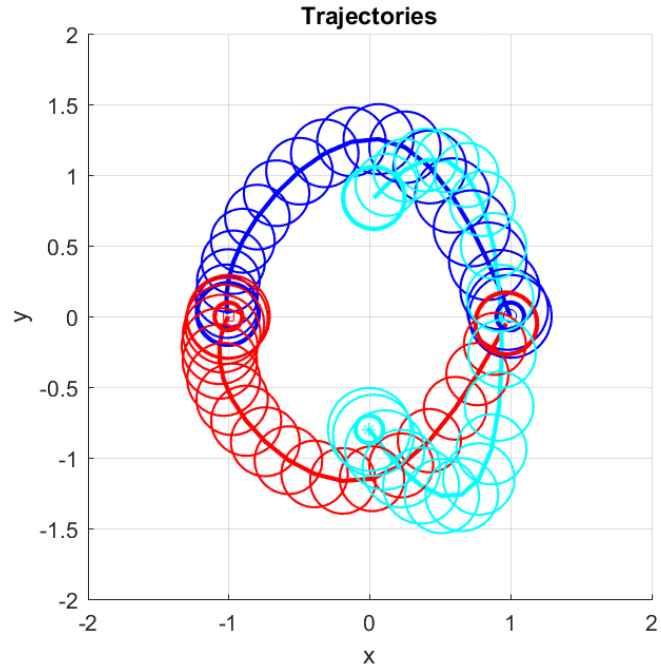


(d) Regions 3.

Figure 4.19: Representation of the feasible region.



(a) Closed loop.



(b) Open loop.

Figure 4.20: Results of two-vehicle collision avoidance using covariance steering.

owing to the requirement that this error ellipse needs to belong to both Regions 1 and 2 (see Fig. 4.11). The decomposition in (4.5) is not unique. In the scenarios we tested, we observed that the performance depends not so much on the number of obstacles, but rather on the way the state space is represented as the union of convex sub-regions. The clearance between obstacles and length of the optimal path does not seem to affect the performance significantly. An interesting question would be to find the “best” decomposition to a union of convex sets for our problem.

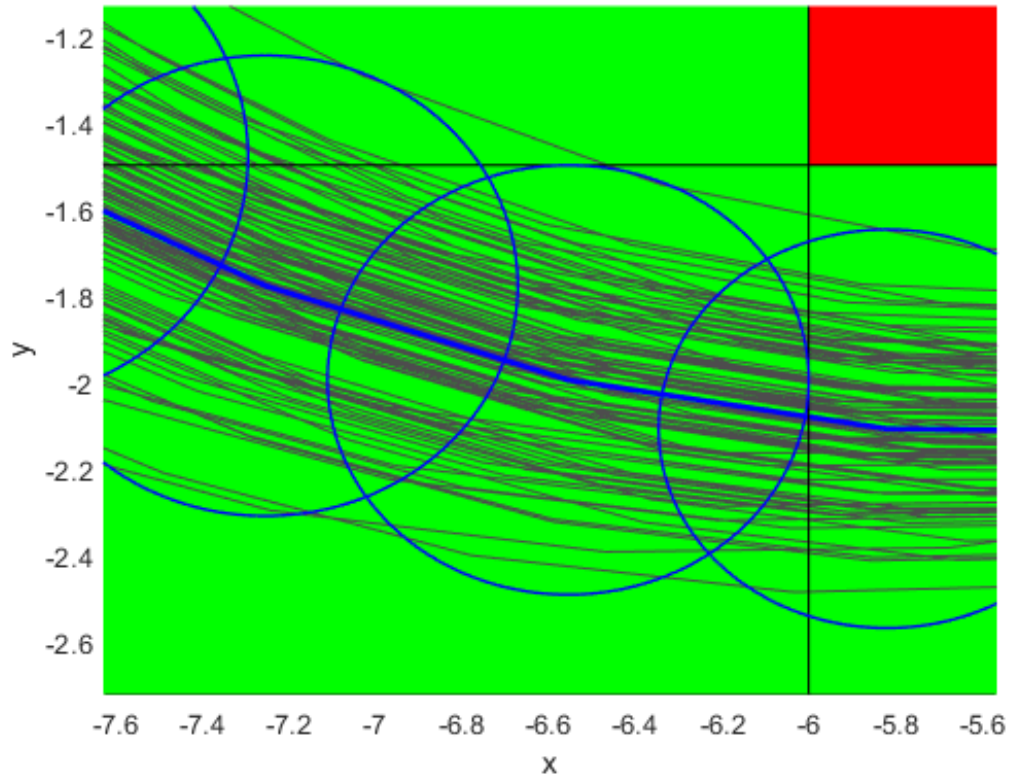


Figure 4.21: Zoom up of the solution illustrated in Fig. 4.10.

In summary, in this chapter, we have addressed the problem of optimal covariance steering under non-convex state chance constraints. We proposed to solve this problem by converting the original problem into a mixed-integer convex programming problem, which can be efficiently solved using an optimization solver. In our numerical simulations, the proposed algorithm successfully found collision-free paths. To the best of our knowledge,

this is the first work to solve the optimal covariance steering problem with non-convex state chance constraints. Future work includes the investigation of an effective approach to separate the feasible state space to a union of convex sets. Also, the application of the covariance steering-based path planning algorithm to belief space planning [58] will be an interesting research topic.

CHAPTER 5

INPUT HARD CONSTRAINED OPTIMAL COVARIANCE STEERING

In this chapter, we investigate the optimal covariance steering theory for systems with input hard constraints. While it is natural to consider probabilistic state chance constraints, i.e., to consider the maximum probability of constraint violation, control constraints are difficult to be formulated probabilistically, because it is hard to interpret what control actions to take when the control command violates the constraints. Thus, for control constraints, hard constraints are preferable. The optimal covariance steering controller we developed in Theorem 1 in Chapter 3 was an affine function of filtered disturbance. It is worth noticing that the control command computed from this approach can be unbounded and thus cannot satisfy input hard constraints. In this chapter, we introduce a covariance steering approach subject to simultaneous state chance and input hard constraints.

The organization of this chapter is as the following. In Section 5.1, we formulate the input-hard constrained optimal covariance steering problem, which is based on the results in Chapter 3. We propose a novel optimal covariance steering controller in Section 5.2 and validate the approach using numerical simulations in Section 5.3. Finally, we provide a brief summary of this chapter in Section 5.4.

5.1 Problem Formulation

This section formulates the input-hard constrained optimal covariance steering problem. We consider the following discrete-time stochastic linear time-varying system with additive uncertainty,

$$x_{k+1} = A_k x_k + B_k u_k + w_k, \quad (5.1)$$

where $x \in \mathbb{R}^{n_x}$ is the state, $u \in \mathbb{R}^{n_u}$ is the control input, and $w \in \mathbb{R}^{n_x}$ is a zero-mean white Gaussian noise with the properties,

$$\mathbb{E}[w_k] = 0, \quad \mathbb{E}[w_{k_1} w_{k_2}^\top] = D_{k_1} D_{k_2}^\top \delta_{k_1, k_2}, \quad (5.2)$$

where δ_{k_1, k_2} is Kronecker's delta function. In addition, A_k , B_k , and D_k are known system matrices having appropriate dimensions. We also assume that the state and control inputs are subject to the constraints

$$x_k \in \mathcal{X}, \quad u_k \in \mathcal{U}, \quad (5.3)$$

for all $k \geq 0$, where $\mathcal{X} \subseteq \mathbb{R}^{n_x}$ and $\mathcal{U} \subseteq \mathbb{R}^{n_u}$ are convex sets. Throughout this chapter, we assume that the sets \mathcal{X} and \mathcal{U} are represented as intersections of linear inequality constraints as follows

$$\mathcal{X} = \bigcap_{i=0}^{N_s-1} \{x : \alpha_{x,i}^\top x \leq \beta_{x,i}\}, \quad (5.4)$$

$$\mathcal{U} = \bigcap_{j=0}^{N_c-1} \{u : \alpha_{u,j}^\top u \leq \beta_{u,j}\}, \quad (5.5)$$

where $\alpha_{x,i} \in \mathbb{R}^{n_x}$ and $\alpha_{u,j} \in \mathbb{R}^{n_u}$ are constant vectors, and $\beta_{x,i} \in \mathbb{R}$ and $\beta_{u,j} \in \mathbb{R}$ are constant scalars. In addition, N_s and N_c denote the number of state and control constraints, respectively. Notice that, since the system noise in (5.1) is possibly unbounded, the state may be unbounded as well. Thus, we formulate the state constraints $x_k \in \mathcal{X}$ probabilistically, as chance constraints, as follows

$$\Pr(x_k \in \mathcal{X}) \geq 1 - \epsilon, \quad k = 0, \dots, N \quad (5.6)$$

where $\epsilon \in [0, 0.5)$. We keep the second set inclusion in (5.3) since for the control inputs, hard constraints are preferable. Using Boole's inequality, (5.4) and (5.6) can be satisfied if

$$\Pr(\alpha_{x,i}^\top x_k > \beta_{x,i}) \leq p_{x,i}, \quad i = 0, \dots, N_s - 1, \quad (5.7)$$

where $p_{x,i}$ are pre-specified such that

$$\sum_{i=0}^{N_s-1} p_{x,i} \leq \epsilon. \quad (5.8)$$

The initial state $x_0 \in \mathbb{R}^{n_x}$ is a random vector that is drawn from a normal distribution according to

$$x_0 \sim \mathcal{N}(\mu_0, \Sigma_0), \quad (5.9)$$

where $\mu_0 \in \mathbb{R}^{n_x}$ and $\Sigma_0 \in \mathbb{R}^{n_x \times n_x}$. We assume that $\Sigma_0 \succeq 0$.

Our objective is to design a control sequence $\{u_0, \dots, u_{N-1}\}$ that steers the system state x_k to a target Gaussian distribution at time step N , that is,

$$x_N \sim \mathcal{N}(\mu_f, \Sigma_f), \quad (5.10)$$

where $\mu_f \in \mathbb{R}^{n_x}$, $\Sigma_f \in \mathbb{R}^{n_x \times n_x}$. We assume that $\Sigma_f \succ 0$ and wish to minimize the following state and control expectation-dependent quadratic cost

$$J(u_0, \dots, u_{N-1}) = \mathbb{E} \left[\sum_{k=0}^{N-1} x_k^\top Q_k x_k + u_k^\top R_k u_k \right], \quad (5.11)$$

where $Q_k \succeq 0$ and $R_k \succ 0$ for $k = 0, \dots, N-1$.

In summary, the following is the problem we solve in this chapter.

Problem 7 (Input Hard Constrained Optimal Covariance Steering).

$$\min J(x, u_0, \dots, u_{N-1}, x_N) = \mathbb{E} \left[\sum_{k=0}^{N-1} x_k^\top Q_k x_k + u_k^\top R_k u_k \right], \quad (5.12a)$$

subject to

$$x_{k+1} = A_k x_k + B_k u_k + w_k, \quad x_0 \sim \mathcal{N}(\mu_0, \Sigma_0), \quad (5.12b)$$

$$\Pr(\alpha_{x,i}^\top x_k > \beta_{x,i}) \leq p_{x,i}, \quad \forall i \in [0, N_s - 1], \quad (5.12c)$$

$$\alpha_{u,j}^\top u_k \leq \beta_{u,j}, \quad \forall j \in [0, N_c - 1], \quad (5.12d)$$

$$x_N = x_f \sim \mathcal{N}(\mu_f, \Sigma_f). \quad (5.12e)$$

Remark 4. It is assumed that system (5.1) is controllable in the absence of constraints and disturbances, that is, x_f is reachable from x_0 for any $x_f \in \mathbb{R}^{n_x}$, provided that $w_k = 0$ for $k = 0, \dots, N - 1$. This assumption implies that given any $x_f \in \mathbb{R}^{n_x}$ and $x_0 \in \mathbb{R}^{n_x}$, there exists a sequence of control inputs $\{u_0, \dots, u_{N-1}\}$ that steers x_0 to x_f in the absence of disturbances or any constraints.

Remark 5. The system dynamics (5.1) looks different from (3.1) in the previous Chapters 3 and 4. It is worth noticing that these two system dynamics are equivalent because of our previous assumption on the noise (3.2). This chapter uses (5.1) with (5.2) because, as we see later in this chapter, it is simpler and easier to describe the proposed approach for input-hard constrained case.

5.2 Proposed Approach

In this section, we propose a novel algorithm that solves Problem 7. Similarly to the approaches in Chapters 3 and 4, we first convert the problem to the following equivalent form.

Problem 8 (Input Hard Constrained Optimal Covariance Steering (Converted)).

$$\min J(X, U) = \mathbb{E} [X^\top \bar{Q} X + U^\top \bar{R} U], \quad (5.13a)$$

subject to

$$X = \mathcal{A}x_0 + \mathcal{B}U + \mathcal{D}W, \quad (5.13b)$$

$$\Pr (\alpha_{x,i}^\top E_k X > \beta_{x,i}) \leq p_{x,i}, \quad (5.13c)$$

$$\alpha_{u,j}^\top F_k U \leq \beta_{u,j}, \quad (5.13d)$$

$$\mu_f = E_N \mathbb{E}[X], \quad (5.13e)$$

$$\Sigma_f = E_N (\mathbb{E}[X X^\top] - \mathbb{E}[X] \mathbb{E}[X]^\top) E_N^\top, \quad (5.13f)$$

where

$$\bar{Q} = \text{blkdiag}(Q_0, \dots, Q_{N-1}, 0) \in \mathbb{R}^{(N+1)n_x \times (N+1)n_x},$$

$$\bar{R} = \text{blkdiag}(R_0, \dots, R_{N-1}) \in \mathbb{R}^{Nn_u \times Nn_u},$$

$$E_k = [0_{n_x, kn_x}, I_{n_x}, 0_{n_x, (N-k)n_x}] \in \mathbb{R}^{n_x \times (N+1)n_x}, \quad k = 0, \dots, N$$

$$F_k = [0_{n_u, kn_u}, I_{n_u}, 0_{n_u, (N-1-k)n_u}] \in \mathbb{R}^{n_u \times Nn_u}, \quad k = 0, \dots, N-1,$$

such that $x_k = E_k X$ and $u_k = F_k U$. In addition, the matrices $\mathcal{A} \in \mathbb{R}^{(N+1)n_x \times n_x}$,

$\mathcal{B} \in \mathbb{R}^{(N+1)n_x \times Nn_u}$, and $\mathcal{D} \in \mathbb{R}^{(N+1)n_x \times Nn_x}$ are defined accordingly.

Note that

$$\mathbb{E}[x_0 x_0^\top] = \Sigma_0 + \mu_0 \mu_0^\top, \quad (5.14a)$$

$$\mathbb{E}[x_0 W^\top] = 0, \quad (5.14b)$$

$$\mathbb{E}[W W^\top] = \begin{bmatrix} D_0 D_0^\top & & \\ & \ddots & \\ & & D_{N-1} D_{N-1}^\top \end{bmatrix} \triangleq \Sigma_W. \quad (5.14c)$$

Notice that terminal covariance equality constraint (5.13f) is non-convex. Thus, similarly to the previous chapters, we relax (5.13f) and instead, solve the following problem.

Problem 9 (Relaxed Input Hard Constrained Optimal Covariance Steering).

$$\min J(X, U) = \mathbb{E} [X^\top \bar{Q} X + U^\top \bar{R} U], \quad (5.15a)$$

subject to

$$X = \mathcal{A}x_0 + \mathcal{B}U + \mathcal{D}W, \quad (5.15b)$$

$$\Pr (\alpha_{x,i}^\top E_k X > \beta_{x,i}) \leq p_{x,i}, \quad (5.15c)$$

$$\alpha_{u,j}^\top F_k U \leq \beta_{u,j}, \quad (5.15d)$$

$$\mu_f = E_N \mathbb{E}[X], \quad (5.15e)$$

$$\Sigma_f \succeq E_N (\mathbb{E}[X X^\top] - \mathbb{E}[X] \mathbb{E}[X]^\top) E_N^\top. \quad (5.15f)$$

In order to solve Problem 9, we propose a novel control policy that is summarized in the following theorem, which is the main result of this chapter. This control policy is a nontrivial extension of the approach in Theorem 1 and is inspired from the approach in [68, 69]

Theorem 2. *The following control law*

$$u_k = v_k + K_k z_k, \quad (5.16)$$

where z_k is governed by the following dynamics

$$z_{k+1} = Az_k + \varphi(w_k), \quad (5.17a)$$

$$z_0 = \varphi(\zeta_0), \quad \zeta_0 = x_0 - \mu_0, \quad (5.17b)$$

where $\varphi(\cdot) : \mathbb{R}^d \mapsto \mathbb{R}^d$ is an element-wise symmetric saturation function, the s th entry of which is

$$\varphi_s(\zeta_s) = \max(-\zeta_s^{\max}, \min(\zeta_s, \zeta_s^{\max})), \quad (5.18)$$

where $\zeta_s^{\max} > 0$ is a predetermined value, converts Problem 9 to the following Problem 10.

Problem 10 (Input Hard Constrained OCS Problem).

$$\begin{aligned} \min J(V, K, \Omega) = & \operatorname{tr} \left(\bar{Q} \begin{bmatrix} I & \mathcal{B}K \end{bmatrix} \Sigma_{XX} \begin{bmatrix} I \\ K^\top \mathcal{B}^\top \end{bmatrix} \right) + \operatorname{tr}(\bar{R}K\Sigma_{UU}K^\top) \\ & + (\mathcal{A}\mu_0 + \mathcal{B}V)^\top \bar{Q}(\mathcal{A}\mu_0 + \mathcal{B}V) + V^\top \bar{R}V \end{aligned} \quad (5.19a)$$

subject to

$$\alpha_{x,i}^\top E_k(\mathcal{A}\mu_0 + \mathcal{B}V) - \beta_{x,i} + \sqrt{\frac{1-p_{x,i}}{p_{x,i}}} \left| S_{XX}^\top \begin{bmatrix} I & \mathcal{B}K \end{bmatrix}^\top E_k^\top \alpha_{x,i} \right| \leq 0, \quad (5.19b)$$

$$HF_k V + \Omega^\top \sigma \leq h, \quad (5.19c)$$

$$HF_k K[\mathcal{A} \mathcal{D}] = \Omega^\top S, \quad (5.19d)$$

$$\Omega \geq 0, \quad (5.19e)$$

$$\mu_f = E_N(\mathcal{A}\mu_0 + \mathcal{B}V), \quad (5.19f)$$

$$\Sigma_f \succeq E_N \begin{bmatrix} I & \mathcal{B}K \end{bmatrix} \Sigma_{XX} \begin{bmatrix} I \\ K^\top \mathcal{B}^\top \end{bmatrix} E_N^\top, \quad (5.19g)$$

where $\Omega \in \mathbb{R}^{2(N+1)n_x \times N_c}$ is a decision (slack) variable,

$$\begin{aligned} \Sigma_{XX} = & \begin{bmatrix} \mathcal{A} \\ \mathcal{A} \end{bmatrix} \begin{bmatrix} \Sigma_0 & \mathbb{E}[\zeta_0 \varphi(\zeta_0)^\top] \\ \mathbb{E}[\varphi(\zeta_0) \zeta_0^\top] & \mathbb{E}[\varphi(\zeta_0) \varphi(\zeta_0)^\top] \end{bmatrix} \begin{bmatrix} \mathcal{A}^\top \\ \mathcal{A}^\top \end{bmatrix} \\ & + \begin{bmatrix} \mathcal{D} \\ \mathcal{D} \end{bmatrix} \begin{bmatrix} \Sigma_W & \mathbb{E}[W \varphi(W)^\top] \\ \mathbb{E}[\varphi(W) W^\top] & \mathbb{E}[\varphi(W) \varphi(W)^\top] \end{bmatrix} \begin{bmatrix} \mathcal{D}^\top \\ \mathcal{D}^\top \end{bmatrix}, \end{aligned} \quad (5.20)$$

$$S_{XX} S_{XX}^\top = \Sigma_{XX}, \quad (5.21)$$

$$\Sigma_{UU} = \mathcal{A} \mathbb{E}[\varphi(\zeta_0) \varphi(\zeta_0)^\top] \mathcal{A}^\top + \mathcal{D} \mathbb{E}[\varphi(W) \varphi(W)^\top] \mathcal{D}^\top, \quad (5.22)$$

and

$$H = \begin{bmatrix} \alpha_{u,0}^\top \\ \vdots \\ \alpha_{u,N_c-1}^\top \end{bmatrix} \in \mathbb{R}^{N_c \times n_u}, \quad h = \begin{bmatrix} \beta_{u,0} \\ \vdots \\ \beta_{u,N_c-1} \end{bmatrix} \in \mathbb{R}^{N_c}, \quad (5.23)$$

and

$$V = \begin{bmatrix} v_0 \\ \vdots \\ v_{N-1} \end{bmatrix}, \quad K = \begin{bmatrix} K_0 & & & 0 \\ & K_1 & & 0 \\ & & \ddots & 0 \\ & & & K_{N-1} & 0 \end{bmatrix}.$$

In addition, $S \in \mathbb{R}^{2(N+1)n_x \times (N+1)n_x}$ and $\sigma \in \mathbb{R}^{2(N+1)n_x}$ are constant. Specifically, for $i = 1, \dots, (N+1)n_x$

$$S_{2i-1} = e_{2i-1}^\top, \quad S_{2i} = -e_{2i}^\top, \quad (5.24a)$$

$$\sigma_{2i-1} = \zeta_i^{\max}, \quad \sigma_{2i} = \zeta_i^{\max}. \quad (5.24b)$$

where S_i denotes the i th row of S , and $e_i \in \mathbb{R}^{2(N+1)n_x}$ is a unit vector with i th element 1.

Proof. It follows from (5.17a) and (5.17b) that

$$Z = \mathcal{A}\varphi(\zeta_0) + \mathcal{D}\varphi(W), \quad (5.25)$$

where

$$Z = \begin{bmatrix} z_0 \\ \vdots \\ z_N \end{bmatrix} \in \mathbb{R}^{(N+1)n_x}, \quad (5.26)$$

In addition, the concatenated control sequence vector U is represented as

$$U = V + KZ, \quad (5.27)$$

and thus,

$$U = V + K(\mathcal{A}\varphi(\zeta_0) + \mathcal{D}\varphi(W)). \quad (5.28)$$

Since the saturation function (5.18) is an odd function and ζ_0 is zero-mean Gaussian distributed, the following holds

$$\begin{aligned} \mathbb{E}[\varphi(\zeta_0)] &= \int_{-\infty}^{\infty} \varphi(\zeta) \rho(\zeta) d\zeta, \\ &= \int_{-\infty}^0 \varphi(\zeta) \rho(\zeta) d\zeta + \int_0^{\infty} \varphi(\zeta) \rho(\zeta) d\zeta, \\ &= \int_0^{\infty} (-\varphi(\zeta)) \rho(\zeta) d\zeta + \int_0^{\infty} \varphi(\zeta) \rho(\zeta) d\zeta \\ &= 0, \end{aligned}$$

where $\rho(\zeta)$ denotes the Gaussian probability distribution function. Similarly,

$$\mathbb{E}[\varphi(W)] = 0, \quad (5.29)$$

and hence,

$$\mathbb{E}[U] = V, \quad \tilde{U} = U - \mathbb{E}[U] = K(\mathcal{A}\varphi(\zeta_0) + \mathcal{D}\varphi(W)).$$

Thus,

$$\bar{X} = \mathbb{E}[X] = \mathcal{A}\mu_0 + \mathcal{B}V, \quad (5.30)$$

$$\begin{aligned} \tilde{X} &= X - \mathbb{E}[X] \\ &= \mathcal{A}(x_0 - \mu_0) + \mathcal{B}(U - V) + \mathcal{D}W, \\ &= \mathcal{A}\zeta_0 + \mathcal{D}W + \mathcal{B}K(\mathcal{A}\varphi(\zeta_0) + \mathcal{D}\varphi(W)), \\ &= \begin{bmatrix} I & \mathcal{B}K \end{bmatrix} \left(\begin{bmatrix} \mathcal{A} \\ \mathcal{A} \end{bmatrix} \begin{bmatrix} \zeta_0 \\ \varphi(\zeta_0) \end{bmatrix} + \begin{bmatrix} \mathcal{D} \\ \mathcal{D} \end{bmatrix} \begin{bmatrix} W \\ \varphi(W) \end{bmatrix} \right). \end{aligned} \quad (5.31)$$

It also follows from (5.14), (5.17b), (5.20), and (5.22) that

$$\mathbb{E}[\tilde{X}\tilde{X}^\top] = \begin{bmatrix} I & \mathcal{B}K \end{bmatrix} \Sigma_{XX} \begin{bmatrix} I \\ K^\top \mathcal{B}^\top \end{bmatrix}, \quad (5.32)$$

$$\mathbb{E}[\tilde{U}\tilde{U}^\top] = K\Sigma_{UU}K^\top. \quad (5.33)$$

Following the discussion in Chapter 3, it can be shown that the cost function (5.15a) may be written as

$$J(V, \tilde{U}) = \text{tr}(\bar{Q}\mathbb{E}[\tilde{X}\tilde{X}^\top]) + \bar{X}^\top \bar{Q} \bar{X} + \text{tr}(\bar{R}\mathbb{E}[\tilde{U}\tilde{U}^\top]) + V^\top \bar{R}V. \quad (5.34)$$

Using (5.30), (5.32), and (5.33), we can further convert (5.34) into

$$J(V, K) = \text{tr} \left(\bar{Q} \begin{bmatrix} I & \mathcal{B}K \end{bmatrix} \Sigma_{XX} \begin{bmatrix} I \\ K^\top \mathcal{B}^\top \end{bmatrix} \right) \\ + (\mathcal{A}\mu_0 + \mathcal{B}V)^\top \bar{Q} (\mathcal{A}\mu_0 + \mathcal{B}V) + \text{tr} (\bar{R}K \Sigma_{UU} K^\top) + V^\top \bar{R}V. \quad (5.35)$$

In addition, using (5.30) and (5.32), the terminal state constraints can be written as

$$\mu_f = E_N (\mathcal{A}\mu_0 + \mathcal{B}V), \quad (5.36a)$$

$$\Sigma_f \succeq E_N \begin{bmatrix} I & \mathcal{B}K \end{bmatrix} \Sigma_{XX} \begin{bmatrix} I \\ K^\top \mathcal{B}^\top \end{bmatrix} E_N^\top. \quad (5.36b)$$

Using the Schur complement, (5.36b) can be further converted to

$$\begin{bmatrix} \Sigma_f & E_N \begin{bmatrix} I & \mathcal{B}K \end{bmatrix} S_{XX} \\ S_{XX}^\top \begin{bmatrix} I & \mathcal{B}K \end{bmatrix}^\top E_N^\top & I \end{bmatrix} \succeq 0.$$

Note that according to Lemma 4 in the Appendix, Σ_{XX} is positive semidefinite.

The state chance constraint (5.15c) can be formulated as follows. First, notice that $\alpha_j^\top E_k X$ is a univariate random variable with mean $\alpha_{x,i}^\top E_k \mathbb{E}[X]$ and variance $\alpha_{x,i}^\top E_k \mathbb{E}[\tilde{X} \tilde{X}^\top] E_k^\top \alpha_{x,i}$. It follows from the Chebyshev-Cantelli inequality (Lemma 5 in the Appendix) that

$$\Pr \left(\alpha_{x,i}^\top E_k X \leq \alpha_{x,i}^\top E_k \mathbb{E}[X] + \sqrt{\frac{1 - p_{x,i}}{p_{x,i}}} \sqrt{\alpha_{x,i}^\top E_k \mathbb{E}[\tilde{X} \tilde{X}^\top] E_k^\top \alpha_{x,i}} \right) > 1 - p_{x,i}.$$

Therefore, the inequality (5.15c) is satisfied if

$$\alpha_{x,i}^\top E_k \mathbb{E}[X] + \sqrt{\frac{1 - p_{x,i}}{p_{x,i}}} \sqrt{\alpha_{x,i}^\top E_k \mathbb{E}[\tilde{X} \tilde{X}^\top] E_k^\top \alpha_{x,i}} \leq \beta_{x,i},$$

is satisfied, which is, from (5.30) and (5.31), equivalent to a second order cone constraint

in terms of V and K (5.19b).

Finally, we rewrite the input hard constraint (5.15d) as follows. Using (5.23), we first rewrite (5.15d) to the following equivalent form

$$HF_k U \leq h. \quad (5.37)$$

Then, using (5.28), this inequality is further converted to

$$HF_k (V + K (\mathcal{A}\varphi(\zeta_0) + \mathcal{D}\varphi(W))) \leq h, \quad (5.38)$$

and thus,

$$HF_k V + HF_k K \begin{bmatrix} \mathcal{A} & \mathcal{D} \end{bmatrix} \begin{bmatrix} \varphi(\zeta_0) \\ \varphi(W) \end{bmatrix} \leq h. \quad (5.39)$$

In addition, using (5.24), the condition (5.18) can be represented as

$$S \begin{bmatrix} \varphi(\zeta_0) \\ \varphi(W) \end{bmatrix} \leq \sigma. \quad (5.40)$$

It follows from the discussion in [68] that the constraint (5.39) can be converted to

$$HF_k V + \Omega^\top \sigma \leq h, \quad (5.41a)$$

$$HF_k K [\mathcal{A} \mathcal{D}] = \Omega^\top S, \quad (5.41b)$$

$$\Omega \geq 0, \quad (5.41c)$$

where $\Omega \in \mathbb{R}^{2(N+1)n_x \times N_c}$ is a design variable. In summary, we have converted Problem (9) to Problem (10). \square

Note that the values of $\mathbb{E}[\zeta_0 \varphi(\zeta_0)^\top]$, $\mathbb{E}[\varphi(\zeta_0) \varphi(\zeta_0)^\top]$, $\mathbb{E}[W \varphi(W)^\top]$, and $\mathbb{E}[\varphi(W) \varphi(W)^\top]$ can be obtained using Monte Carlo or Lemma 3 in the Appendix.

Remark 6. When designing u_k in (5.16), the value of z_k can be obtained from z_{k-1} and $\varphi(w_{k-1})$. The noise w_{k-1} is obtained from the system dynamics (5.1), i.e.,

$$w_{k-1} = x_k - A_{k-1}x_{k-1} - B_{k-1}u_{k-1}, \quad (5.42)$$

and thus, $\varphi(w_{k-1})$ can be computed before computing the value of u_k at time step k .

5.3 Numerical Simulation

In this section we validate the proposed algorithm using a numerical example. We consider the same path-planning problem for a vehicle under the double integrator time-invariant dynamics in Section 3.4 in Chapter 3. The feasible state space is

$$0.2(x - 1) \leq y \leq -0.2(x - 1).$$

The mean and the covariance of the initial and target terminal distributions are set to

$$\begin{aligned} \mu_0 &= [-10, 1, 0, 0], \quad \Sigma_0 = \text{diag}(0.05, 0.05, 0.01, 0.01), \\ \mu_f &= [0, 0, 0, 0], \quad \Sigma_f = \text{diag}(0.025, 0.025, 0.005, 0.005). \end{aligned}$$

The cost function weights are chosen as

$$Q = \text{diag}(0.5, 4.0, 0.05, 0.05), \quad R = \text{diag}(20, 20).$$

The horizon is set to $N = 20$ and the probability threshold to $p_{x,i} = 0.05$ for $i = 0, 1$.

Finally, we restrict the maximum acceleration at $U_{\max} = 2.9 \text{ m/s}^2$ along each axis, i.e.,

$$\|u_k\|_{\infty} \leq U_{\max}, \quad (5.43)$$

for $k = 0, \dots, N - 1$. We also set the saturation function (5.18) to be saturated when the input exceeds the 3σ values. We employ YALMIP [111] to model the problem and the MOSEK [112] solver for the relevant optimization problems.

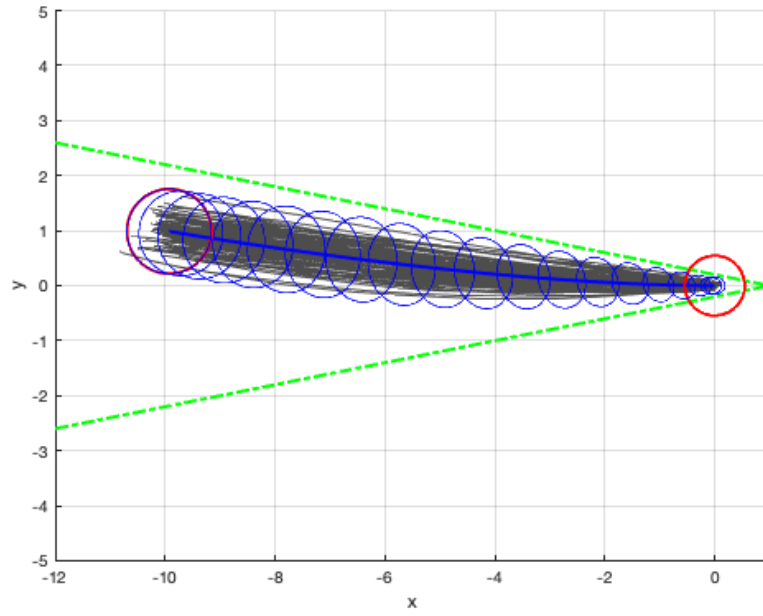
We first show the results when the controller from Chapter 3 is used. Figure 5.1 illustrates the results. The trajectories are depicted in Fig. 5.1(a), and they satisfy the state chance constraints. However, the controller cannot deal with input hard constraints, and as shown in Fig. 5.1(b), the acceleration value violates the constraint (5.43). The cost for this scenario is 2,285.

Next, we show the results when the newly developed optimal covariance steering controller in Theorem 2 is used. Figure 5.2 depicts the results. As shown in Fig. 5.2(a), state chance constraints are satisfied, and, unlike the control profiles in Fig. 5.1(b), the control profiles depicted in Fig. 5.2(a) satisfy the input hard constraint (5.43). The cost for this constrained scenario is 2,301, which is, as expected, a bit larger than the cost for the unconstrained case owing to the additional input constraint.

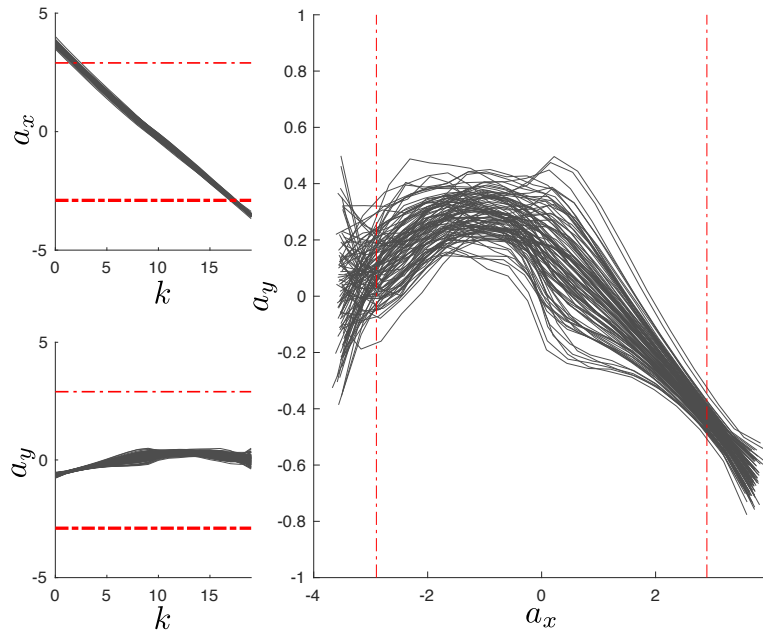
5.4 Summary

In this chapter, we have developed a novel optimal covariance steering controller that can deal with state chance constraints and input hard constraints. Similarly to the approaches in the previous chapters, we converted the original OCS problem to a convex programming problem. The input hard constraints are formulated using saturation functions to limit the effect of possibly unbounded disturbance. In our numerical simulations, the proposed algorithm successfully found the optimal paths while satisfying the input constraints.

Future work includes the application of the algorithm to more complex systems such as the Mars powered descent guidance and self-driving vehicle control problems. In addition, extending the framework to time-varying environment is also an interesting research topic.

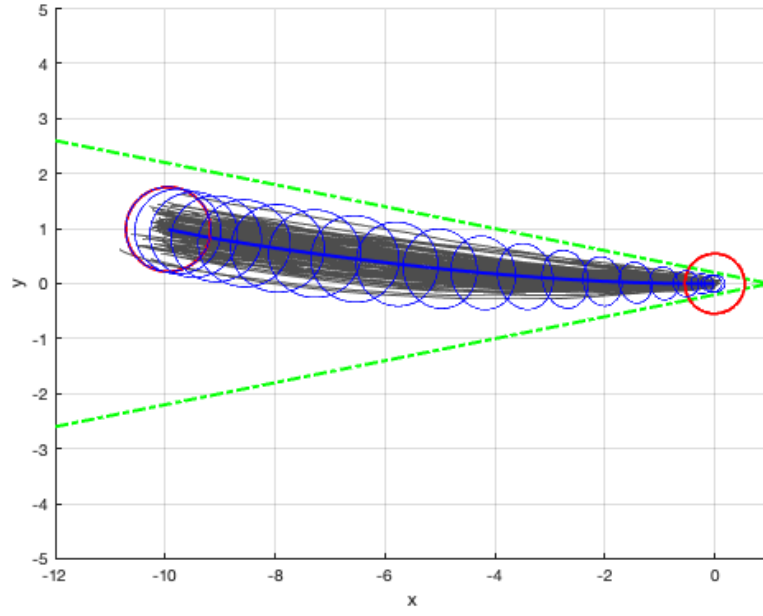


(a) Trajectory.

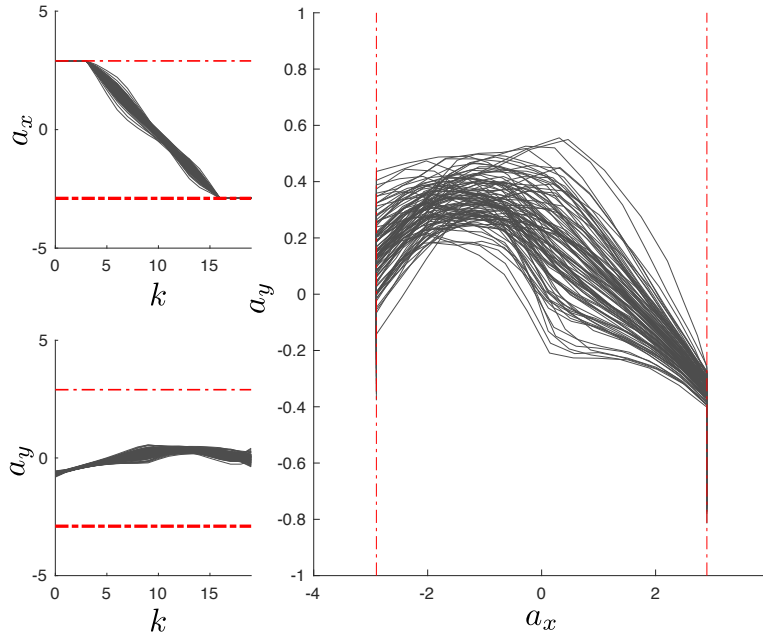


(b) Input accelerations from Monte Carlo simulation with randomly selected 100 samples. Red dashed lines indicate $\pm 2.9\text{m/s}^2$

Figure 5.1: Results when input is constraint free.



(a) Trajectory.



(b) Input accelerations from Monte Carlo simulation with randomly selected 100 samples. Red dashed lines indicate the acceleration bounds $\pm 2.9 \text{ m/s}^2$.

Figure 5.2: Results when input constraints are imposed.

CHAPTER 6

STOCHASTIC MODEL PREDICTIVE CONTROL USING OPTIMAL COVARIANCE STEERING

In this chapter, we develop the optimal covariance steering-based stochastic model predictive control (CS-SMPC) theory for stochastic linear time-invariant (LTI) systems with additive Gaussian noise subject to probabilistic state and control constraints. In addition to the conventional terminal cost and terminal mean constraints, we introduce terminal covariance constraints in the stochastic model predictive control theory. The optimal covariance steering theory efficiently computes the control commands that satisfy the terminal covariance constraints.

In Section 6.1, we formulate the CS-SMPC problem followed by the introduction of some mathematical preliminaries in Section 6.2. In Section 6.3 we introduce the proposed CS-SMPC approach and prove stability and recursive feasibility of the closed-loop system. The effectiveness of the proposed approach is demonstrated with a simple two-dimensional dynamics and an self-driving vehicle control examples in Section 6.4. Finally, Section 6.5 provides a brief summary of the proposed CS-SMPC approach.

6.1 Problem Statement

In this section we formulate the general SMPC problem and introduce the necessary mathematical preliminaries along with the optimal covariance steering background theory used in the proposed approach.

In this chapter, $\mathbb{E}_k[\cdot] = \mathbb{E}[\cdot|x_k]$ denotes the expectation conditioned on the measured state x_k at time step k . In addition, $\Pr_k(\cdot) = \Pr(\cdot|x_k)$ denotes the conditional probability given x_k .

6.1.1 Problem Formulation

We consider the following discrete-time stochastic linear time-invariant (LTI) system with additive noise,

$$x_{k+1} = Ax_k + Bu_k + Dw_k, \quad (6.1)$$

where k is the time-step index, $x \in \mathbb{R}^{n_x}$ is the state, $u \in \mathbb{R}^{n_u}$ is the control input, and $w \in \mathbb{R}^{n_w}$ is a zero-mean independently and identically distributed (i.i.d.) Gaussian noise. In addition, $A \in \mathbb{R}^{n_x \times n_x}$, $B \in \mathbb{R}^{n_x \times n_u}$, and $D \in \mathbb{R}^{n_x \times n_w}$ are system matrices. The noise w_k has the following properties,

$$\mathbb{E}[w_k] = 0, \quad \mathbb{E}[w_{k_1} w_{k_2}^\top] = I_{n_w} \delta_{k_1, k_2}, \quad (6.2)$$

where δ_{k_1, k_2} is the Kronecker delta function. Note that the previous assumption is not stringent because the covariance of the added disturbance is DD^\top , which we can be tuned based on observations of the real-world system. In addition, the following holds

$$\mathbb{E}[x_{k_1} w_{k_2}^\top] = 0, \quad 0 \leq k_1 \leq k_2, \quad (6.3)$$

which stems from causality considerations.

Furthermore, it is assumed that the state and control inputs are subject to the constraints

$$x_k \in \mathcal{X}, \quad u_k \in \mathcal{U}, \quad (6.4)$$

for all $k \geq 0$, where $\mathcal{X} \subseteq \mathbb{R}^{n_x}$ and $\mathcal{U} \subseteq \mathbb{R}^{n_u}$ are convex sets containing the origin. Throughout this chapter, we assume that the sets \mathcal{X} and \mathcal{U} are convex polytopes, represented as the

intersection of a finite number of linear inequality constraints as follows

$$\mathcal{X} = \bigcap_{i=0}^{N_s-1} \{x : \alpha_{x,i}^\top x \leq \beta_{x,i}\}, \quad (6.5)$$

$$\mathcal{U} = \bigcap_{j=0}^{N_c-1} \{u : \alpha_{u,j}^\top u \leq \beta_{u,j}\}, \quad (6.6)$$

where $\alpha_{x,i} \in \mathbb{R}^{n_x}$ and $\alpha_{u,j} \in \mathbb{R}^{n_u}$ are constant vectors, and $\beta_{x,i} \in \mathbb{R}$ and $\beta_{u,j} \in \mathbb{R}$ are constant scalars. In (6.5) and (6.6), N_s and N_c denote the number of state and control constraints defining the polytopes, respectively. Notice that, since the system noise w is possibly unbounded, the state may be unbounded as well. Thus, we formulate the state constraints $x_k \in \mathcal{X}$ probabilistically, as chance constraints

$$\Pr(x_k \in \mathcal{X}) \geq 1 - \epsilon_x, \quad (6.7)$$

where $\epsilon_x \geq 0$ is the maximum probability of constraint violation. In this chapter we restrict the range of ϵ_x to the interval $\epsilon_x \in [0, 0.5)$. Using Boole's inequality [109], (6.5) and (6.7) can be satisfied, assuming

$$\Pr(\alpha_{x,i}^\top x_k \leq \beta_{x,i}) \geq 1 - p_{x,i}, \quad (6.8)$$

for all $i = 0, \dots, N_s - 1$, where $p_{x,i}$ are such that

$$\sum_{i=0}^{N_s-1} p_{x,i} \leq \epsilon_x, \quad (6.9)$$

where $p_{x,i} \in [0, 0.5)$ for all $i = 0, \dots, N_s - 1$. Similarly, by replacing the second inclusion in (6.4) with the chance constraint

$$\Pr(u_k \in \mathcal{U}) \geq 1 - \epsilon_u, \quad (6.10)$$

where $\epsilon_u \in [0, 0.5)$, and along with (6.6), we impose the following conditions

$$\Pr(\alpha_{u,j}^\top u_k \leq \beta_{u,j}) \geq 1 - p_{u,j}, \quad (6.11)$$

$$\sum_{j=0}^{N_c-1} p_{u,j} \leq \epsilon_u, \quad (6.12)$$

where $p_{u,j} \in [0, 0.5)$ for all $j = 0, \dots, N_c - 1$. Finally, we assume perfect state information and ignore the measurement noise, and thus

$$\begin{aligned} \mathbb{E}[x_0] &= x_0, \\ \Sigma_0 &= 0. \end{aligned} \quad (6.13)$$

Our objective is to design a control sequence $\{u_0, u_1, \dots\}$ that minimizes the following infinite horizon optimal control problem with state and control expectation-dependent quadratic cost.

$$\min_{u_0, u_1, \dots} J_\infty(x_0; u_0, u_1, \dots) = \mathbb{E} \left[\sum_{k=0}^{\infty} x_k^\top Q x_k + u_k^\top R u_k \right], \quad (6.14a)$$

subject to

$$x_{k+1} = Ax_k + Bu_k + Dw_k, \quad (6.14b)$$

$$\Pr(\alpha_{x,i}^\top x_k \leq \beta_{x,i}) \geq 1 - p_{x,i}, \quad i = 0, \dots, N_s - 1, \quad (6.14c)$$

$$\Pr(\alpha_{u,j}^\top u_k \leq \beta_{u,j}) \geq 1 - p_{u,j}, \quad j = 0, \dots, N_c - 1, \quad (6.14d)$$

where $Q \succeq 0$ and $R \succ 0$.

Remark 7. It is worth noticing that, as discussed in [115, 68], SMPC with input hard constraints is not possible if the disturbance is unbounded and the system is not Schur stable [98] nor Lyapunov stable [99]. Therefore, we use input chance constraints here, as indicated in (6.14d).

6.1.2 SMPC Formulation

The SMPC aims to solve the infinite-horizon optimal control problem (6.14) by solving, at each time step k , the following *finite* horizon optimal control problem, instead.

$$\min_{u_{k|k}, \dots, u_{k+N-1|k}} J_N(\mu_k, \Sigma_k; u_{k|k}, \dots, u_{k+N-1|k}) = \mathbb{E}_k \left[\sum_{t=k}^{k+N-1} x_{t|k}^\top Q x_{t|k} + u_{t|k}^\top R u_{t|k} \right] + J_f(x_{k+N|k}), \quad (6.15a)$$

subject to

$$x_{t+1|k} = Ax_{t|k} + Bu_{t|k} + Dw_t, \quad x_{k|k} = x_k \sim \mathcal{N}(\mu_k, \Sigma_k), \quad (6.15b)$$

$$\Pr_k(\alpha_{x,i}^\top x_{t|k} \leq \beta_{x,i}) \geq 1 - p_{x,i}, \quad i = 0, \dots, N_s - 1, \quad (6.15c)$$

$$\Pr_k(\alpha_{u,j}^\top u_{t|k} \leq \beta_{u,j}) \geq 1 - p_{u,j}, \quad j = 0, \dots, N_c - 1, \quad (6.15d)$$

where $t = k, \dots, k + N - 1$ and N is the horizon.

The notation $x_{t|k}$ denotes the state at time step t predicted at time step $k \geq 0$ where $t \geq k$. The variables μ_k and Σ_k in (6.15b)) are the mean and the covariance of the state x_k , and assumed to be given at step k .

We denote the optimal solution to (6.15) as $\{u_{k|k}^*, \dots, u_{k+N-1|k}^*\}$. At time step k , we apply $u_{k|k}^*$ to the system (6.1), i.e., $u_k = u_{k|k}^*$. Then, at time step $k + 1$, we solve the finite horizon optimal control problem (6.15) again, with the new initial condition

$$x_{k+1|k+1} = x_{k+1} = Ax_k + Bu_{k|k}^* + Dw_k, \quad (6.16)$$

which leads to a receding horizon control strategy that solves the original infinite horizon optimal control problem (6.14). The function $J_f(\cdot) : \mathbb{R}^{n_x} \mapsto \mathbb{R}$ is a terminal cost that needs to be designed properly to ensure stability [74]. In this chapter, we show that optimal covariance steering theory helps us choose an appropriate expression for $J_f(\cdot)$ and solves

Problem (6.15) efficiently and robustly.

6.2 Mathematical Preliminaries of Optimal Covariance Steering

In this section, we introduce the basic theory behind optimal covariance steering controller design under state and control chance constraints, which will be applied to solve the SMPC problem. In the discrete-time optimal covariance steering problem setup, we wish to steer the state distribution of system (6.1) from an initial Gaussian distribution

$$x_0 \sim \mathcal{N}(\mu_0, \Sigma_0), \quad (6.17)$$

to a prescribed Gaussian distribution at a given time step N , i.e.,

$$x_N = x_f \sim \mathcal{N}(\mu_f, \Sigma_f). \quad (6.18)$$

Specifically, given an initial distribution (6.17), we wish to solve the following optimization problem.

$$\min_{u_0, \dots, u_{N-1}} J(u_0, \dots, u_{N-1}) = \mathbb{E} \left[\sum_{k=0}^{N-1} x_k^\top Q x_k + u_k^\top R u_k \right], \quad (6.19a)$$

subject to

$$x_{k+1} = Ax_k + Bu_k + Dw_k, \quad x_0 \sim \mathcal{N}(\mu_0, \Sigma_0) \quad (6.19b)$$

$$\Pr(\alpha_{x,i}^\top x_k \leq \beta_{x,i}) \geq 1 - p_{x,i}, \quad i = 0, \dots, N_s - 1, \quad (6.19c)$$

$$\Pr(\alpha_{u,j}^\top u_k \leq \beta_{u,j}) \geq 1 - p_{u,j}, \quad j = 0, \dots, N_c - 1, \quad (6.19d)$$

$$x_N = x_f \sim \mathcal{N}(\mu_f, \Sigma_f), \quad (6.19e)$$

for $k = 0, \dots, N - 1$, where we assume that $\Sigma_0 \succeq 0$ and $\Sigma_f \succ 0$. In addition, w_k , $p_{x,i}$, and $p_{u,j}$ are as in Chapter (6.2), (6.9), and (6.12) respectively.

Henceforth, we make the following assumptions.

Assumption 1. *The pair (A, B) in (6.1) is controllable.*

Assumption 2. *All control channels are corrupted by noise, that is, $\mathcal{R}(B) \subseteq \mathcal{R}(D)$. This assumption along with Assumption 1 ensures that the pair (A, D) is controllable.*

Assumption 3. *The horizon $N \geq n_x$. This assumption implies that the N -step reachability matrix*

$$\begin{bmatrix} A^{N-1}D & A^{N-2}D & \dots & AD & D \end{bmatrix}. \quad (6.20)$$

is full row rank. Thus, along with Assumption 1, ensures that x_f is reachable from x_0 for any $x_f \in \mathbb{R}^{n_x}$, provided that $w_k = 0$ for $k = 0, \dots, N-1$ with no state and control constraints. This assumption implies that, given any $x_f \in \mathbb{R}^{n_x}$ and $x_0 \in \mathbb{R}^{n_x}$, there exists a sequence of control inputs $\{u_0, \dots, u_{N-1}\}$ that steers x_0 to x_f in the absence of disturbances or any constraints.

In order to proceed, we need the following lemma.

Lemma 2. *One can derive the following equivalent form of Problem (6.19).*

$$\min_U J(U) = \mathbb{E} [X^\top \bar{Q} X + U^\top \bar{R} U], \quad (6.21a)$$

subject to

$$X = \mathcal{A}x_0 + \mathcal{B}U + \mathcal{D}W, \quad x_0 \sim \mathcal{N}(\mu_0, \Sigma_0), \quad (6.21b)$$

$$\Pr(\alpha_{x,i}^\top E_k X \leq \beta_{x,i}) \geq 1 - p_{x,i}, \quad (6.21c)$$

$$\Pr(\alpha_{u,j}^\top F_k U \leq \beta_{u,j}) \geq 1 - p_{u,j}, \quad (6.21d)$$

$$\mu_f = E_N \mathbb{E}[X], \quad (6.21e)$$

$$\Sigma_f = E_N (\mathbb{E}[X X^\top] - \mathbb{E}[X] \mathbb{E}[X]^\top) E_N^\top, \quad (6.21f)$$

where

$$\bar{Q} = \text{blkdiag}(Q, \dots, Q, 0) \in \mathbb{R}^{(N+1)n_x \times (N+1)n_x},$$

$$\bar{R} = \text{blkdiag}(R, \dots, R) \in \mathbb{R}^{Nn_u \times Nn_u},$$

and

$$E_k = [0_{n_x, kn_x}, I_{n_x}, 0_{n_x, (N-k)n_x}] \in \mathbb{R}^{n_x \times (N+1)n_x}, \quad k = 0, \dots, N,$$

$$F_k = [0_{n_u, kn_u}, I_{n_u}, 0_{n_u, (N-k-1)n_u}] \in \mathbb{R}^{n_u \times Nn_u}, \quad k = 0, \dots, N-1,$$

and thus $x_k = E_k X$ and $u_k = F_k U$.

Proof. The proof is straightforward from the discussion in Chapter 3. Note also that, because $Q \succeq 0$ and $R \succ 0$, it follows that $\bar{Q} \succeq 0$ and $\bar{R} \succ 0$. \square

The following theorem shows that Problem (6.21) can be relaxed to a convex programming problem.

Theorem 3. *Given the relaxation of (6.21f)*

$$\Sigma_f \succeq E_N \left(\mathbb{E}[XX^\top] - \mathbb{E}[X]\mathbb{E}[X]^\top \right) E_N^\top, \quad (6.22)$$

along with the control law

$$u_k = v_k + K_k y_k, \quad (6.23)$$

where $v_k \in \mathbb{R}^{n_u}$, $K_k \in \mathbb{R}^{n_u \times n_x}$, and $y_k \in \mathbb{R}^{n_x}$ from

$$y_{k+1} = Ay_k + Dw_k, \quad (6.24a)$$

$$y_0 = x_0 - \mu_0, \quad (6.24b)$$

reformulates Problem (6.21) as the following convex programming problem.

$$\begin{aligned} \min_{V, K} J(V, K) = & \text{tr} \left[((I + \mathcal{B}K)^\top \bar{Q} (I + \mathcal{B}K) + K^\top \bar{R} K) \Sigma_y \right] \\ & + (\mathcal{A}\mu_0 + \mathcal{B}V)^\top \bar{Q} (\mathcal{A}\mu_0 + \mathcal{B}V) + V^\top \bar{R} V. \end{aligned} \quad (6.25a)$$

subject to

$$\alpha_{x,i}^\top E_k(\mathcal{A}\mu_0 + \mathcal{B}V) - \beta_{x,i} + |S^\top (I + \mathcal{B}K)^\top E_k^\top \alpha_{x,i}| \Phi^{-1}(1 - p_{x,i}) \leq 0, \quad (6.25b)$$

$$\alpha_{u,j}^\top F_k V - \beta_{u,j} + |S^\top K^\top F_k^\top \alpha_{u,j}| \Phi^{-1}(1 - p_{u,j}) \leq 0, \quad (6.25c)$$

$$\mu_f = E_N(\mathcal{A}\mu_0 + \mathcal{B}V), \quad (6.25d)$$

$$\Sigma_f \succeq E_N(I + \mathcal{B}K) \Sigma_y (I + \mathcal{B}K)^\top E_N^\top, \quad (6.25e)$$

for $i = 0, \dots, N_s - 1$ and $j = 0, \dots, N_c - 1$, where

$$\begin{aligned} \Sigma_y &= \mathcal{A} \Sigma_0 \mathcal{A}^\top + \mathcal{D} \mathcal{D}^\top, \\ SS^\top &= \Sigma_y, \end{aligned}$$

and

$$V = \begin{bmatrix} v_0 \\ \vdots \\ v_{N-1} \end{bmatrix}, \quad K = \begin{bmatrix} K_0 & & & 0 \\ & K_1 & & 0 \\ & & \ddots & 0 \\ & & & K_{N-1} & 0 \end{bmatrix},$$

and where $\Phi^{-1}(\cdot)$ is the inverse function of the cumulative distribution function of the standard normal distribution.

Proof. All the steps to convert Problem (6.21) to Problem (6.25) have already been discussed in the previous chapters, except for the conversion from (6.21d) to (6.25c). Thus, we only need to outline the step of converting (6.21d) to (6.25c).

Using the control law (6.23), the control sequence vector U is represented as

$$U = V + KY, \quad (6.26)$$

where $Y = \begin{bmatrix} y_0^\top & \dots & y_N^\top \end{bmatrix}^\top \in \mathbb{R}^{Nn_x}$. It follows from (6.24) that

$$Y = \mathcal{A}y_0 + \mathcal{D}W, \quad (6.27)$$

and thus, using the facts that $\mathbb{E}[y_0] = 0$, $\mathbb{E}[y_0 y_0^\top] = \Sigma_0$, and $\mathbb{E}[y_0 W^\top] = 0$, one obtains

$$\mathbb{E}[Y] = 0, \quad \mathbb{E}[Y Y^\top] = \Sigma_y. \quad (6.28)$$

Therefore,

$$\mathbb{E}[U] = V, \quad \mathbb{E}[\tilde{U} \tilde{U}^\top] = K \Sigma_y K^\top, \quad (6.29)$$

where $\tilde{U} = U - \mathbb{E}[U]$. The inequality (6.21d) can be rewritten as

$$\Pr(\alpha_{u,j}^\top F_k (V + KY) \leq \beta_{u,j}) \geq 1 - p_{u,j}. \quad (6.30)$$

Notice that $\alpha_{u,j}^\top F_k (V + KY)$ is a Gaussian distributed random scalar with mean $\alpha_{u,j}^\top F_k V$ and variance $\alpha_{u,j}^\top F_k K \Sigma_y K^\top F_k^\top \alpha_{u,j}$. Thus, inequality (6.30) becomes

$$\begin{aligned} & \Pr(\alpha_{u,j}^\top F_k (V + KY) \leq \beta_{u,j}) \\ &= \frac{1}{\sqrt{2\pi \alpha_{u,j}^\top F_k K \Sigma_y K^\top F_k^\top \alpha_{u,j}}} \int_{-\infty}^{\beta_{u,j}} \exp\left(-\frac{(\xi - \alpha_{u,j}^\top F_k V)^2}{2\alpha_{u,j}^\top F_k K \Sigma_y K^\top F_k^\top \alpha_{u,j}}\right) d\xi, \\ &= \Phi\left(\frac{\beta_{u,j} - \alpha_{u,j}^\top F_k V}{\sqrt{\alpha_{u,j}^\top F_k K \Sigma_y K^\top F_k^\top \alpha_{u,j}}}\right) \geq 1 - p_{u,j}. \end{aligned} \quad (6.31)$$

Using the inverse function of $\Phi(\cdot)$, we obtain

$$\alpha_{u,j}^\top F_k V - \beta_{u,j} + \sqrt{\alpha_{u,j}^\top F_k K \Sigma_y K^\top F_k^\top \alpha_{u,j}} \Phi^{-1}(1 - p_{u,j}) \leq 0, \quad (6.32)$$

which can be readily converted to (6.25c). \square

As Problem (6.25) is convex, one can efficiently solve the problem using a convex programming solver.

Since $p_{x,i} \in [0, 0.5)$ and $p_{u,j} \in [0, 0.5)$, the constraints (6.25b) and (6.25c) are convex. Since Problem (6.25) is convex, one can efficiently solve the problem using a convex programming solver. Specifically, because the terminal covariance constraint (6.25e) can be converted to a linear matrix inequality (LMI),

$$\begin{bmatrix} \Sigma_f & E_N(I + \mathcal{B}K)S \\ S^\top(I + \mathcal{B}K)^\top E_N^\top & I \end{bmatrix} \succeq 0, \quad (6.33)$$

a semidefinite programming (SDP) solver such as Mosek [112] is needed.

6.3 CS-SMPC Design

In the previous section, we introduced the optimal covariance steering controller under state and control chance constraints. We are now ready to discuss the CS-SMPC algorithm, followed by a proof of recursive feasibility and guaranteed stability.

6.3.1 CS-SMPC Formulation

In this section, we solve Problem (6.14) approximately by solving Problem (6.15) at each time step in a receding horizon manner. Specifically, at time step k , we wish to solve the following *finite* horizon stochastic optimal control problem.

$$\min_{u_{k|k}, u_{k+1|k}, \dots, u_{k+N-1|k}} J_N(x_k; u_{k|k}, u_{k+1|k}, \dots, u_{k+N-1|k}) = \mathbb{E}_k \left[\sum_{t=k}^{k+N-1} x_{t|k}^\top Q x_{t|k} + u_{t|k}^\top R u_{t|k} \right] + \mathbb{E}_k[x_{k+N|k}]^\top P_{\text{mean}} \mathbb{E}_k[x_{k+N|k}], \quad (6.34a)$$

subject to

$$x_{t+1|k} = Ax_{t|k} + Bu_{t|k} + Dw_t, \quad x_{k|k} = x_k \sim \mathcal{N}(\mu_k, \Sigma_k), \quad (6.34b)$$

$$\Pr_k(\alpha_{x,i}^\top x_{t|k} \leq \beta_{x,i}) \geq 1 - p_{x,i}, \quad i = 0, \dots, N_s - 1, \quad (6.34c)$$

$$\Pr_k(\alpha_{u,j}^\top u_{t|k} \leq \beta_{u,j}) \geq 1 - p_{u,j}, \quad j = 0, \dots, N_c - 1, \quad (6.34d)$$

$$\mathbb{E}_k[x_{k+N|k}] \in \mathcal{X}_f^\mu, \quad (6.34e)$$

$$\mathbb{E}_k[(x_{k+N|k} - \mathbb{E}[x_{k+N|k}])(x_{k+N|k} - \mathbb{E}[x_{k+N|k}])^\top] \preceq \Sigma_f, \quad (6.34f)$$

where $\mu_k \in \mathbb{R}^{n_x}$, $\Sigma_k \in \mathbb{R}^{n_x \times n_x}$, $P_{\text{mean}} \in \mathbb{R}^{n_x \times n_x}$, $\mathcal{X}_f^\mu \subset \mathbb{R}^{n_x}$, and $\Sigma_f \in \mathbb{R}^{n_x \times n_x}$ are given.

Problem (6.34f) is illustrated in Fig. 6.1. At each time step, the *predicted* system state and the *predicted* control have to satisfy the constraints. In addition, at the end of the horizon, the state mean has to be in a subset \mathcal{X}_f^μ , denoted by a yellow polytope, and the system covariance has to be smaller than Σ_f , denoted by the yellow ellipse in Fig. 6.1.

Problem (6.34) results from Problem (6.15) by setting

$$J_f(x) = \mathbb{E}[x]^\top P_{\text{mean}} \mathbb{E}[x], \quad (6.35a)$$

along with the state terminal constraints (6.34e) and (6.34f). Adding terminal constraints is a common methodology to ensure recursive feasibility and stability for MPC [74]. In this section, we show that, by properly designing the terminal parameters of Problem (6.34), i.e., \mathcal{X}_f^μ , Σ_f , and P_{mean} , we can achieve recursive feasibility and guaranteed stability.

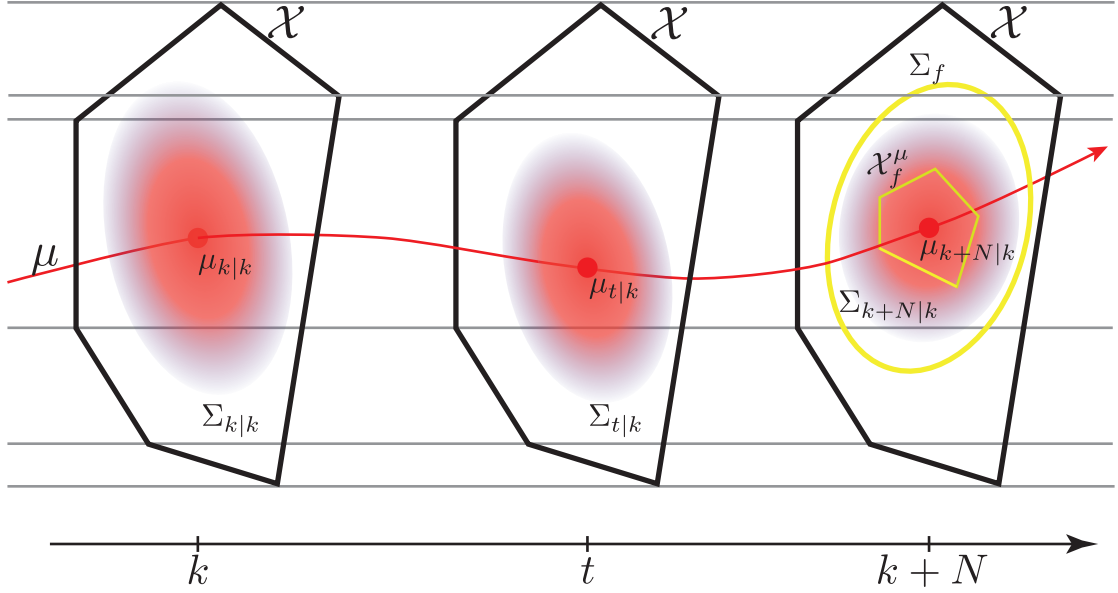


Figure 6.1: A schematic describing the proposed CS-SMPC approach.

We start from the following theorem that converts Problem (6.34) to a more convenient form to solve.

Theorem 4. Given μ_k , \mathcal{X}_f^μ , $\Sigma_f \succ 0$, and $P_{\text{mean}} \succ 0$, and using the following control law

$$u_{t|k} = v_{t|k} + K_{t|k}y_{t|k}, \quad (6.36a)$$

where $v_{t|k} \in \mathbb{R}^{n_u}$, $K_{t|k} \in \mathbb{R}^{n_u \times n_x}$, and $y_t \in \mathbb{R}^{n_x}$ from

$$y_{t+1|k} = Ay_{t|k} + Dw_t, \quad (6.36b)$$

$$y_{k|k} = x_{k|k} - \mu_{k|k}, \quad (6.36c)$$

for $t = k, \dots, k + N - 1$, Problem (6.34) can be cast as a convex programming problem as follows.

$$\begin{aligned} \min_{V, K} J_N(\mu_k, \Sigma_k; V, K) = & \text{tr} \left[((I + \mathcal{B}K)^\top \bar{Q}_{P, \text{cov}}(I + \mathcal{B}K) + K^\top \bar{R}K) \Sigma_y \right] \\ & + (\mathcal{A}\mu_{k|k} + \mathcal{B}V)^\top \bar{Q}_{P, \text{mean}}(\mathcal{A}\mu_{k|k} + \mathcal{B}V) + V^\top \bar{R}V. \end{aligned} \quad (6.37a)$$

subject to

$$\alpha_{x,i}^\top E_{t-k}(\mathcal{A}\mu_{k|k} + \mathcal{B}V) + |S^\top(I + \mathcal{B}K)^\top E_{t-k}^\top \alpha_{x,i}| \Phi^{-1}(1 - p_{x,i}) - \beta_{x,i} \leq 0, \quad (6.37b)$$

$$\alpha_{u,j}^\top F_{t-k}V + |S^\top K^\top F_{t-k}^\top \alpha_{u,j}| \Phi^{-1}(1 - p_{u,j}) - \beta_{u,j} \leq 0, \quad (6.37c)$$

$$E_N(\mathcal{A}\mu_{k|k} + \mathcal{B}V) \in \mathcal{X}_f^\mu, \quad (6.37d)$$

$$\Sigma_f \succeq E_N(I + \mathcal{B}K)\Sigma_y(I + \mathcal{B}K)^\top E_N^\top, \quad (6.37e)$$

for all $i = 0, \dots, N_s - 1$, $j = 0, \dots, N_c - 1$, and $t = k, \dots, k + N - 1$, where

$$\mu_{k|k} = \mu_k, \quad \Sigma_{k|k} = \Sigma_k, \quad \Sigma_y = \mathcal{A}\Sigma_{k|k}\mathcal{A}^\top + \mathcal{D}\mathcal{D}^\top, \quad SS^\top = \Sigma_y,$$

$$\begin{aligned} V &= \begin{bmatrix} v_{k|k} \\ \vdots \\ v_{k+N-1|k} \end{bmatrix}, \quad K = \begin{bmatrix} K_{k|k} & & & 0 \\ & K_{k+1|k} & & 0 \\ & & \ddots & 0 \\ & & & K_{k+N-1|k} & 0 \end{bmatrix}, \\ \bar{Q}_{P, \text{mean}} &= \begin{bmatrix} Q & & & \\ & \ddots & & \\ & & Q & \\ & & & P_{\text{mean}} \end{bmatrix}, \quad \bar{Q}_{P, \text{cov}} = \begin{bmatrix} Q & & & \\ & \ddots & & \\ & & Q & \\ & & & 0 \end{bmatrix}, \quad \bar{R} = \begin{bmatrix} R & & \\ & \ddots & \\ & & R \end{bmatrix}. \end{aligned}$$

Proof. The proof follows directly from the discussion in Section 6.2. \square

As discussed in Section 6.2, Problem (6.37) can be efficiently solved using a SDP solver. The remaining issue is whether Problem (6.37) is always feasible or not. To this end, we need to properly design the initial and terminal conditions.

Initial Condition Strategy

In this work, we assume that, at time step $k = 0$, Problem (6.37) is feasible subject to the following initial condition

$$\mu_0 = x_0, \tag{6.38a}$$

$$\Sigma_0 = 0. \tag{6.38b}$$

Notice that, as we assume perfect state measurement, the value of x_0 is available. Contrary to the deterministic MPC case, here we are dealing with unbounded additive noise, the state variable may be unbounded as well, and thus Problem (6.37) can become infeasible if we always set

$$\mu_k = x_k, \tag{6.39a}$$

$$\Sigma_k = 0. \tag{6.39b}$$

In order to keep Problem (6.37) feasible for all time steps $k \geq 1$, several approaches have been proposed to deal with this problem [95, 68, 91]. In this work we follow a similar initialization strategy to the one in [95], and set μ_k and Σ_k according to Algorithm 1. Notice that the choice of line 4 in Algorithm 1 is the result when SMPC implicitly closes the loop, while the choice in line 6 is does not use the most recent measurement and thus it can be regarded as an open-loop control. It follows from this strategy that it is necessary for line 6 to be always feasible. To this end, we need to properly design the terminal constraints. In [95], the authors defined $\Sigma_f \succ 0$ as the steady-state solution of the following discrete-time Lyapunov equation

$$\Sigma_f = (A + BK_{\text{LQR}})\Sigma_f(A + BK_{\text{LQR}})^\top + DD^\top, \tag{6.40}$$

where K_{LQR} is the infinite-horizon LQR gain. Because K_{LQR} is determined from the Q and R matrices in (6.34a), this approach results in Σ_f being an implicit function of Q and R and not of the terminal penalty. Thus, it is difficult to tune the matrix Σ_f except by trial and error. The approach we propose in this work utilizes the results from the covariance assignment theory to allow Σ_f to be chosen independent from the Q and R matrices as long as Σ_f is *assignable*.

Algorithm 1: Initial Condition Update Strategy

```

1 if  $k = 0$  then
2   | Set  $\mu_0 = x_0$  and  $\Sigma_0 = 0$  and solve (6.37) ;
3 else
4   | Set  $\mu_k = x_k$ ,  $\Sigma_k = 0$  and try to solve (6.37) ;
5   | if Infeasible then
6     | Set  $\mu_k = \mu_{k|k-1}^*$ ,  $\Sigma_k = \Sigma_{k|k-1}^*$  and solve (6.37) ;
7    $u_k \leftarrow u_{k|k}^*$ ;
```

Covariance Assignment Theory

Before introducing how we choose \mathcal{X}_f^μ , Σ_f , and P_{mean} , we introduce the following results from the covariance assignment theory [25, 26].

Definition 5 (Assignable Covariance). The state covariance $\Sigma \succ 0$ is *assignable* to the closed-loop system

$$x_{k+1} = (A + B\tilde{K})x_k + Dw_k, \quad (6.41)$$

if Σ satisfies

$$\Sigma = (A + B\tilde{K})\Sigma(A + B\tilde{K})^\top + DD^\top, \quad (6.42)$$

where \tilde{K} is a state-feedback gain.

Since $\mathcal{R}(B) \subseteq \mathcal{R}(D)$ and (A, D) is controllable, it follows that the pair $(A + B\tilde{K}, D)$ is

controllable as well. Since the pair (A, B) is controllable, if \tilde{K} is stabilizing, the matrix Σ in (6.42) is positive definite. Conversely, if $\Sigma \succ 0$ is pre-specified, from Lyapunov stability theory, any \tilde{K} that satisfies (6.42) is stabilizing. Such Σ and \tilde{K} can be computed as follows.

Proposition 3 ([25]). *The set of assignable state covariances Σ can be parameterized by the following set of linear matrix inequalities (LMIs)*

$$(I - BB^+)(\Sigma - A\Sigma A^\top - DD^\top)(I - BB^+) = 0, \quad (6.43a)$$

$$\Sigma \succ 0, \quad (6.43b)$$

$$\Sigma \succeq DD^\top, \quad (6.43c)$$

where B^+ denotes the Moore-Penrose pseudoinverse of B .

Proposition 4 ([25]). *If $\Sigma \succ 0$ is an assignable covariance matrix, then all state-feedback gains \tilde{K} that satisfy (6.42) are parametrized by*

$$\tilde{K} = B^+ \left((\Sigma - DD^\top)^{1/2} G_1 \begin{bmatrix} I_r & 0 \\ 0 & T \end{bmatrix} G_2^\top S_\Sigma^{-1} - A \right) + (I_{n_u} - B^+ B)Z, \quad (6.44)$$

where T is an arbitrary orthogonal matrix, $S_\Sigma S_\Sigma^\top = \Sigma$, $Z \in \mathbb{R}^{n_u \times n_x}$ is an arbitrary matrix, and G_1 and G_2 are defined from the singular-value decompositions

$$(I - BB^+)(\Sigma - DD^\top)^{1/2} = L\Lambda G_1^\top, \quad (6.45a)$$

$$(I - BB^+)AS_\Sigma = L\Lambda G_2^\top, \quad (6.45b)$$

where L , G_1 , and G_2 are orthogonal matrices, and $\Lambda = \text{diag}(\sigma_1, \dots, \sigma_r, 0, \dots, 0)$ with $\sigma_1 \geq \sigma_2 \geq \dots \geq \sigma_r > 0$.

Remark 8. It is worth noticing from [25] that, if A is nonsingular and B is full column rank, then the rank r in (6.45) is computed from $r = n_x - n_u$. In addition, $I_{n_u} - B^+ B = 0$, and thus the second term in (6.44) vanishes.

We are now ready to prove the recursive feasibility and guaranteed stability of the closed-loop system with the proposed CS-SMPC algorithm in (6.37). Let us denote the optimal cost of Problem (6.37) at time step k by $J_N^*(x_{k|k})$ and the associated optimal control sequence by

$$\{u_{k|k}^*, \dots, u_{k+N-1|k}^*\} = \{v_{k|k}^* + K_{k|k}^* y_{k|k}, \dots, v_{k+N-1|k}^* + K_{k+N-1|k}^* y_{k+N-1|k}\}, \quad (6.46)$$

which generates the corresponding optimal state sequence $\{x_{k|k}^*, x_{k+1|k}^*, \dots, x_{k+N|k}^*\}$. Since we are dealing with systems having additive uncertainty, it is difficult to design a control law that ensures the mean square stability of the state [87]. Instead, and similarly to [88], we will show that the average of the stage cost value is bounded from above.

Theorem 5. *Suppose that Σ_f satisfies (6.43), μ_f satisfies $\mu_f \in \mathcal{X}_f^\mu$, where the set $\mathcal{X}_f^\mu \subset \mathbb{R}^{n_x}$ is a positively invariant set [104] such that, for any $\mu \in \mathcal{X}_f^\mu$,*

$$(A + B\tilde{K})\mu \in \mathcal{X}_f^\mu, \quad (6.47a)$$

$$\alpha_{x,i}^\top \mu + |S^\top \alpha_{x,i}| \Phi^{-1}(1 - p_{x,i}) - \beta_{x,i} \leq 0, \quad i = 0, \dots, N_s - 1 \quad (6.47b)$$

$$\alpha_{u,j}^\top \tilde{K}\mu + |S^\top \tilde{K}^\top \alpha_{u,j}| \Phi^{-1}(1 - p_{u,j}) - \beta_{u,j} \leq 0, \quad j = 0, \dots, N_c - 1, \quad (6.47c)$$

where \tilde{K} is derived from (6.44), and P_{mean} is the solution of the following discrete-time Lyapunov equation

$$(A + B\tilde{K})^\top P_{\text{mean}}(A + B\tilde{K}) - P_{\text{mean}} + Q + \tilde{K}^\top R \tilde{K} = 0. \quad (6.48)$$

Then, the solution of Problem (6.37) ensures recursive feasibility and stability. Namely, the following two properties hold:

- a) *If Problem (6.37) is feasible at time step k , i.e., the control sequence (6.46) satisfies (6.37b), (6.37c), (6.37d), and (6.37e), then Problem (6.37) is feasible for all $k + n$, where $n \geq 1$.*

b) The average stage cost is bounded from above. Specifically,

$$\lim_{n \rightarrow \infty} \frac{1}{n} \sum_{t=0}^{n-1} \mathbb{E}_k [x_{k+t|k}^{*\top} Q x_{k+t|k}^* + u_{k+t|k}^{*\top} R u_{k+t|k}^*] \leq \ell_{\max}, \quad (6.49)$$

where $\ell_{\max} > 0$.

Proof. In order to simplify notation, henceforth we will rewrite the cost function J_N in (6.34a) as

$$J_N(x_{k|k}; u_{k|k}, \dots, u_{k+N-1|k}) = \sum_{t=k}^{k+N-1} \ell(x_{t|k}, u_{t|k}) + J_f(x_{k+N|k}), \quad (6.50)$$

where

$$\ell(x, u) = \mathbb{E}_k [x^\top Q x + u^\top R u], \quad (6.51)$$

and $J_f(\cdot)$ is as in (6.35a).

In order to prove recursive feasibility, it is sufficient to show that, given that Problem (6.37) is feasible at time step k , it is feasible at time step $k + 1$. To this end, we consider Problem (6.37), or equivalently Problem (6.34), with the following control sequence of length N

$$\mathbf{u} = \{v_{k+1|k}^* + K_{k+1|k}^* y_{k+1|k}, \dots, v_{k+N-1|k}^* + K_{k+N-1|k}^* y_{k+N-1|k}, \tilde{K} x_{k+N|k}^*\}, \quad (6.52)$$

where the first $N - 1$ elements are derived from the optimal control sequence at time step k in (6.46), and the last step is a covariance assignment control with gain as in (6.44). This control sequence steers the state trajectory from $x_{k+1|k}^*$ to

$$\mathbf{x} = \{x_{k+1|k}^*, \dots, x_{k+N|k}^*, (A + B\tilde{K})x_{k+N|k}^* + Dw_{k+N}\}. \quad (6.53)$$

Note that the control sequence (6.52) can be separated to the mean control sequence

$$\{v_{k+1|k}^*, \dots, v_{k+N-1|k}^*, \tilde{K} \mu_{k+N|k}^*\}, \quad (6.54)$$

and the covariance steering sequence

$$\{K_{k+1|k}^* y_{k+1|k}, \dots, K_{k+N-1|k}^* y_{k+N-1|k}, \tilde{K}(x_{k+N|k}^* - \mu_{k+N|k}^*)\}. \quad (6.55)$$

Since the state sequence (6.53) follows the same path as the solution at time step k , we only need to check the satisfaction of the constraints (6.34c) (6.34d) (6.34e), and (6.34f) at the end of the horizon.

We first show that the state mean at the end of the horizon satisfies the terminal mean constraint (6.34e). The first $N - 1$ mean control subsequence in (6.54) steers $\mu_{k+1|k}^*$ to $\mu_{k+N|k}^*$. Because of the fact that $\mu_{k+N|k}^* \in \mathcal{X}_f^\mu$, the last entry in (6.54) steers the system mean to

$$\mu_{k+N+1|k} = (A + B\tilde{K})\mu_{k+N|k}^* \in \mathcal{X}_f^\mu. \quad (6.56)$$

Thus, the constraint (6.34e) is satisfied at the end of the horizon.

Next, we show that the terminal covariance constraint (6.34f) is satisfied at the end of the horizon. Note that the first $N - 1$ covariance control subsequence in (6.55) steers $\Sigma_{k+1|k}^*$ to $\Sigma_{k+N|k}^*$. It follows from (6.41) that

$$\Sigma_{k+N+1|k} = (A + B\tilde{K})\Sigma_{k+N|k}^*(A + B\tilde{K})^\top + DD^\top. \quad (6.57)$$

In addition, since Σ_f is designed to be assignable, it follows from (6.42) that

$$\Sigma_f = (A + B\tilde{K})\Sigma_f(A + B\tilde{K})^\top + DD^\top. \quad (6.58)$$

It then follows from (6.57), (6.58), and the fact that $\Sigma_{k+N|k}^* \preceq \Sigma_f$, that

$$\Sigma_{k+N+1|k} \preceq \Sigma_f, \quad (6.59)$$

which indicates the satisfaction of the condition (6.34f) at the end of the horizon.

The remaining constraints needed to be satisfied are (6.34c) and (6.34d). Note that, because of (6.56),

$$\alpha_{x,i}^\top \mu_{k+N+1|k} + |S^\top \alpha_{x,i}| \Phi^{-1}(1 - p_{x,i}) - \beta_{x,i} \leq 0, \quad i = 0, \dots, N_s - 1, \quad (6.60)$$

holds. In addition, because $\epsilon_x \in [0, 0.5]$, it follows that $p_{x,i} \leq 0.5$, and thus, $\Phi^{-1}(1 - p_{x,i}) \geq 0$ for $i = 0, \dots, N_s - 1$. Therefore, along with (6.59),

$$\alpha_{x,i}^\top \mu_{k+N+1|k} + |\Sigma_{k+N+1|k}^{1/2} \alpha_{x,i}| \Phi^{-1}(1 - p_{x,i}) - \beta_{x,i} \leq 0, \quad i = 0, \dots, N_s - 1, \quad (6.61)$$

which means that (6.34c) is satisfied at the end of the horizon. Following a similar discussion, we can show that (6.34d) is also satisfied at the end of the horizon. Namely,

$$\alpha_{u,j}^\top \tilde{K} \mu_{k+N+1|k} + |\Sigma_{k+N+1|k}^{1/2} \tilde{K}^\top \alpha_{u,j}| \Phi^{-1}(1 - p_{u,j}) - \beta_{u,j} \leq 0, \quad j = 0, \dots, N_c - 1. \quad (6.62)$$

Thus, we have shown that, given that Problem (6.37) is feasible at time step k , the control sequence in (6.54) leads to the satisfaction of all the constraints in Problem (6.37) and (6.34). The remaining issue is to show that the proposed control policy $u_{k+N|k} = v_{k+N|k} + K_{k+N|k} y_{k+N|k}$ reproduces the same control input as $u_{k+N|k} = \tilde{K} x_{k+N|k}^*$. This can be achieved by letting

$$\tilde{K} \mu_{k+N|k}^* = v_{k+N|k} + K_{k+N|k} A^N y_{k|k}, \quad (6.63a)$$

$$\tilde{K} (x_{k+N|k}^* - \mu_{k+N|k}^*) = K_{k+N|k} (y_{k+N|k} - A^N y_{k|k}), \quad (6.63b)$$

where

$$y_{k+N|k} = A^N y_{k|k} + \begin{bmatrix} A^{N-1}D & \cdots & AD & D \end{bmatrix} \begin{bmatrix} w_k \\ \vdots \\ w_{k+N-1} \end{bmatrix}. \quad (6.64)$$

If $y_{k+N|k} \neq A^N y_{k|k}$, by letting

$$K_{k+N|k} = \tilde{K}(x_{k+N|k}^* - \mu_{k+N|k}^*) \frac{1}{|y_{k+N|k} - A^N y_{k|k}|^2} (y_{k+N|k} - A^N y_{k|k})^\top, \quad (6.65a)$$

$$v_{k+N|k} = \tilde{K} \mu_{k+N|k}^* - K_{k+N|k} A^N y_{k|k}. \quad (6.65b)$$

yields the desired result. If, on the other hand, $y_{k+N|k} = A^N y_{k|k}$, it follows from (6.64) that

$$y_{k+N|k} - A^N y_{k|k} = \begin{bmatrix} A^{N-1}D & \cdots & AD & D \end{bmatrix} \begin{bmatrix} w_k \\ \vdots \\ w_{k+N-1} \end{bmatrix} = 0, \quad (6.66)$$

and hence,

$$\begin{aligned} x_{k+N|k}^* &= A^N x_{k|k} + \begin{bmatrix} A^{N-1}B & \cdots & B \end{bmatrix} \begin{bmatrix} u_{k|k}^* \\ \vdots \\ u_{k+N-1|k}^* \end{bmatrix} + \begin{bmatrix} A^{N-1}D & \cdots & D \end{bmatrix} \begin{bmatrix} w_k \\ \vdots \\ w_{k+N-1} \end{bmatrix}, \\ &= A^N x_{k|k} + \begin{bmatrix} A^{N-1}B & \cdots & AB & B \end{bmatrix} \begin{bmatrix} u_{k|k}^* \\ \vdots \\ u_{k+N-1|k}^* \end{bmatrix}. \end{aligned} \quad (6.67)$$

Thus $x_{k+N|k}^*$ can be computed deterministically from the control inputs. In this case,

we can thus choose

$$v_{k+N|k} = \tilde{K}x_{k+N|k}^*, \quad (6.68a)$$

$$K_{k+N|k} = 0. \quad (6.68b)$$

So far, we have shown the recursive feasibility of the closed-loop system with CS-SMPC. Next, we discuss the issue of stability. Note that the cost $J_N(x_{k+1|k}^*; \mathbf{u})$ can be represented as

$$\begin{aligned} J_N(x_{k+1|k}^*; \mathbf{u}) &= J_N^*(x_{k|k}) - \ell(x_{k|k}, u_{k|k}^*) + \ell(x_{k+N|k}^*, \tilde{K}x_{k+N|k}^*) \\ &\quad - J_f(x_{k+N|k}^*) + J_f((A + B\tilde{K})x_{k+N|k}^* + Dw_{k+N}). \end{aligned} \quad (6.69)$$

We first show that

$$J_N^*(x_{k+1|k}^*) \leq J_N^*(x_{k|k}) - \ell(x_{k|k}, u_{k|k}^*) + \text{tr} \left((Q + \tilde{K}^\top R \tilde{K}) \Sigma_f \right). \quad (6.70)$$

It follows from (6.35a) that

$$J_f(x_{k+N|k}^*) = \mu_{k+N|k}^{*\top} P_{\text{mean}} \mu_{k+N|k}^*. \quad (6.71)$$

In addition, since the mean of the system state at the horizon is $(A + B\tilde{K})\mu_{k+N|k}^*$, the following holds

$$J_f((A + B\tilde{K})x_{k+N|k}^* + Dw_{k+N}) = \mu_{k+N|k}^{*\top} (A + B\tilde{K})^\top P_{\text{mean}} (A + B\tilde{K}) \mu_{k+N|k}^*.$$

Furthermore, it follows from (6.51) that

$$\ell(x_{k+N|k}^*, \tilde{K}x_{k+N|k}^*) = \mu_{k+N|k}^{*\top} (Q + \tilde{K}^\top R \tilde{K}) \mu_{k+N|k}^* + \text{tr} \left((Q + \tilde{K}^\top R \tilde{K}) \Sigma_{k+N|k}^* \right).$$

Thus, using the conditions (6.48) and (6.42), it follows from (6.69) that

$$\begin{aligned}
& J_N(x_{k+1|k}^*, \mathbf{u}) - J_N^*(x_{k|k}) + \ell(x_{k|k}, u_{k|k}^*) \\
&= \ell(x_{t+N|t}^*, \tilde{K}x_{k+N|k}^*) - J_f(x_{t+N|t}^*) + J_f((A + B\tilde{K})x_{t+N|t}^* + Dw_{t+N}), \\
&= \mu_{t+N|t}^{*\top} \left(Q + \tilde{K}^\top R \tilde{K} - P_{\text{mean}} + (A + B\tilde{K})^\top P_{\text{mean}} (A + B\tilde{K}) \right) \mu_{t+N|t}^* \\
&\quad + \text{tr} \left((Q + \tilde{K}^\top R \tilde{K}) \Sigma_{t+N|t}^* \right), \\
&= \text{tr} \left((Q + \tilde{K}^\top R \tilde{K}) \Sigma_{t+N|t}^* \right) = \text{tr} \left((Q + \tilde{K}^\top R \tilde{K})^{1/2} \Sigma_{t+N|t}^* (Q + \tilde{K}^\top R \tilde{K})^{1/2} \right), \\
&\leq \text{tr} \left((Q + \tilde{K}^\top R \tilde{K})^{1/2} \Sigma_f (Q + \tilde{K}^\top R \tilde{K})^{1/2} \right) = \text{tr} \left((Q + \tilde{K}^\top R \tilde{K}) \Sigma_f \right). \tag{6.72}
\end{aligned}$$

Note also that since

$$J_N^*(x_{k+1|k}^*) \leq J_N(x_{k+1|k}^*, \mathbf{u}),$$

inequality (6.70) holds. It then follows from (6.70) that

$$\begin{aligned}
\ell(x_{k|k}, u_{k|k}^*) &\leq J_N^*(x_{k|k}) - J_N^*(x_{k+1|k}^*) + \text{tr} \left((Q + \tilde{K}^\top R \tilde{K}) \Sigma_f \right), \\
\ell(x_{k+1|k}^*, u_{k+1|k}^*) &\leq J_N^*(x_{k+1|k}^*) - J_N^*(x_{k+2|k}^*) + \text{tr} \left((Q + \tilde{K}^\top R \tilde{K}) \Sigma_f \right), \\
&\vdots \\
\ell(x_{k+n-1|k}^*, u_{k+n-1|k}^*) &\leq J_N^*(x_{k+n-1|k}^*) - J_N^*(x_{k+n|k}^*) + \text{tr} \left((Q + \tilde{K}^\top R \tilde{K}) \Sigma_f \right),
\end{aligned}$$

and thus,

$$\lim_{n \rightarrow \infty} \frac{1}{n} \sum_{t=0}^{n-1} \ell(x_{k+t|k}^*, u_{k+t|k}^*) \leq \lim_{n \rightarrow \infty} \frac{1}{n} (J_N^*(x_{k|k}) - J_N^*(x_{k+n|k}^*)) + \text{tr} \left((Q + \tilde{K}^\top R \tilde{K}) \Sigma_f \right).$$

Since $J_N^*(\cdot)$ has a finite lower bound, the right-hand-side of this inequality is bounded from

above. Thus, there exists a positive value ℓ_{\max} such that

$$\lim_{n \rightarrow \infty} \frac{1}{n} \sum_{k=0}^n \ell(x_{t+k|t}^*, u_{t+k|t}^*) \leq \text{tr} \left((Q + \tilde{K}^\top R \tilde{K}) \Sigma_f \right) = \ell_{\max}.$$

which leads to (6.49). □

Remark 9. As (6.44) indicates, the gain matrix \tilde{K} that satisfies (6.42) is not unique. Thus, in our numerical examples, we use the following

$$\tilde{K} = B^+ \left((\Sigma_f - DD^\top)^{1/2} G_1 G_2^\top \Sigma_f^{-1/2} - A \right), \quad (6.73)$$

which can be derived by setting $T = I$ and $Z = 0$.

Remark 10. We choose \mathcal{X}_f^μ to be the maximal positively invariant set for the mean system dynamics

$$\mu_{k+1} = A\mu_k + Bv_k, \quad (6.74)$$

subject to, for $k = 0, 1, \dots, N$,

$$\alpha_{x,i}^\top \mu_k + |\Sigma_f^{1/2} \alpha_{x,i}| \Phi^{-1}(1 - p_{x,i}) - \beta_{x,i} \leq 0, \quad i = 0, \dots, N_s - 1 \quad (6.75a)$$

$$\alpha_{u,j}^\top \tilde{K} \mu_k + |\Sigma_f^{1/2} \tilde{K}^\top \alpha_{u,j}| \Phi^{-1}(1 - p_{u,j}) - \beta_{u,j} \leq 0, \quad j = 0, \dots, N_c - 1. \quad (6.75b)$$

Such a set can be computed efficiently from the results in [104].

Remark 11. Because the eigenvalues of $A + B\tilde{K}$ lie inside the unit ball and $Q + \tilde{K}R\tilde{K} \succeq 0$, it follows from (6.48) that $P_{\text{mean}} \succeq 0$, and thus, the cost function (6.34a) is convex.

Remark 12. In fact, the matrix Σ_f that satisfies (6.40) is an assignable covariance with a corresponding state-feedback gain K_{LQR} .

6.4 Numerical Simulation

In this section we validate the proposed algorithm using two numerical examples. In the first example, we clarify the benefit of CS-SMPC using a problem with simple dynamics. In the second example, we demonstrate that CS-SMPC can be applied to control an autonomous vehicle. We use YALMIP [111] along with the MPT3 toolbox [116] to compute the maximal invariant sets and with MOSEK [112] to solve the relevant optimization problems.

6.4.1 Illustrative Example with 2D Dynamics

In this section, we demonstrate the benefit of CS-SMPC using a numerical example similar to the one used in [94]. We set the system dynamics matrices in (6.1) to be

$$A = \begin{bmatrix} 1.02 & -0.1 \\ 0.1 & 0.98 \end{bmatrix}, \quad B = \begin{bmatrix} 0.1 & 0 \\ 0.05 & 0.01 \end{bmatrix}, \quad D = \begin{bmatrix} 0.01 & 0 \\ 0 & 0.01 \end{bmatrix}. \quad (6.76)$$

The initial condition is set to $x_0 = \begin{bmatrix} -0.3 & 1.2 \end{bmatrix}^\top$. Notice that the eigenvalues of the A matrix lie outside the unit disk ($\lambda_{1,2} = 1.0 \pm i 0.098$). Figure 6.2 shows 100 sample trajectories of the uncontrolled system. The trajectories follow increasingly large spiral paths.

In addition, we consider the following chance constraint

$$\Pr \left(\begin{bmatrix} -2 & 1 \end{bmatrix} x_k \leq 2.5 \right) \geq 1 - 10^{-3}, \quad (6.77)$$

for all $k = 0, 1, \dots$. We wish to minimize the cost function in (6.14) with the following

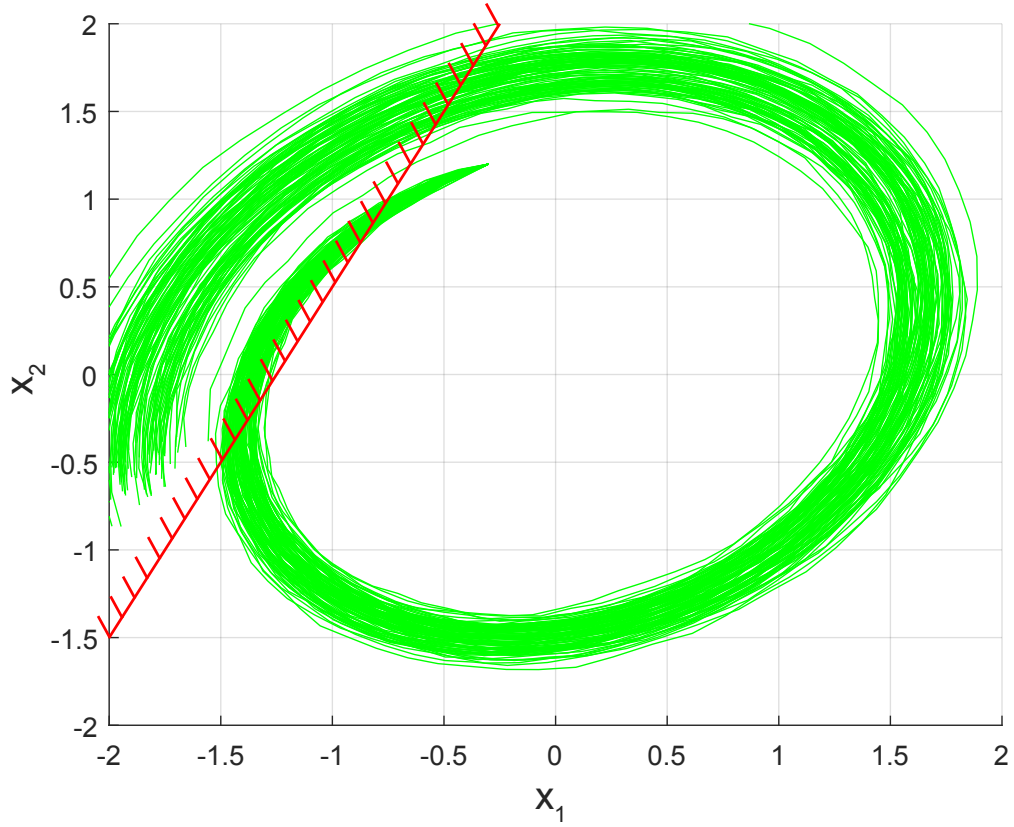


Figure 6.2: Uncontrolled system state trajectories.

matrices

$$Q = \begin{bmatrix} 2 & 0 \\ 0 & 1 \end{bmatrix}, \quad R = \begin{bmatrix} 5 & 0 \\ 0 & 20 \end{bmatrix}, \quad (6.78)$$

while satisfying the constraints. Figure 6.3 shows the results of 100 sample trajectories using a controller with the infinite-horizon LQR gain corresponding to (6.78). As LQR controllers do not take into account any constraints, the majority of the trajectories in Fig. 6.3 violate the state constraint (6.77).

We first apply the MPC approach proposed in [95] with some modifications. The necessary modifications along with the difference between our approach and [95] are summa-

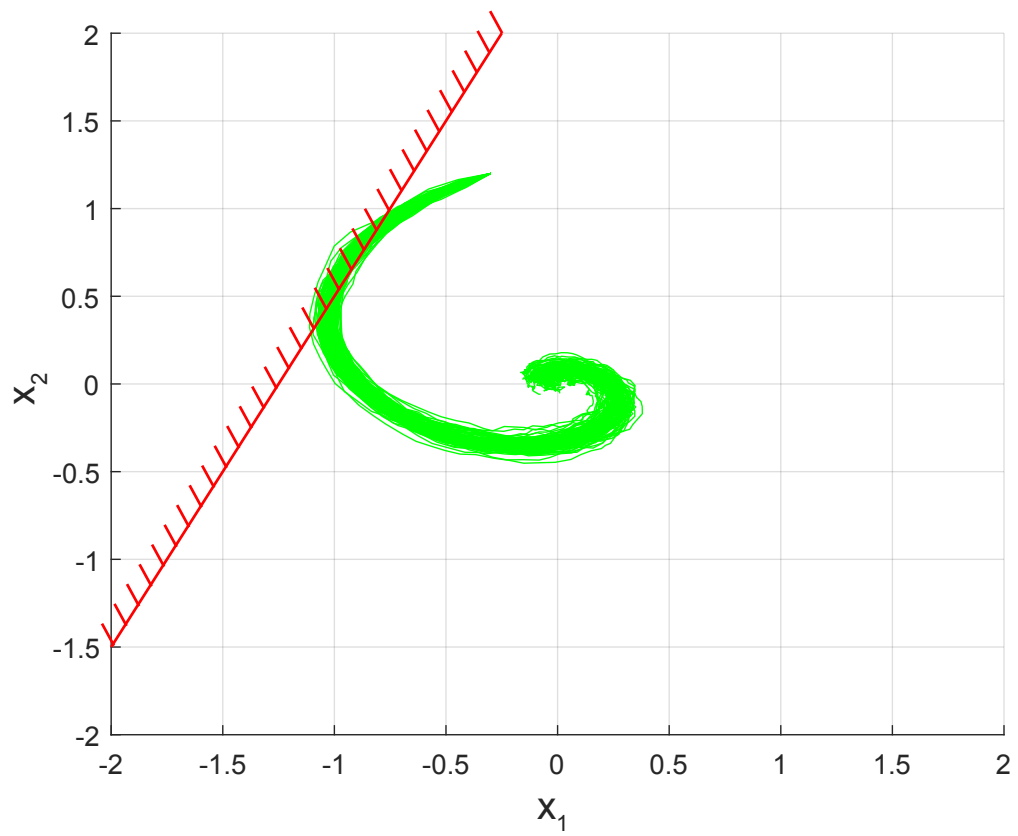


Figure 6.3: System state trajectories controlled by an LQR controller

rized as follows. The terminal cost in [95] is

$$\min_{u_{k|k}, u_{k+1|k}, \dots, u_{k+N-1|k}} J_N(x_k; u_{k|k}, u_{k+1|k}, \dots, u_{k+N-1|k}) = \mathbb{E}_k \left[x_{k+N|k}^\top Q_N x_{k+N|k} + \sum_{t=k}^{k+N-1} x_{t|k}^\top Q x_{t|k} + u_{t|k}^\top R u_{t|k} \right], \quad (6.79)$$

where Q_N is the solution of the following discrete-time algebraic Riccati equation

$$A^\top Q_N A - Q_N - A^\top Q_N B (B^\top Q_N B + R)^{-1} B^\top Q_N A + Q = 0. \quad (6.80)$$

In [95], the covariance at the horizon is bounded from above by the solution of the discrete-time Lyapunov equation (6.40). The terminal mean set in [95] $\bar{\mathcal{X}}_f^\mu$ is the positive invariant set such that

$$(A + BK_{\text{LQR}})\mu \in \bar{\mathcal{X}}_f^\mu, \quad \forall \mu \in \bar{\mathcal{X}}_f^\mu. \quad (6.81)$$

The control policy in [95] involves a feedback of the state deviation from the mean, which leads to the following covariance dynamics

$$\Sigma_{t+1|k} = (A + BK_{t|k})\Sigma_{t|k}(A + BK_{t|k})^\top + DD^\top, \quad (6.82)$$

which is non-convex due to the coupling between $K_{t|k}$ and $\Sigma_{t|k}$. The authors of [95] mentioned in [117] that they used the following convex relaxation technique proposed in [94] with the mild assumption that $\Sigma_{t|k} \succ 0$ for all $t > k$,

$$\Sigma_{t+1|k} \succeq (A + B\Theta_{t|k})\Sigma_{t|k}^{-1}(A + B\Theta_{t|k})^\top + DD^\top, \quad (6.83)$$

which is, using Schur complement, equivalent to the following LMI

$$\begin{bmatrix} \Sigma_{t+1|k} & A + B\Theta_{t|k} & D \\ (A + B\Theta_{t|k})^\top & \Sigma_{t|k} & 0 \\ D^\top & 0 & I_{n_w} \end{bmatrix} \succeq 0, \quad (6.84)$$

where $\Theta_{t|k} = K_{t|k}\Sigma_{t|k}$ is a new design variable. However, in this example, we observed that this relaxation led to imprecise computation of the covariance, implying a difficulty in properly assessing the state chance constraint (6.77). Instead, we use the disturbance feedback approach used in [93, 68], where the control input is an affine function of the past disturbance sequence

$$u_{t|k} = v_{t|k} + \sum_{\tau=k}^{t-1} M_{t,\tau} D w_\tau, \quad (6.85)$$

which is known to lead to a convex formulation of the covariance dynamics [97].

We assume that the problem is feasible with initial condition $\mu_0 = x_0, \Sigma_0 = 0$. In order to maintain feasibility we use the approach in Algorithm 1 for $k \geq 1$. Figure 6.4(a) illustrates 100 sample trajectories of the system controlled by (6.85) with horizon $N = 10$. The trajectories successfully avoid the constraint and converge to the origin.

The proposed CS-SMPC algorithm with the same horizon length is also applied to the system. Figure 6.4(b) shows 100 sample trajectories. We used the same terminal target covariance as the one in (6.40). Similarly to the trajectories in Fig. 6.4(a), the trajectories successfully satisfy the constraint and converge to the origin. The main difference between the two methods is the computational cost. As shown in Fig. 6.5, the CS-SMPC algorithm exhibits faster computational speed. This superior performance is due to the difference in the control approach formulation. The CS-SMPC algorithm uses the current value of the y variable, and thus, the K matrix in (6.37) is block diagonal, while the disturbance feedback controller (6.85) uses the past disturbance sequence, implying that a lower block triangular

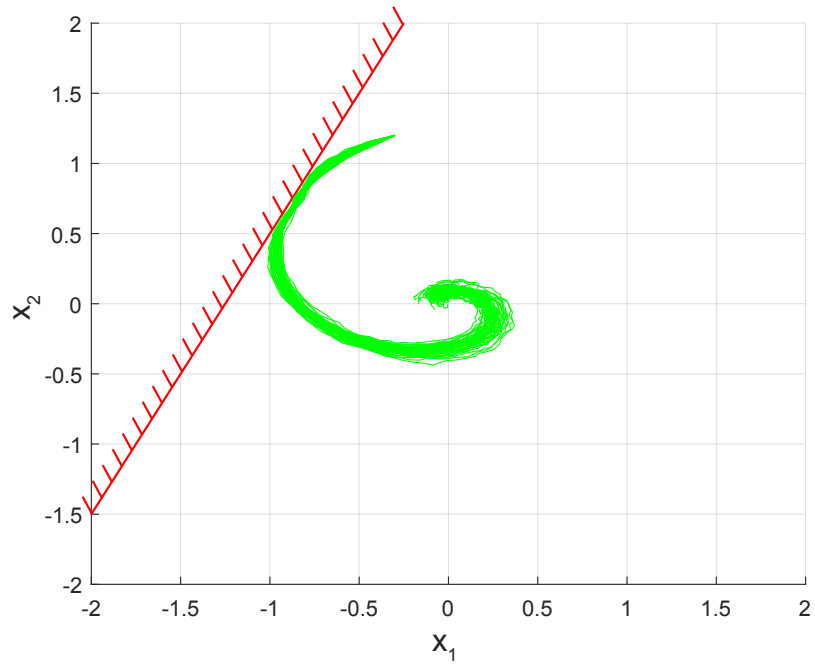
matrix is needed (see [93, 97]), which leads to more computations.

6.4.2 Self-Driving Vehicle Control

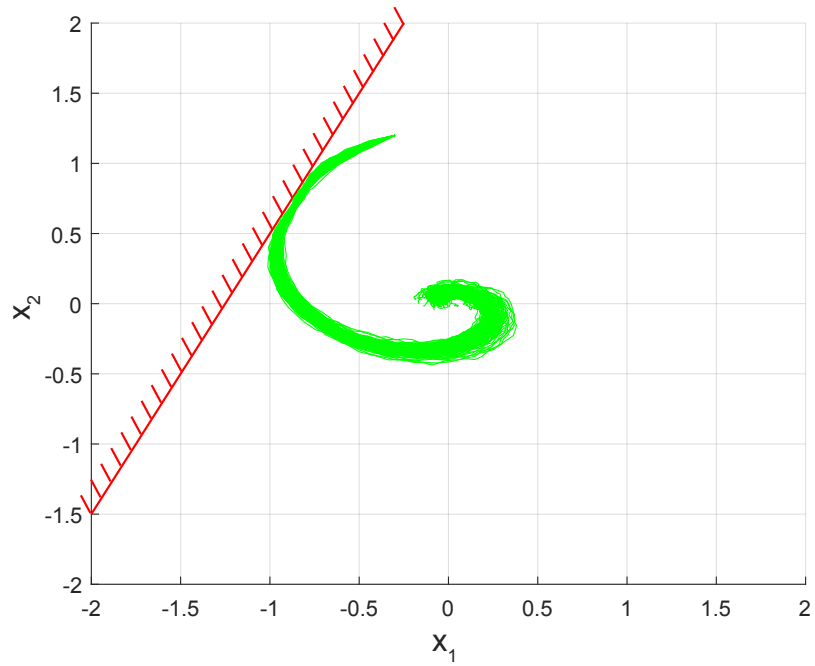
The previous simple numerical example illustrated the computational benefits of the CS-SMPC approach stemming from the convexity of the problem formulation and the block diagonal structure of the feedback gain matrix. In this section, we validate the efficacy of the proposed CS-SMPC algorithm with a more realistic example of a vehicle driving around a road circuit.

The key benefit of using CS-SMPC for this example is illustrated in Fig. 6.6. A deterministic MPC approach, as shown in Fig. 6.6(a), neglects the effect of stochastic disturbances, and thus, a safety margin to the constraint boundaries is needed. It thus requires trial-and-error to find reasonable values to achieve good performance while not violating the constraints. Figure 6.6(b) shows an example of a planned trajectory using a stochastic MPC controller with open-loop vehicle dynamics. Since the effect of noise increases with time, it is difficult to have a long time horizon. Stochastic tube-MPC uses closed-loop vehicle dynamics as shown in Fig. 6.6(c). As the stabilizing gain of a stochastic tube-MPC is generally constant, the resulting state covariance converges to a constant value. In addition, a priori calculation of appropriate values of the feedback gains is not straightforward and requires trial and error. Fig. 6.6(d) illustrates the benefit of the proposed CS-SMPC approach. By directly controlling the covariance of the system state, the mean trajectory is steered to the inner edge of the road, which leads to a better performance for a race car that is trying to minimize lap time.

We use the linearized bicycle model assuming constant longitudinal vehicle speed [118] shown in Fig. 6.7. The continuous dynamics is described as follows.



(a) Trajectories from the controller in [95] with some modifications.



(b) Trajectories from the CS-SMPC approach.

Figure 6.4: System state trajectories.

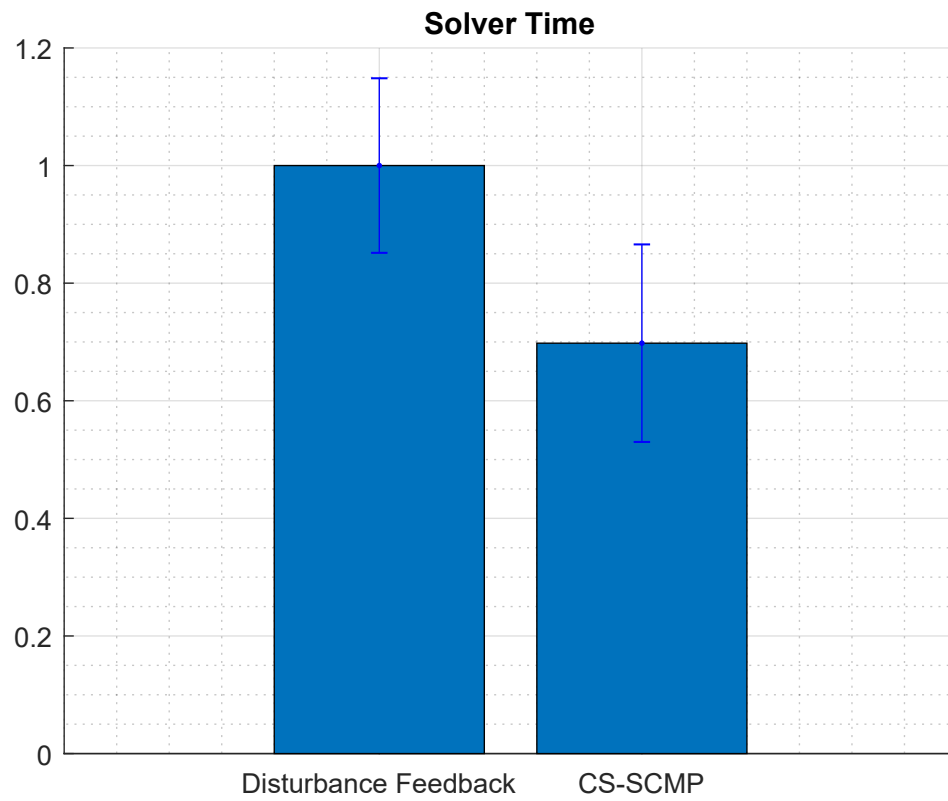
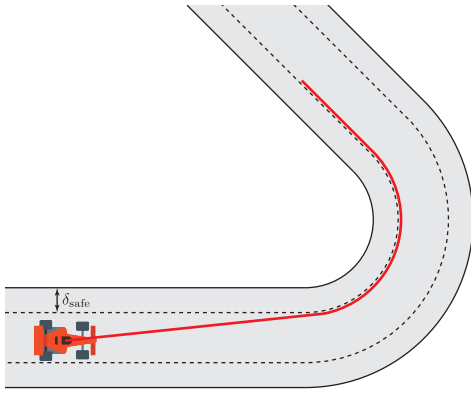
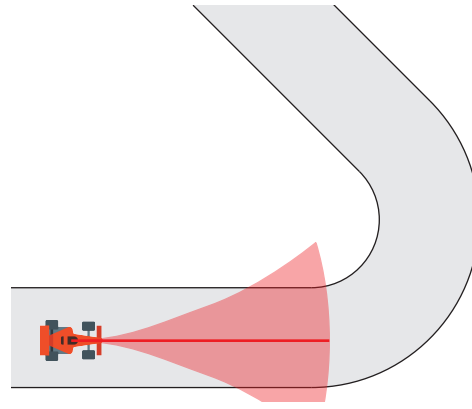


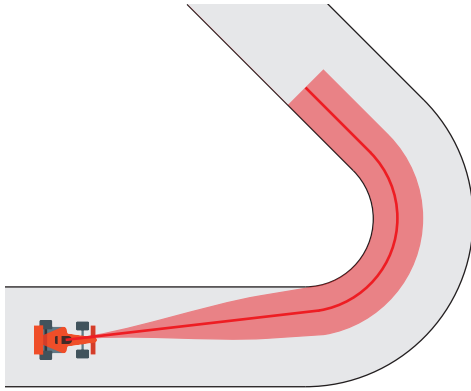
Figure 6.5: Mean and standard deviation of the computation time of each method. The time is normalized by the computation time of the disturbance feedback method.



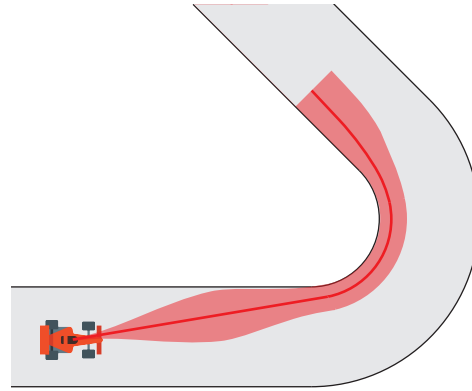
(a) Deterministic MPC.



(b) Stochastic MPC with open-loop vehicle dynamics.



(c) Stochastic MPC with closed-loop constant gain vehicle dynamics.



(d) Stochastic MPC with closed-loop time-varying gain vehicle dynamics.

Figure 6.6: Comparison of MPC approaches for vehicle control example. Each figure shows a planned trajectory for a race car using different MPC approaches. The bold lines indicate the mean trajectories, and the shaded areas represent $1-\epsilon$ confidence regions. By directly controlling the covariance, it is possible to design more aggressive controllers that operate closer to the constraints.

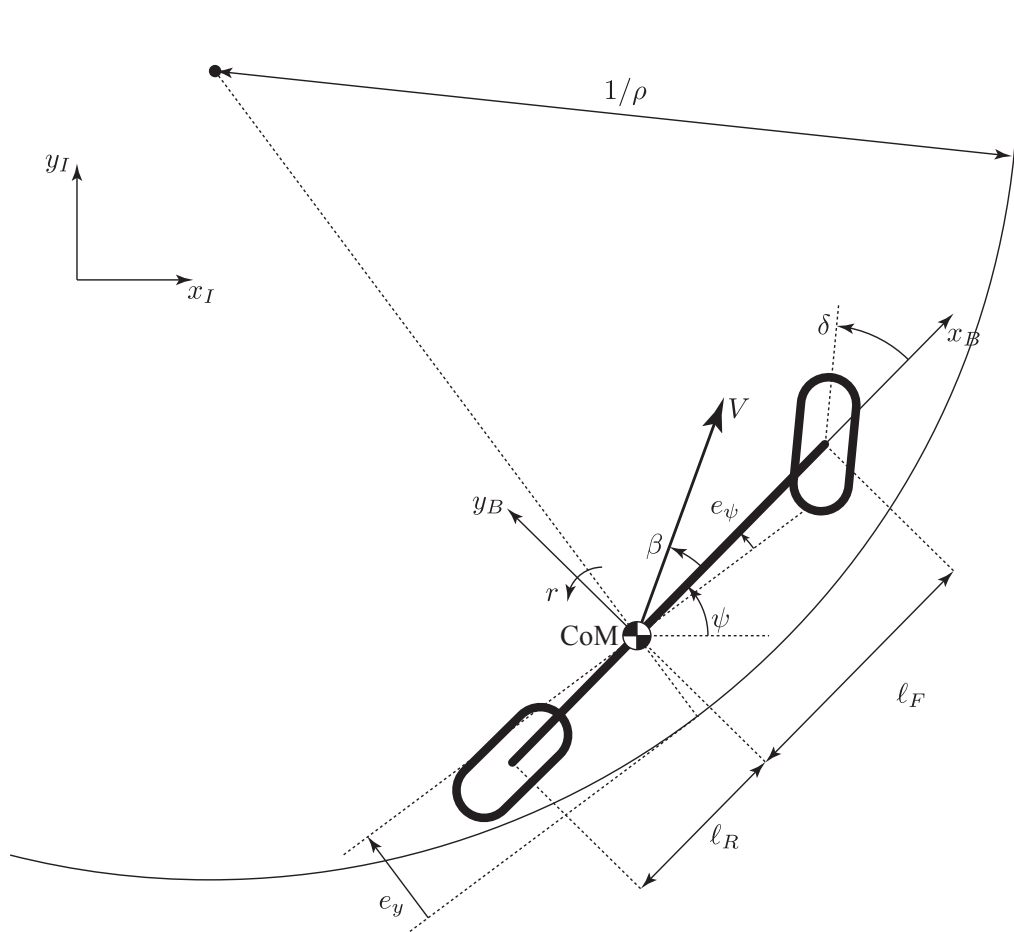


Figure 6.7: Bicycle model. (x_I, y_I) is the inertial frame, and (x_B, y_B) is the body frame.

$$\dot{\beta}(t) = -\frac{C_r + C_f}{mV_x}\beta(t) + \left(-1 + \frac{\ell_R C_r - \ell_F C_f}{mV_x^2}\right)r(t) + \frac{C_f}{mV_x}\delta(t), \quad (6.86a)$$

$$\dot{r}(t) = \frac{\ell_R C_r - \ell_F C_f}{I_z}\beta(t) - \frac{\ell_R^2 C_r + \ell_F^2 C_f}{I_z V_x}r(t) + \frac{\ell_F C_f}{I_z}\delta(t), \quad (6.86b)$$

$$\dot{e}_\psi(t) = r(t) - V_x \rho(t), \quad (6.86c)$$

$$\dot{e}_y(t) = V_x \beta(t) + V_x e_\psi(t). \quad (6.86d)$$

The state variables in (6.86) are the side-slip angle β , the vehicle yaw rate r , the heading angle error e_ψ , and the lateral deviation error e_y . The inputs to the system are the front wheel angle δ and the curvature of the road centerline ρ , which is a function of the distance along the road centerline s . In this model, since we assume constant longitudinal velocity, it follows that $s(t) = V_x t$, and thus, ρ can be regarded as a function of time only. The system parameters are listed in Table 6.1 along with the numerical values used in this example. Note also that the vehicle direction angle ψ can be computed from

$$\dot{\psi}(t) = r(t). \quad (6.87)$$

The vehicle dynamics (6.86) can be represented as an LTI system.

$$\dot{x}(t) = A_c x(t) + B_c u(t) + C_c \rho(t), \quad (6.88)$$

where $x = \begin{bmatrix} \beta & r & e_\psi & e_y \end{bmatrix}^\top \in \mathbb{R}^4$ and $u = \delta \in \mathbb{R}$. Using zero-order hold with $\Delta t = 0.5$ sec, we represent the discretized LTI dynamics as

$$x_{k+1} = A x_k + B u_k + C \rho_k. \quad (6.89)$$

Setting (6.89) as the nominal dynamics, our interest is to control the following stochastic

dynamics

$$x_{k+1} = Ax_k + Bu_k + C\rho_k + Dw_k, \quad (6.90)$$

where $D = \text{diag}(0.01, 0.01, 0.01, 0.01)$ using the CS-MPC framework. The noise term represents modeling errors and the disturbance from the ground. The geometry of the road circuit is depicted in Fig. 6.8. The vehicle starts from the origin and drives around the track counter-clockwise. The state constraint is to keep the vehicle on the road and the system state close enough to the origin. Namely,

$$\begin{bmatrix} \beta_{\min} \\ r_{\min} \\ e_{\psi, \min} \\ e_{y, \min} \end{bmatrix} \leq x_k \leq \begin{bmatrix} \beta_{\max} \\ r_{\max} \\ e_{\psi, \max} \\ e_{y, \max} \end{bmatrix}, \quad (6.91)$$

for all $k \geq 0$. Notice that, although the road circuit in Fig. 6.8 is non-convex in the global coordinate frame, the state constraint (6.91) is convex. We set $\beta_{\max} = 0.1$ rad, $\beta_{\min} = -0.1$ rad, $r_{\min} = -1.5$ rad/s, $r_{\max} = 1.5$ rad/s, $e_{\psi, \min} = -0.5$ rad, $e_{\psi, \max} = 0.5$ rad, $e_{y, \min} = -2$ m, and $e_{y, \max} = 2$ m. In addition, the steering wheel angle is restricted to

$$\delta_{\min} \leq u_k \leq \delta_{\max}, \quad (6.92)$$

for all $k \geq 0$. In this work we set $\delta_{\min} = -0.25$ rad and $\delta_{\max} = 0.25$ rad. We set $p_{x,i} = 1.0 \times 10^{-3}$ and $p_{u,j} = 1.0 \times 10^{-3}$ for all i and j in this example. The length of the horizon is set to $N = 8$, which corresponds to 4 sec. The cost matrices are set as

$$Q = \text{diag}(10^{-2}, 0, 10^{-2}, 10^{-8}), \quad R = 1. \quad (6.93)$$

We chose these values to have the vehicle minimize the control energy while fully utilizing

Table 6.1: Vehicle parameters and values. (CoM: the center of mass of the vehicle).

Notation	Meaning	Used numerical value
m	Vehicle mass	1,653 kg
I_z	Vehicle yaw inertia	2,765 kgm ²
V_x	Longitudinal velocity	15 m/s
ℓ_F	Distance from CoM to the front axle	1.402 m
ℓ_R	Distance from CoM to the rear axle	1.646 m
C_f	Front tire cornering stiffness	42 kN/rad
C_r	Rear tire cornering stiffness	81 kN/rad

the width of the road.

Note that, unlike the previous example in Section 6.4.1, the approach in [95] does not work for this scenario, because the terminal covariance in (6.40) becomes

$$\Sigma_f = \begin{bmatrix} 0.0001 & -0.0000 & 0.0000 & 0.0002 \\ -0.0000 & 0.0001 & -0.0001 & -0.0072 \\ 0.0000 & -0.0001 & 0.0005 & -0.0003 \\ 0.0002 & -0.0072 & -0.0003 & 26.9796 \end{bmatrix}, \quad (6.94)$$

and the variance of e_y is too large and \mathcal{X}_f^μ becomes null due to the constraint (6.91)). Since Σ_f in (6.40) is an implicit function of the Q and R matrices, the only way to satisfy the constraint is by changing the Q and/or R weight matrices in the cost. Specifically, for this problem, one has to choose a larger value in the (4,4) component of the Q matrix, which eventually makes the vehicle stay on the centerline of the road. This will require trial-and-error, till a suitable value for Q_{44} is found. The CS-SMPC approach, on the other hand, allows us to directly shape Σ_f so that the state satisfies the probabilistic constraints at the end of the horizon. This also results in the mean state of the vehicle operating closer to the road boundaries, thus making full advantage of the available operational region.

We also compared against a deterministic MPC controller. Specifically, if we ignore

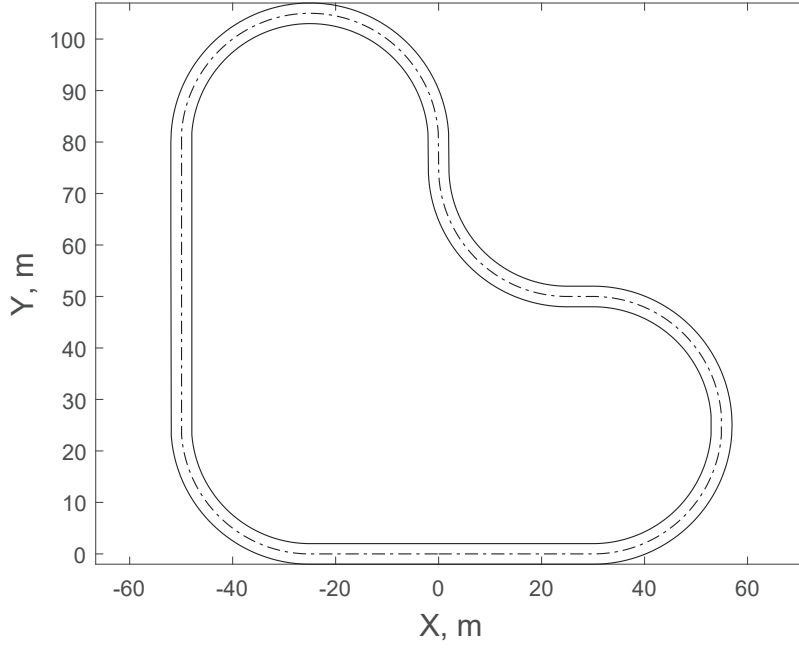


Figure 6.8: Geometry of the road circuit.

the additive noise in (6.90) at each time step, we minimize the following quadratic cost

$$J = \sum_{k=0}^{N-1} (x_k^\top Q x_k + u_k^\top R u_k) + x_N^\top Q_p x_N, \quad (6.95)$$

where Q_p is the solution of the following discrete-time algebraic Riccati equation

$$A^\top Q_p A - A^\top Q_p B (B^\top Q_p B + R)^{-1} B^\top Q_p A + Q = Q_p. \quad (6.96)$$

In addition, the terminal state x_N is constrained to be in the maximal control invariant set. The initial condition of the state is set to zero. The resulting trajectory without noise is depicted in Fig. 6.9. However, if noise is added to the system, this controller cannot satisfy the constraints as the vehicle gets too close to the inner edge of the road since the controller does not consider the additive noise. This case demonstrates the benefits of the stochastic control formulation.

Next, we present the result with the proposed CS-SMPC approach. In order to deter-

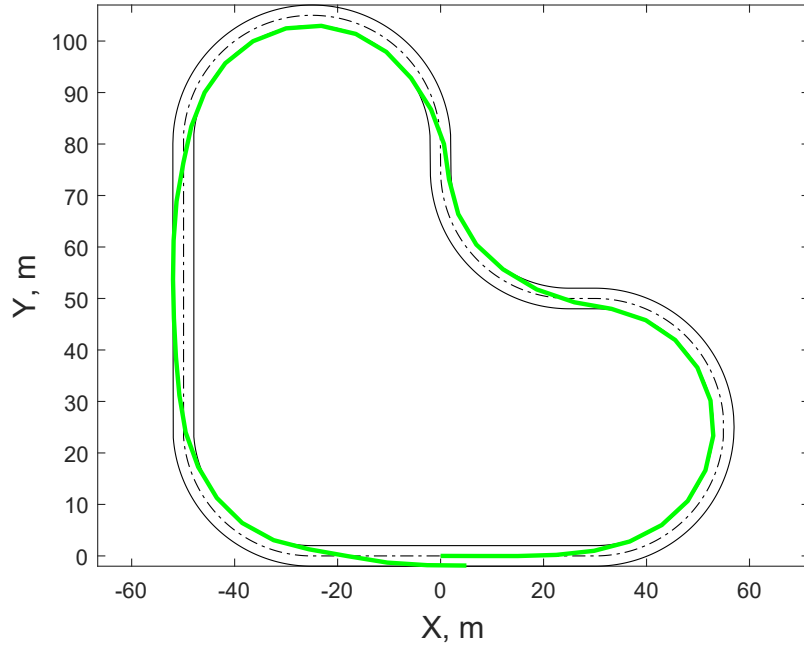


Figure 6.9: Result of Deterministic MPC without noise.

mine the terminal covariance, we first solve the following problem to obtain an assignable covariance.

$$\min \|\Sigma_f - \Sigma_f^d\|_F, \quad (6.97a)$$

$$\text{subject to (6.43)}, \quad (6.97b)$$

where Σ_f^d is a desired terminal covariance computed as the terminal covariance when the system is controlled by an LQR controller. Specifically, the covariance dynamics is

$$\Sigma_{t+1|k} = (A + BK_{\text{LQR}})\Sigma_{t|k}(A + BK_{\text{LQR}})^\top + DD^\top, \quad (6.98)$$

$$\Sigma_{k|k} = 0, \quad (6.99)$$

and we set $\Sigma_{k+N|k} = \Sigma_f^d$. In this example, the values of Σ_f^d and Σ_f were computed as

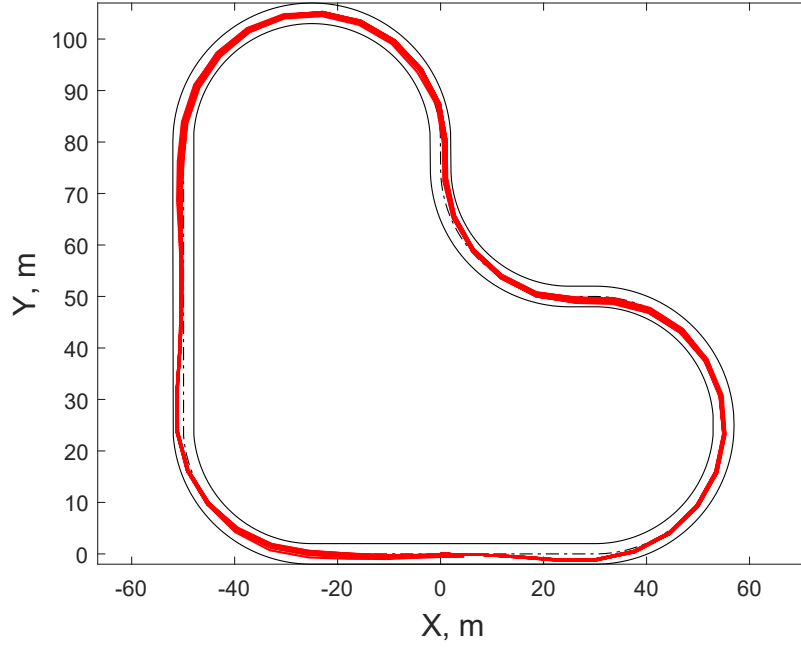


Figure 6.10: 100 sample trajectories controlled by CS-SMPC approach.

follows

$$\Sigma_f^d = \begin{bmatrix} 0.0001 & -0.0000 & 0.0000 & 0.0001 \\ -0.0000 & 0.0001 & -0.0001 & -0.0026 \\ 0.0000 & -0.0001 & 0.0004 & 0.0087 \\ 0.0001 & -0.0026 & 0.0087 & 0.3595 \end{bmatrix},$$

$$\Sigma_f = \begin{bmatrix} 0.0001 & -0.0000 & 0.0000 & 0.0001 \\ -0.0000 & 0.0002 & -0.0001 & -0.0023 \\ 0.0000 & -0.0001 & 0.0002 & -0.0002 \\ 0.0001 & -0.0023 & -0.0002 & 0.3640 \end{bmatrix}.$$

Using this value of Σ_f , we compute \tilde{K} based on (6.73) and P_{mean} based on (6.48). Figure 6.10 shows 100 sample trajectories controlled by the CS-SMPC algorithm. The vehicle successfully satisfies the constraints and stays on the road.

6.5 Discussion and Summary

In this chapter, we introduced a novel stochastic model predictive control scheme for constrained linear systems with additive Gaussian noise. The proposed approach makes use of the recently developed finite horizon optimal covariance steering theory, which converts the original stochastic optimal control problem at each iteration of the MPC algorithm to a deterministic convex programming problem. In addition to the conventional terminal cost and terminal mean constraints, we introduced terminal covariance constraints in the stochastic model predictive control theory and showed that the CS-SMPC approach ensures recursive feasibility and guaranteed stability even when the system has unbounded additive Gaussian noise. In addition, in the numerical simulations, we showed that the approach of covariance steering to compute future state covariance is more precise and computationally more efficient than the previously proposed approaches in the literature.

Future work include the investigation of CS-SMPC with measurement noise. In addition, a more efficient initialization strategy will be an interesting research topic.

CHAPTER 7

CONCLUSIONS

In this chapter, we provide a brief summary of the contribution of this thesis in Section 7.1. Furthermore, future work and open problems are introduced in Section 7.2.

7.1 Contributions

In this thesis, we have presented a novel stochastic optimal control algorithm, the optimal covariance steering (OCS) theory. Unlike conventional optimal control approaches that controls a single state, the proposed OCS theory computes the control commands simultaneously for the state mean and the state covariance. Because we focus on the control of linear systems with additive Gaussian noise, the state variable remains Gaussian distributed. Thus, since a Gaussian distribution can be fully described by the first two moments, the proposed OCS theory allows us to control the whole state distribution and quantify the effect of uncertainty without conducting computationally demanding Monte-Carlo simulations.

In the following, we provide the list of specific contributions of this dissertation.

1. Incorporation of State Constraints to Optimal Covariance Steering Theory
 - (a) First work that solves covariance steering problem with state chance constraints.
 - i. Utilization of convex optimization theory.
 - ii. Problem reformulation as a semidefinite programming problem.
 - (b) Proof of the coupling between the state mean and covariance trajectories when state constraints exist.
 - i. Demonstration of the reason simultaneously optimizing the mean and covariance trajectories are preferable.

- ii. Analytical treatment of the state chance constraints with polytopic feasible state space and additive Gaussian noise assumptions.
 - (c) Proposition of an efficient control policy.
 - i. Relaxation of the nonconvex terminal covariance constraint.
 - ii. Proposition of a novel affine parameterization approach for stochastic optimal control.
2. Application of the Optimal Covariance Steering Theory to Path Planning Problems
- (a) Nontrivial extension of the optimal covariance steering theory to incorporate non-convex state constraints.
 - i. Problem formulation as a mixed-integer convex programming problem.
 - ii. Introduction of an efficient approach that represents the non-convex feasible state space as a union of over-lapping convex state sub-spaces.
 - (b) Application to path planning with closed-loop prediction.
 - i. Simultaneous optimization of feedforward and feedback control actions.
 - ii. Analytical computation of feasible nominal paths without using sampling-based approaches.
 - iii. Extension to multi-vehicle path planning under uncertainty.
3. Introduction of Input Hard Constraints to Optimal Covariance Steering
- (a) Utilized element-wise saturation functions to limit the effect of unbounded disturbance to the control command.
 - i. Minor modification to the original formulation with additional linear equality and inequality constraints.
 - ii. Introduction of the Chebyshev-Cantelli inequality to deal with chance constraints with non-Gaussian state distributions.

- (b) Demonstration of the approach with a more realistic scenario such as the control of aircraft that has minimum and maximum thrust.
 - i. Probabilistic state chance constraints.
 - ii. Deterministic input hard constraints.
4. Application to Stochastic Model Predictive Control Theory
- (a) First work to apply the optimal covariance steering theory to stochastic model predictive control for linear systems with additive unbounded Gaussian noise.
 - i. Incorporation of terminal covariance constraints in addition to conventional terminal cost and terminal mean constraints.
 - ii. Efficient computation of control commands that satisfy the constraints by utilizing the OCS theory.
 - iii. A new method that can be categorized as an affine parameterization approach.
 - (b) Proof of the following properties of the proposed CS-SMPC algorithm.
 - i. Recursive feasibility.
 - ii. Guaranteed stability.
 - (c) Application to an autonomous driving problem.
 - i. Design of terminal maximal covariance based on covariance assignment theory.
 - ii. Demonstration of the efficiency of the algorithm.

7.2 Future Work and Open Problems

The idea of steering the covariance encompasses new research directions. Specifically, as future research directions, we can propose the following:

7.2.1 Optimal Risk Allocation for Optimal Covariance Steering

In this thesis, we converted state chance constraints to second-order cone constraints. This conversion was possible with the assumption that the probabilistic threshold values were pre-specified constant. In some scenarios, however, this setting may be restrictive, and one may want to use joint state chance constraint setting and formulate the probabilistic thresholds to be design variables, the value of which are optimally assigned. There are a number of algorithms proposed to optimally allocate risk for chance-constrained optimal control problem [119, 102, 120, 121, 68]. Notice that this problem formulation makes the state chance constraint a non-convex multiplicative constraint, and thus, many local optima exist. It will be interesting to investigate a fast algorithm to find a local minimum or a method to find the global minimum for the joint state chance constrained optimal covariance steering.

7.2.2 Variable Horizon Optimal Covariance Steering

The optimal covariance steering theories we have developed so far have assumed that the terminal time step N is given a priori. There are some situations that involve the difficulty of pre-determining the terminal time step. The approach in [122] introduced a binary design variable in the objective function and penalized the length of the horizon for the problem of control energy minimization. A similar approach can be applied to the optimal covariance steering problem as follows. We deal with the following cost function

$$J(u_0, \dots, u_N - 1) = \mathbb{E} \left[\sum_{k=0}^{N-1} (kb_k + u_k^\top R_k u_k) \right],$$

where $b_k \in \{0, 1\}^N$ are subject to the constraint

$$\sum_{k=0}^{N-1} b_k = 1.$$

With a sufficiently large constant $M \in \mathbb{R}$, we deal with the state mean dynamics as

$$\begin{aligned}\mu_{k+1} &\leq A_k \mu_k + B_k v_k + \sum_{j=0}^{k-1} b_j M, \\ \mu_{k+1} &\geq A_k \mu_k + B_k v_k - \sum_{j=0}^{k-1} b_j M,\end{aligned}$$

for all $k = 0, \dots, N-1$. These conditions imply that the state mean has to follow the dynamics when $k \leq N^*$, where N^* is the optimal step size, but when $k > N^*$, the state mean does not have to follow the dynamics. The terminal mean constraint can be represented as

$$\begin{aligned}\mu_k &\leq \mu_f + (1 - b_k)M, \\ \mu_k &\geq \mu_f - (1 - b_k)M,\end{aligned}$$

which is equivalent to

$$\mu_k = \begin{cases} \mu_f, & \text{if } k = N^*, \\ \text{free}, & \text{otherwise.} \end{cases}$$

Similarly, the terminal covariance constraint can be formulated as

$$(1 - b_k)M + 1 - \|S(I + \mathcal{B}K)^\top E_k^\top \Sigma_f^{-1/2}\| \geq 0.$$

While the approach above can solve some problems, we found that this approach is computationally demanding. A more computationally efficient approach is preferable.

7.2.3 Optimal Covariance Steering with Measurement Noise

A natural extension of the optimal covariance steering theory is to incorporate measurement noise. A covariance controller for such system has been proposed in [107], which requires all the state information from the initial time step. By modifying the proposed OCS theory

in this thesis, which requires only the current value of the filtered noise, we will be able to design a computationally more efficient controller. In addition, stochastic model predictive control with measurement noise is also a major research topic [80, 81], and the OCS theory with measurement noise is also expected to contribute to this research community.

7.2.4 Path Planning under Uncertainty using Optimal Covariance Steering

The path planning algorithm we discussed in Chapter 4 has some room for improvement. One interesting extension is to combine the algorithm with a sampling based method. For example, the work in [48, 49] proposed the chance-constrained RRT and RRT* algorithms. These approaches consider only the open-loop trajectories of the state and future corrective action to the nominal path was not considered. Thus combining the RRT algorithm with the optimal covariance steering method is expected to generate less conservative nominal trajectories.

7.2.5 Swarm Control using Optimal Covariance Steering

The problem of moving a swarm of robots from a initial spatial configuration to a target configuration in finite time can be formulated as a density control problem [12, 13, 14]. In fact, such multi-robot control approaches have been implemented [123, 124] and the effectiveness has been demonstrated [125]. It will be interesting to apply the OCS theory to compute density functions that optimally controls a swarm of robots and experimentally validate the performance.

7.2.6 Optimal Covariance Steering Theory for Linear Systems with Multiplicative Noise

An interesting research topic is the optimal covariance steering theory for linear systems with multiplicative noise. Such systems are of interest for financial applications, e.g., stock price dynamics can be represented as a linear system with multiplicative noise [126, 127]. While stochastic model predictive control of such systems has been attempted by a number

of researchers, e.g., [94, 128], to the author's knowledge, covariance steering theory has not been developed for linear systems with multiplicative noise. The system can be described as the following.

$$x_{k+1} = A_k x_k + B_k u_k + \sum_{i=1}^q [\bar{A}_{k,i} x_k + \bar{B}_{k,i} u_k] w_{k,i},$$

where $\{w_{k,i}\} \in \mathbb{R}$ ($i = 1, \dots, q$) are independent and identically distributed (i.i.d.) Gaussian noise with zero-mean unit variance, i.e.,

$$\mathbb{E}[w_{k,j}] = 0, \quad \mathbb{E}[w_{k_1,i_1} w_{k_2,i_2}] = \begin{cases} 1, & \text{if } k_1 = k_2 \text{ \& } i_1 = i_2, \\ 0, & \text{otherwise.} \end{cases}$$

Notice that the system dynamics can be also described as

$$\begin{aligned} x_{k+1} &= \tilde{A}_k x_k + \tilde{B}_k u_k, \\ \tilde{A}_k &= A_k + \sum_{i=1}^q \bar{A}_{k,i} w_{k,i}, \\ \tilde{B}_k &= B_k + \sum_{i=1}^q \bar{B}_{k,i} w_{k,i}. \end{aligned}$$

It will be interesting to import some results from the stochastic model predictive control research and solve the optimal covariance steering problem for systems with multiplicative noise.

7.2.7 Optimal Covariance Steering-based ADAS or Human Robot Interaction

Last, but not least, the application of the CS-SMPC algorithm to advanced driver assist systems (ADAS) and investigate human robot interaction will be an interesting research topic. Similar to the work in [129, 130], a haptic-shared ADAS can be a good application for the CS-SMPC as it can efficiently compute the future closed-loop motion of the system.

Specifically, we can consider the following system.

$$x_{k+1} = A_k x_k + B_k u_k + D_k w_k + g_k,$$

where g_k is the nominal prediction of the human control to the system, which can be predicted based on some algorithms [131], and we can regard the term $D_k w_k$ as the error between the actual and the predicted human control actions. As the new algorithm considers the uncertainty in the system, this formulation allows the ADAS to compute the most appropriate commands by taking into account human corrective actions, where human drivers are expected to be more robustly and properly assisted than when deterministic systems are employed. Furthermore, the following are possible applications.

7.2.8 Corrective Steering while Obstacle Avoidance

The work in [132] computed supportive actions while avoiding obstacles using a stochastic-tube MPC algorithm. While the authors of [132] claimed that the approach computed the smallest corrective steering action needed to satisfy the safety constraints, this approach assumed that the feedback gain is a constant, which leads to conservativeness and the algorithm may execute some unnecessary corrective actions. The CS-SMPC approach is able to compute time-varying feedback gains efficiently and is expected to produce less conservative results.

7.2.9 ADAS for Aggressive Driving

Vehicle power-sliding is one of the maneuvers that only skilled drivers can deal with, and there are a number of works on autonomously conduct such aggressive maneuvers, e.g., [133]. An interesting topic is the development of an ADAS that supports the driver only when necessary, and the capability of efficiently computing the closed-loop future vehicle motion by the CS-SMPC will play a key role. Applying this approach to aggressive

driving will enhance the safety of the road by assisting the driver in emergency situations such as slipping on a slippery road.

Appendices

APPENDIX A

AUTHOR'S PUBLICATIONS

This chapter provides the complete list of publications by the author.

A.1 Journals

1. **K. Okamoto**, P. Tsiotras, “Stochastic Model Predictive Control for Constrained Linear Systems Using Optimal Covariance Steering,” *Automatica* (under review).
2. **K. Okamoto**, P. Tsiotras, “Optimal Stochastic Vehicle Path Planning Using Covariance Steering,” *IEEE Robotics and Automation Letters*, vol. 4, no. 3, pp. 2276 – 2281, 2019.
3. **K. Okamoto**, L. Itti, P. Tsiotras, “Vision-Based Autonomous Path Following Using a Human Driver Control Model with Reliable Input-Feature Value Estimation,” *IEEE Transactions on Intelligent Vehicles*, vol. 4, no. 3, pp. 497 – 506, 2019.
4. **K. Okamoto**, P. Tsiotras, “Data-Driven Human Driver Lateral Control Models for Developing Haptic-Shared Control Advanced Driver Assist Systems,” *Robotics and Autonomous Systems*, vol. 114, pp 155 – 171, 2019.
5. **K. Okamoto**, M. Goldshtein, P. Tsiotras, “Optimal Covariance Control for Stochastic Systems Under Chance Constraints,” *IEEE Control Systems Letters*, vol. 2, no. 2, pp. 266 - 271, 2018.
6. **K. Okamoto**, T. Tsuchiya, “Optimal Aircraft Control in Stochastic Severe Weather Conditions,” *Journal of Guidance, Control, and Dynamics*, vol. 39, no. 1, pp. 77-85, 2016.

A.2 Conferences

1. **K. Okamoto**, P. Tsiotras, “Input Hard Constrained Optimal Covariance Steering,” *IEEE Conference on Decision and Control*, Dec. 2019, Nice, France (to appear).
2. J. Ridderhof, **K. Okamoto**, P. Tsiotras, “Nonlinear Uncertainty Control with Iterative Covariance Steering,” *IEEE Conference on Decision and Control*, Dec. 2019, Nice, France (to appear).
3. **K. Okamoto**, P. Tsiotras, “Optimal Stochastic Vehicle Path Planning Using Covariance Steering,” *IEEE International Conference on Robotics and Automation*, May 2019, Montreal, Canada.
4. **K. Okamoto**, M. Goldshtein, P. Tsiotras, “Optimal Covariance Control for Stochastic Systems Under Chance Constraints,” *IEEE Conference on Decision and Control*, Dec. 2018, Miami Beach, Florida.
5. **K. Okamoto**, P. Tsiotras, “A Comparative Study of Data-Driven Human Driver Lateral Control Models,” *American Control Conference*, June 2018, Milwaukee, Wisconsin.
6. **K. Okamoto**, K. Berntorp, S. Di Cairano, “Driver Intention-based Vehicle Threat Assessment using Random Forests and Particle Filtering,” *The World Congress of the International Federation of Automatic Control*, July 2017, Toulouse, France.
7. **K. Okamoto**, K. Berntorp, S. Di Cairano, “Similarity-Based Vehicle-Motion Prediction,” *American Control Conference*, May 2017, Seattle, Washington.
8. **K. Okamoto**, P. Tsiotras, “A New Hybrid Sensorimotor Driver Model with Model Predictive Control,” *IEEE International Conference on Systems, Man, and Cybernetics Society*, Oct. 2016, Budapest, Hungary (Best Student Paper Finalist).

9. Y. Matsuno, **K. Okamoto**, T. Tsuchiya, “Conflict-free 4D Trajectory Optimization in Uncertain Environments,” *Asia-Pacific International Symposium on Aerospace Technology*, Nov. 2013, Takamatsu, Japan.
10. **K. Okamoto**, Y. Matsuno, T. Tsuchiya “Trajectory Optimization of a Small UAV in a Stochastic Environment,” *Asia-Pacific International Symposium on Aerospace Technology*, Nov. 2013, Takamatsu, Japan.
11. **K. Okamoto**, T. Tsuchiya, “Guidance Strategy for Small UAVs to Extend Mission Range by Utilizing Atmospheric Energy,” *AIAA Infotech@Aerospace 2013 Conference*, Aug. 2013, Boston, Massachusetts.
12. **K. Okamoto**, T. Tsuchiya, “Guidance Strategy to Minimize Airplane Fuel Usage by Utilizing Wind Field,” *SICE Navigation and Control Symposium*, May 2013, Sagami-hara, Japan (Japanese).

A.3 Patents

1. K. Berntorp, **K. Okamoto**, S. Di Cairano, “System and Method for Controlling Motion of Vehicle in Shared Environment,” US 10,324,469.

APPENDIX B
SUPPLEMENTARY MATERIAL FOR CHAPTER 5

Lemma 3. *If a random variable $z \in \mathbb{R}$ is sampled from a Gaussian distribution $\mathcal{N}(0, \sigma_z^2)$ and the saturation function $\varphi(\cdot)$ is such that*

$$\varphi(z) = \begin{cases} \zeta & \text{if } \zeta \leq z, \\ z & \text{if } -\zeta \leq z \leq \zeta, \\ -\zeta & \text{if } z \leq -\zeta, \end{cases} \quad (\text{B.1})$$

then the following holds.

$$\mathbb{E}[\varphi(z)^2] = \zeta^2 \left(1 - \Phi \left(\frac{\zeta}{\sqrt{2}\sigma_z} \right) \right) + \sigma_z^2 \Phi \left(\frac{\zeta}{\sqrt{2}\sigma_z} \right) - \frac{2\zeta\sigma_z}{\sqrt{2\pi}} e^{-\frac{\zeta^2}{2\sigma_z^2}}, \quad (\text{B.2})$$

$$\mathbb{E}[z\varphi(z)] = \sigma_z^2 \Phi \left(\frac{\zeta}{\sqrt{2}\sigma_z} \right), \quad (\text{B.3})$$

where $\Phi(\cdot)$ is the error function.

Proof. It follows from (B.1) and the definition of the expectation that

$$\begin{aligned} \mathbb{E}[\varphi(z)^2] &= \frac{1}{\sqrt{2\pi}\sigma_z} \int_{-\infty}^{\infty} \varphi(z)^2 e^{-\frac{z^2}{2\sigma_z^2}} dz, \\ &= \frac{1}{\sqrt{2\pi}\sigma_z} \left\{ \int_{-\infty}^{-\zeta} \zeta^2 e^{-\frac{z^2}{2\sigma_z^2}} dz + \int_{-\zeta}^{\zeta} z^2 e^{-\frac{z^2}{2\sigma_z^2}} dz + \int_{\zeta}^{\infty} \zeta^2 e^{-\frac{z^2}{2\sigma_z^2}} dz \right\}, \end{aligned}$$

which leads to (B.2), and that

$$\begin{aligned} \mathbb{E}[z\varphi(z)] &= \frac{1}{\sqrt{2\pi}\sigma_z} \int_{-\infty}^{\infty} z\varphi(z) e^{-\frac{z^2}{2\sigma_z^2}} dz, \\ &= \frac{1}{\sqrt{2\pi}\sigma_z} \left\{ \int_{-\infty}^{-\zeta} z(-\zeta) e^{-\frac{z^2}{2\sigma_z^2}} dz + \int_{-\zeta}^{\zeta} z^2 e^{-\frac{z^2}{2\sigma_z^2}} dz + \int_{\zeta}^{\infty} z\zeta e^{-\frac{z^2}{2\sigma_z^2}} dz \right\}, \end{aligned}$$

which leads to (B.3). □

Lemma 4. *Let the matrix $\Sigma_{XX} \in \mathbb{R}^{2(N+1)n_x \times 2(N+1)n_x}$ be defined as*

$$\begin{aligned} \Sigma_{XX} = & \begin{bmatrix} \mathcal{A} \\ \mathcal{A} \end{bmatrix} \begin{bmatrix} \Sigma_0 & \mathbb{E}[\zeta_0 \varphi(\zeta_0)^\top] \\ \mathbb{E}[\varphi(\zeta_0) \zeta_0^\top] & \mathbb{E}[\varphi(\zeta_0) \varphi(\zeta_0)^\top] \end{bmatrix} \begin{bmatrix} \mathcal{A}^\top \\ \mathcal{A}^\top \end{bmatrix} \\ & + \begin{bmatrix} \mathcal{D} \\ \mathcal{D} \end{bmatrix} \begin{bmatrix} \Sigma_W & \mathbb{E}[W \varphi(W)^\top] \\ \mathbb{E}[\varphi(W) W^\top] & \mathbb{E}[\varphi(W) \varphi(W)^\top] \end{bmatrix} \begin{bmatrix} \mathcal{D}^\top \\ \mathcal{D}^\top \end{bmatrix}, \end{aligned}$$

where $\Sigma_0 = \mathbb{E}[\zeta_0 \zeta_0^\top]$ and $\Sigma_W = \mathbb{E}[W W^\top]$. Then, $\Sigma_{XX} \succeq 0$.

Proof. Consider vectors $x \in \mathbb{R}^{(N+1)n_x}$ and $y \in \mathbb{R}^{(N+1)n_x}$. Then,

$$\begin{aligned}
& \begin{bmatrix} x^\top & y^\top \end{bmatrix} \Sigma_{XX} \begin{bmatrix} x \\ y \end{bmatrix} \\
&= \begin{bmatrix} x^\top \mathcal{A} & y^\top \mathcal{A} \end{bmatrix} \begin{bmatrix} \Sigma_0 & \mathbb{E}[\zeta_0 \varphi(\zeta_0)^\top] \\ \mathbb{E}[\varphi(\zeta_0) \zeta_0^\top] & \mathbb{E}[\varphi(\zeta_0) \varphi(\zeta_0)^\top] \end{bmatrix} \begin{bmatrix} \mathcal{A}^\top x \\ \mathcal{A}^\top y \end{bmatrix} \\
&+ \begin{bmatrix} x^\top \mathcal{D} & y^\top \mathcal{D} \end{bmatrix} \begin{bmatrix} \Sigma_W & \mathbb{E}[W \varphi(W)^\top] \\ \mathbb{E}[\varphi(W) W^\top] & \mathbb{E}[\varphi(W) \varphi(W)^\top] \end{bmatrix} \begin{bmatrix} \mathcal{D}^\top x \\ \mathcal{D}^\top y \end{bmatrix}, \\
&= \begin{bmatrix} x^\top \mathcal{A} & y^\top \mathcal{A} \end{bmatrix} \mathbb{E} \left[\begin{bmatrix} \zeta_0 \\ \varphi(\zeta_0) \end{bmatrix} \begin{bmatrix} \zeta_0^\top & \varphi(\zeta_0)^\top \end{bmatrix} \right] \begin{bmatrix} \mathcal{A}^\top x \\ \mathcal{A}^\top y \end{bmatrix} \\
&+ \begin{bmatrix} x^\top \mathcal{D} & y^\top \mathcal{D} \end{bmatrix} \mathbb{E} \left[\begin{bmatrix} W \\ \varphi(W) \end{bmatrix} \begin{bmatrix} W^\top & \varphi(W)^\top \end{bmatrix} \right] \begin{bmatrix} \mathcal{D}^\top x \\ \mathcal{D}^\top y \end{bmatrix}, \\
&= \mathbb{E} \left[\begin{bmatrix} x^\top \mathcal{A} & y^\top \mathcal{A} \end{bmatrix} \begin{bmatrix} \zeta_0 \\ \varphi(\zeta_0) \end{bmatrix} \begin{bmatrix} \zeta_0^\top & \varphi(\zeta_0)^\top \end{bmatrix} \begin{bmatrix} \mathcal{A}^\top x \\ \mathcal{A}^\top y \end{bmatrix} \right] \\
&+ \mathbb{E} \left[\begin{bmatrix} x^\top \mathcal{D} & y^\top \mathcal{D} \end{bmatrix} \begin{bmatrix} W \\ \varphi(W) \end{bmatrix} \begin{bmatrix} W^\top & \varphi(W)^\top \end{bmatrix} \begin{bmatrix} \mathcal{D}^\top x \\ \mathcal{D}^\top y \end{bmatrix} \right], \\
&= \mathbb{E} [(x^\top \mathcal{A} \zeta_0 + y^\top \mathcal{A} \varphi(\zeta_0))(\zeta_0^\top \mathcal{A}^\top x + \varphi(\zeta_0)^\top \mathcal{A}^\top y)] \\
&+ \mathbb{E} [(x^\top \mathcal{D} W + y^\top \mathcal{D} \varphi(W))(W^\top \mathcal{D}^\top x + \varphi(W)^\top \mathcal{D}^\top y)], \\
&= \mathbb{E} [(x^\top \mathcal{A} \zeta_0 + y^\top \mathcal{A} \varphi(\zeta_0))^2] \\
&\quad + \mathbb{E} [(x^\top \mathcal{D} W + y^\top \mathcal{D} \varphi(W))^2] \geq 0.
\end{aligned}$$

It follows that $\Sigma_{XX} \succeq 0$. □

Lemma 5 (Chebyshev-Cantelli inequality [134]). *Let $z \in \mathbb{R}$ be a random variable with*

mean μ_z and variance Σ_z . Then, for any $c \geq 0$, the following inequality holds

$$\Pr(z \geq \mu_z + c) \leq \frac{\Sigma_z}{\Sigma_z + c^2}. \quad (\text{B.4})$$

APPENDIX 2

In this section, we describe the derivation of the new chance constraints in more detail. It follows from Lemma 5 that the following inequality on the random scalar variable $\alpha_j^\top E_k X$ holds

$$\Pr(\alpha_j^\top E_k X \geq \alpha_j^\top E_k \mathbb{E}[X] + c) \leq \frac{\alpha_j^\top E_k \mathbb{E}[\tilde{X} \tilde{X}^\top] E_k^\top \alpha_j^\top}{\alpha_j^\top E_k \mathbb{E}[\tilde{X} \tilde{X}^\top] E_k^\top \alpha_j^\top + c^2}, \quad (\text{B.5})$$

which is equivalent to

$$\Pr(\alpha_j^\top E_k X \leq \alpha_j^\top E_k \mathbb{E}[X] + c) > 1 - \frac{\alpha_j^\top E_k \mathbb{E}[\tilde{X} \tilde{X}^\top] E_k^\top \alpha_j^\top}{\alpha_j^\top E_k \mathbb{E}[\tilde{X} \tilde{X}^\top] E_k^\top \alpha_j^\top + c^2}, \quad (\text{B.6})$$

In addition, because of (5.15c), we are interested in

$$\Pr(\alpha_{x,i}^\top E_k X \leq \beta_{x,i}) \geq 1 - p_{x,i}, \quad (\text{B.7})$$

We wish to compute $c > 0$ that satisfies

$$p_{x,i} = \frac{\alpha_j^\top E_k \mathbb{E}[\tilde{X} \tilde{X}^\top] E_k^\top \alpha_j^\top}{\alpha_j^\top E_k \mathbb{E}[\tilde{X} \tilde{X}^\top] E_k^\top \alpha_j^\top + c^2}, \quad (\text{B.8})$$

and obtain

$$c = \sqrt{\frac{1 - p_{x,i}}{p_{x,i}}} \sqrt{\alpha_{x,i}^\top E_k \mathbb{E}[\tilde{X} \tilde{X}^\top] E_k^\top \alpha_{x,i}^\top}. \quad (\text{B.9})$$

Therefore, the following inequality holds

$$\begin{aligned} \Pr\left(\alpha_{x,i}^\top E_k X \leq \alpha_{x,i}^\top E_k \mathbb{E}[X] \right. \\ \left. + \sqrt{\frac{1-p_{x,i}}{p_{x,i}}} \sqrt{\alpha_{x,i}^\top E_k \mathbb{E}[\tilde{X} \tilde{X}^\top] E_k^\top \alpha_{x,i}^\top}\right) > 1 - p_{x,i}. \end{aligned} \quad (\text{B.10})$$

By comparing (B.7) and (B.10), we can claim that (B.7) is satisfied if

$$\alpha_{x,i}^\top E_k \mathbb{E}[X] + \sqrt{\frac{1-p_{x,i}}{p_{x,i}}} \sqrt{\alpha_{x,i}^\top E_k \mathbb{E}[\tilde{X} \tilde{X}^\top] E_k^\top \alpha_{x,i}^\top} \leq \beta_{x,i}, \quad (\text{B.11})$$

which is equivalent to the second order cone constraint in terms of V and K (5.19b).

APPENDIX C

MATLAB CODE

This chapter provides sample MATLAB codes of covariance steering. For comparison, the main.m file runs the mean steering and the covariance steering without chance constraints (See Chapter 3). One also needs the error_ellipse.m from https://www.mathworks.com/matlabcentral/fileexchange/4705-error_ellipse

main.m

```
1 clear all;
2 clc;
3
4 % Set Horizon
5 Ncands = [5, 10, 20, 30, 40, 50];
6 lenN = length(Ncands);
7 SolverTime = zeros(1, lenN);
8 SolverTimeMS = zeros(1, lenN);
9 SolverTimenoChance = zeros(1, lenN);
10 objValue = zeros(1, lenN);
11 objValueMS = zeros(1, lenN);
12 objValuenoChance = zeros(1, lenN);
13 drawProblemSetup(3*lenN+1);
14 for i = 1:lenN
15     PS = loadProblemSetup(Ncands(i));
16     % Solve Mean Steering Problem
17     [SolverTimeMS(i), objValueMS(i)] = SolveMS(PS,3*i-2);
18     % Solve Covariance Steering Problem ignoring Chance Constraints
```

```

19     [SolverTimeNoChance(i), objValueNoChance(i)] = SolveOCSnoChance(PS
        ,3*i-1);
20     % Solve Covariance Steering Problem
21     [SolverTime(i), objValue(i)] = SolveOCS(PS,3*i);
22 end

```

drawProblemSetup.m

```

1 function drawProblemSetup(fignum)
2     figure(fignum);clf;
3     PS = loadProblemSetup(1);
4     rl = 0.9973;% 3 Sigma
5     hold on;
6     error_ellipse('C',PS.Sigma0(1:2,1:2),'mu',PS.mu0(1:2),'conf',rl,'
        style','r','linewidth',2);
7     error_ellipse('C',PS.Sigmaf(1:2,1:2),'mu',PS.muf(1:2),'conf',rl,'
        style','m','linewidth',2);
8     x = linspace(-12,1);
9     plot(x,-1/5*x + 1/5,'g-','linewidth',2);
10    plot(x, 1/5*x - 1/5,'g-','linewidth',2);
11    hold off;
12    grid on;
13    axis equal;
14    axis equal;set(gca,'fontsize',16);
15    xlabel('x');
16    ylabel('y');
17 end

```

loadProblemSetup.m

```

1  % This function returns the problem setup (PS) given the length of the
2  % horizon N.
3
4  function PS = loadProblemSetup(N)
5      PS.N = N;
6      % Initial condition
7      PS.mu0 = [-10;1;0;0];
8      PS.Sigma0 = blkdiag(0.05,0.05,0.01,0.01);
9      % Terminal Condition
10     PS.muf = [0;0;0;0];
11     PS.Sigmaf = blkdiag(0.01,0.01,0.001,0.001);
12     % Linear System
13     dt = 0.2;
14     PS = defineDynamics(PS, dt);
15     % Probability threshold
16     PS.alpha = [1 5 0 0;
17                 1 -5 0 0]';
18     PS.beta = 1;
19     PS.delta = 0.0005;
20     % Objective function
21     PS = makeCost(PS, blkdiag(0.5,4,0.05,0.05),blkdiag(20,20));
22     % Make Large Matrices
23     PS = makeLargeMatrices(PS);
24 end
25
26 function PS = defineDynamics(PS, dt)

```

```

27     PS.nx = 4;
28     PS.nu = 2;
29     PS.nw = 4;
30     PS.A = [1 0 dt 0; 0 1 0 dt; 0 0 1 0; 0 0 0 1];
31     PS.B = [dt^2/2 0; 0 dt^2/2; dt 0; 0 dt];
32     PS.D = 0.01*eye(PS.nx);
33 end
34
35 function PS = makeCost(PS,Q0,R0)
36     Q = [];
37     R = [];
38     for i = 1:PS.N
39         Q = blkdiag(Q,Q0);
40         R = blkdiag(R,R0);
41     end
42     Q = blkdiag(Q,zeros(PS.nx));
43     PS.Q = Q;
44     PS.R = R;
45 end
46
47 function PS = makeLargeMatrices(PS)
48     nx = PS.nx;
49     nu = PS.nu;
50     nw = PS.nw;
51     N = PS.N;
52     A = PS.A;
53     B = PS.B;

```



```

54     D = PS.D;
55     ScriptA = eye(nx);
56     ScriptB = zeros(nx,nu*N);
57     ScriptD = zeros(nx,nw*N);
58     for k = 1:N
59         ScriptA = [ScriptA; A*ScriptA(end-nx+1:end,:)];
60         ScriptB = [ScriptB; A*ScriptB(end-nx+1:end,1:(k-1)*nu) B zeros
                    (nx,(N-k)*nu)];
61         ScriptD = [ScriptD; A*ScriptD(end-nx+1:end,1:(k-1)*nw) D zeros
                    (nx,(N-k)*nw)];
62     end
63     PS.ScriptA = ScriptA;
64     PS.ScriptB = ScriptB;
65     PS.ScriptD = ScriptD;
66 end

```

solveMS.m

```

1  % This file solves the mean steering problem.
2  % State chance constraints and terminal covariance constraints are NOT
   imposed.
3
4  function [time,obj] = SolveMS(PS,fignum)
5      N = PS.N;
6      nx = PS.nx;
7      nu = PS.nu;
8      ScriptA = PS.ScriptA;
9      ScriptB = PS.ScriptB;

```

```

10 % Define optimization variables
11 V = sdpvar(nu*N,1);
12 % Useful matrices
13 EN = [zeros(nx,N*nx) eye(nx)];
14 % System Dynamics
15 EX = ScriptA * PS.mu0 + ScriptB * V;
16 % Define constraints
17 Constraints = [];
18 % Boundary condition
19 Constraints = [Constraints, EN*EX == PS.muf];
20 % Objective Function
21 Objective = EX'*PS.Q*EX + V'*PS.R*V;
22 % Solve the Problem
23 options = sdpsettings('solver','mosek');
24 sol = optimize(Constraints,Objective,options);
25 % Get performance measure values
26 time = sol.solvertime;
27 obj = value(Objective);
28 % Extract and display value
29 V = value(V);
30 K = [];
31 for i = 1:N
32     K = blkdiag(K,zeros(nu,nx));
33 end
34 K = [K,zeros(nu*N,nx)];
35 drawResult(fignum,100,V,K,PS);
36 end

```

solveOCSnoChance.m

```

1  % This file solves the OCS problem WITHOUT state chance constraints
2  function [time,obj,NonZeroElements] = SolveOCSnoChance(PS,fignum)
3      N = PS.N;
4      nx = PS.nx;
5      nu = PS.nu;
6      ScriptA = PS.ScriptA;
7      ScriptB = PS.ScriptB;
8      ScriptD = PS.ScriptD;
9      % Define optimization variables
10     V = sdpvar(nu*N,1);
11     K = [];
12     for i = 1:N
13         K = blkdiag(K,sdpvar(nu,nx));
14     end
15     K = [K,zeros(nu*N,nx)];
16     % Useful matrices
17     SigmaY = ScriptA*PS.Sigma0*ScriptA'+ScriptD*ScriptD';
18     IplusBK = eye((N+1)*nx)+ScriptB*K;
19     EN = [zeros(nx,N*nx) eye(nx)];
20     S = computeS(SigmaY);
21
22     % System Dynamics
23     EX = ScriptA * PS.mu0 + ScriptB * V;
24     Z = EN*IplusBK*S;
25
26     % Define constraints

```

```

27 Constraints = [];
28 % Boundary condition
29 Constraints = [Constraints, EN*EX == PS.muf];
30 Constraints = [Constraints, [PS.Sigmaf Z; Z' eye((N+1)*nx)] >= 0];
31 % Objective Function
32 Objective = EX'*PS.Q*EX + V'*PS.R*V + trace((IplusBK'*PS.Q*
    IplusBK + K'*PS.R*K)*SigmaY);
33 % Solve the Problem
34 options = sdpsettings('solver','mosek');
35 sol = optimize(Constraints,Objective,options);
36 % Get performance measure values
37 time = sol.solvertime;
38 obj = value(Objective);
39 NonZeroElements = nnz(value(V)) + nnz(value(K));
40 % Draw result
41 drawResult(fignum,100,value(V),value(K),PS);
42 end

```

solveOCS.m

```

1 % This file solves the OCS problem with state chance constraints
2 function [time,obj] = SolveOCS(PS,fignum)
3     N = PS.N;
4     nx = PS.nx;
5     nu = PS.nu;
6     ScriptA = PS.ScriptA;
7     ScriptB = PS.ScriptB;
8     ScriptD = PS.ScriptD;

```

```

9      % Define optimization variables
10     V = sdpvar(nu*N,1);
11     K = [];
12     for i = 1:N
13         K = blkdiag(K,sdpvar(nu,nx));
14     end
15     K = [K,zeros(nu*N,nx)];
16     % Useful matrices
17     SigmaY = ScriptA*PS.Sigma0*ScriptA'+ScriptD*ScriptD';
18     IplusBK = eye((N+1)*nx)+ScriptB*K;
19     EN = [zeros(nx,N*nx) eye(nx)];
20     S = computeS(SigmaY);
21
22     % System Dynamics
23     EX = ScriptA * PS.mu0 + ScriptB * V;
24     Z = EN*IplusBK*S;
25
26     % Define constraints
27     Constraints = [];
28     % Boundary condition
29     Constraints = [Constraints, EN*EX == PS.muf];
30     Constraints = [Constraints, [PS.Sigmaf Z; Z' eye((N+1)*nx)] >= 0];
31     % Chance Constraints
32     Constraints = chanceConstraints(Constraints,EX,S,IplusBK,PS);
33     % Objective Function
34     Objective = EX'*PS.Q*EX + V'*PS.R*V + trace((IplusBK'*PS.Q*
        IplusBK + K'*PS.R*K)*SigmaY);

```

```

35 % Solve the Problem
36 options = sdpsettings('solver','mosek');
37 sol = optimize(Constraints,Objective,options);
38 % Get performance measure values
39 time = sol.solvertime;
40 obj = value(Objective);
41 % Draw result
42 drawResult(fignum,100,value(V),value(K),PS);
43 end
44
45 function Constraints = chanceConstraints(Constraints,EX,S,IplusBK,PS)
46     a = PS.alpha;
47     b = PS.beta;
48     ICDF = norminv(1-PS.delta);
49     nx = PS.nx;
50     for k = 1:PS.N
51         Ek = [zeros(nx,k*nx) eye(nx) zeros(nx,(PS.N-k)*nx)];
52         for j = 1:2
53             Constraints = [Constraints, a(:,j)'*Ek*EX+ICDF*norm(S'*
54                             IplusBK'*Ek'*a(:,j))<=b];
55         end
56     end
57 end

```

computeS.m

```

1
2 function S = computeS(SigmaY)

```

```

3     [L,D] = ldl(SigmaY);
4     S = L * sqrtm(D);
5 end

```

drawResult.m

```

1 function drawResult(fignum,MCnum,V,K,PS)
2     figure(fignum);clf;
3     nx = PS.nx;
4     nu = PS.nu;
5     nw = PS.nw;
6     N = PS.N;
7     EX = PS.ScriptA*PS.mu0 + PS.ScriptB*V;
8     rng(0);
9     for mc = 1:MCnum
10         x0_MC = PS.mu0 + sqrtm(PS.Sigma0)*randn(nx,1);
11         U = zeros(nu,N);
12         x_MC = zeros(nx,N+1);
13         y_MC = zeros(nx,N+1);
14         x_MC(:,1) = x0_MC;
15         y_MC(:,1) = x0_MC - PS.mu0;
16         for k = 1:N
17             U(:,k) = V((k-1)*nu+1:k*nu) + K((k-1)*nu+1:k*nu,(k-1)*nx
                +1:k*nx) * y_MC(:,k);
18             w = randn(nw,1);
19             x_MC(:,k+1) = PS.A*x_MC(:,k) + PS.B*U(:,k) + PS.D*w;
20             y_MC(:,k+1) = PS.A*y_MC(:,k) + PS.D*w;
21         end

```

```

22     figure(fignum);hold on;plot(x_MC(1,:),x_MC(2:,:), 'color'
    ,[0.3,0.3,0.3]);hold off;
23 end
24 nominal = value(EX);
25 rl = 0.9973;% 3 Sigma
26 figure(fignum);
27 hold on;
28 plot(nominal(1:nx:end),nominal(2:nx:end),'r','linewidth',2);
29 error_ellipse('C',PS.Sigma0(1:2,1:2),'mu',PS.mu0(1:2),'conf',rl,'
    style','r','linewidth',2);
30 error_ellipse('C',PS.Sigmaf(1:2,1:2),'mu',PS.muf(1:2),'conf',rl,'
    style','m','linewidth',2);
31 IplusBK = eye((N+1)*nx)+PS.ScriptB*K;
32 SigmaY = PS.ScriptA*PS.Sigma0*PS.ScriptA'+PS.ScriptD*PS.ScriptD';
33 SX = IplusBK*SigmaY*IplusBK';
34 for k = 0:N
35     Ek = [zeros(nx,k*nx) eye(nx) zeros(nx,(PS.N-k)*nx)];
36     muk = Ek*nominal;
37     SXk = Ek*SX*Ek';
38     error_ellipse('C',SXk(1:2,1:2),'mu',muk(1:2),'conf',rl,'style'
    , 'b','linewidth',1);
39 end
40 x = linspace(-12,1);
41 plot(x,-1/5*x + 1/5,'g-.','linewidth',2);
42 plot(x, 1/5*x - 1/5,'g-.','linewidth',2);
43 hold off;
44 grid on;

```



```
45     titlestr = sprintf('N = %d',PS.N);
46     title(titlestr);
47     axis equal;set(gca,'fontsize',16);
48     xlabel('x');
49     ylabel('y');
50 end
```

REFERENCES

- [1] R. Bellman, “The theory of dynamic programming,” *Bulletin of the American Mathematical Society*, vol. 60, no. 6, pp. 503–515, 1954.
- [2] L. S. Pontryagin, E. Mishchenko, V. Boltyanskii, and R. Gamkrelidze, *The mathematical theory of optimal processes*. Fizmatgiz, Moscow, 1961 (in Russian); Pergamon, Oxford, 1964.
- [3] B. Açıkmeşe and S. R. Ploen, “Convex programming approach to powered descent guidance for Mars landing,” *Journal of Guidance, Control, and Dynamics*, vol. 30, no. 5, pp. 1353–1366, 2007.
- [4] B. Açıkmeşe, J. M. Carson, and L. Blackmore, “Lossless convexification of non-convex control bound and pointing constraints of the soft landing optimal control problem,” *IEEE Transactions on Control Systems Technology*, vol. 21, no. 6, pp. 2104–2113, 2013.
- [5] J. Ridderhof and P. Tsiotras, “Uncertainty quantification and control during mars powered descent and landing using covariance steering,” in *AIAA Guidance, Navigation, and Control Conference*, Kissimmee, FL, 2018, p. 0611.
- [6] G. Monge, “Mémoire sur la théorie des déblais et des remblais,” *Histoire de l’Académie Royale des Sciences de Paris*, 1781.
- [7] J.-D. Benamou and Y. Brenier, “A computational fluid mechanics solution to the monge-kantorovich mass transfer problem,” *Numerische Mathematik*, vol. 84, no. 3, pp. 375–393, 2000.
- [8] R. W. Brockett, “Optimal control of the liouville equation,” *AMS IP Studies in Advanced Mathematics*, vol. 39, p. 23, 2007.
- [9] R. Brockett, “Notes on the control of the liouville equation,” in *Control of partial differential equations*, 2012, pp. 101–129.
- [10] S. Mazurenko, “The dynamic programming method in systems with states in the form of distributions,” *Moscow University Computational Mathematics and Cybernetics*, vol. 35, pp. 133–141, 2011.
- [11] E. Bakolas, “Dynamic output feedback control of the liouville equation for discrete-time SISO linear systems,” *IEEE Transactions on Automatic Control*, 2019.

- [12] B. Açıkmeşe and D. S. Bayard, “Markov chain approach to probabilistic guidance for swarms of autonomous agents,” *Asian Journal of Control*, vol. 17, no. 4, pp. 1105–1124, 2015.
- [13] S. Bandyopadhyay, S.-J. Chung, and F. Y. Hadaegh, “Probabilistic swarm guidance using optimal transport,” in *2014 IEEE Conference on Control Applications*, Antibes, France, 2014, pp. 498–505.
- [14] L. C. Pimenta, N. Michael, R. C. Mesquita, G. A. Pereira, and V. Kumar, “Control of swarms based on hydrodynamic models,” in *IEEE International Conference on Robotics and Automation*, Pasadena, CA, 2008, pp. 1948–1953.
- [15] A Vinante, M Bignotto, M. Bonaldi, M Cerdonio, L Conti, P. Falferi, N Liguori, S Longo, R Mezzena, A Ortolan, *et al.*, “Feedback cooling of the normal modes of a massive electromechanical system to submillikelvin temperature,” *Physical review letters*, vol. 101, no. 3, p. 033 601, 2008.
- [16] M. Bonaldi, L Conti, P De Gregorio, L Rondoni, G Vedovato, A Vinante, M Bignotto, M Cerdonio, P. Falferi, N Liguori, *et al.*, “Nonequilibrium steady-state fluctuations in actively cooled resonators,” *Physical review letters*, vol. 103, no. 1, p. 010 601, 2009.
- [17] A. Geletu, M. Klöppel, H. Zhang, and P. Li, “Advances and applications of chance-constrained approaches to systems optimisation under uncertainty,” *International Journal of Systems Science*, vol. 44, no. 7, pp. 1209–1232, 2013.
- [18] K. J. Åström, *Introduction to Stochastic Control Theory*, R. Bellman, Ed. Academic Press New York and London, 1970.
- [19] W. H. Fleming and R. W. Rishel, *Deterministic and stochastic optimal control*. Springer Science & Business Media, 2012, vol. 1.
- [20] A. F. Hotz and R. E. Skelton, “A covariance control theory,” in *IEEE Conference on Decision and Control*, vol. 24, Fort Lauderdale, FL, 1985, pp. 552–557.
- [21] A. Hotz and R. E. Skelton, “Covariance control theory,” *International Journal of Control*, vol. 46, no. 1, pp. 13–32, 1987.
- [22] T Iwasaki and R. E. Skelton, “Quadratic optimization for fixed order linear controllers via covariance control,” in *American Control Conference*, Chicago, IL, 1992, pp. 2866–2870.
- [23] J.-H. Xu and R. E. Skelton, “An improved covariance assignment theory for discrete systems,” *IEEE transactions on Automatic Control*, vol. 37, no. 10, pp. 1588–1591, 1992.

- [24] K. Yasuda, R. E. Skelton, and K. M. Grigoriadis, "Covariance controllers: A new parametrization of the class of all stabilizing controllers," *Automatica*, vol. 29, no. 3, pp. 785–788, 1993.
- [25] E. Collins and R. Skelton, "A theory of state covariance assignment for discrete systems," *IEEE Transactions on Automatic Control*, vol. 32, no. 1, pp. 35–41, 1987.
- [26] K. M. Grigoriadis and R. E. Skelton, "Minimum-energy covariance controllers," *Automatica*, vol. 33, no. 4, pp. 569–578, 1997.
- [27] Y. Chen, T. T. Georgiou, and M. Pavon, "Optimal steering of a linear stochastic system to a final probability distribution, Part I," *IEEE Transactions on Automatic Control*, vol. 61, no. 5, pp. 1158–1169, 2016.
- [28] Y. Chen, T. Georgiou, and M. Pavon, "Optimal steering of a linear stochastic system to a final probability distribution, Part II," *IEEE Transactions on Automatic Control*, vol. 61, no. 5, pp. 1170–1180, 2016.
- [29] Y. Chen, T. T. Georgiou, and M. Pavon, "Optimal steering of a linear stochastic system to a final probability distribution, Part III," *IEEE Transactions on Automatic Control*, vol. 63, no. 9, pp. 3112–3118, 2018.
- [30] E. Schrödinger, *Über die Umkehrung der Naturgesetze*. Verlag Akademie der Wissenschaften in Kommission bei Walter de Gruyter u. Company, 1931.
- [31] L. V. Kantorovich, "On the transfer of masses," in *Dokl. Akad. Nauk. SSSR*, vol. 37, 1942, pp. 227–229.
- [32] A. Halder and E. D. Wendel, "Finite horizon linear quadratic Gaussian density regulator with Wasserstein terminal cost," in *American Control Conference*, Boston, MA, 2016, pp. 7249–7254.
- [33] E. Bakolas, "Optimal covariance control for stochastic linear systems subject to integral quadratic state constraints," in *American Control Conference*, Boston, MA, 2016, pp. 7231–7236.
- [34] A. Beghi, "On the relative entropy of discrete-time markov processes with given end-point densities," *IEEE Transactions on Information Theory*, vol. 42, no. 5, pp. 1529–1535, 1996.
- [35] B. C. Levy and A. Beghi, "Discrete-time gauss-markov processes with fixed reciprocal dynamics," *Journal of Mathematical Systems Estimation and Control*, vol. 7, pp. 55–80, 1997.

- [36] B. Jamison, “Reciprocal processes: The stationary gaussian case,” *The Annals of Mathematical Statistics*, vol. 41, no. 5, pp. 1624–1630, 1970.
- [37] I. G. Vladimirov and I. R. Petersen, “State distributions and minimum relative entropy noise sequences in uncertain stochastic systems: The discrete-time case,” *SIAM Journal on Control and Optimization*, vol. 53, no. 3, pp. 1107–1153, 2015.
- [38] M. Goldshtein and P. Tsiotras, “Finite-horizon covariance control of linear time-varying systems,” in *IEEE Conference on Decision and Control*, Melbourne, Australia, 2017, pp. 3606–3611.
- [39] E. Bakolas, “Optimal covariance control for discrete-time stochastic linear systems subject to constraints,” in *IEEE Conference on Decision and Control*, Las Vegas, NV, 2016, pp. 1153–1158.
- [40] —, “Finite-horizon covariance control for discrete-time stochastic linear systems subject to input constraints,” *Automatica*, vol. 91, pp. 61–68, 2018.
- [41] S. Boyd and L. Vandenberghe, *Convex optimization*. Cambridge university press, 2004.
- [42] L. Blackmore, M. Ono, and B. C. Williams, “Chance-constrained optimal path planning with obstacles,” *IEEE Transactions on Robotics*, vol. 27, no. 6, pp. 1080–1094, 2011.
- [43] S. M. LaValle, *Planning Algorithms*. Cambridge, UK: Cambridge University Press, 2006.
- [44] S. M. LaValle, “Rapidly-exploring random trees: A new tool for path planning,” Iowa State University, Tech. Rep., 1998.
- [45] S. Karaman and E. Frazzoli, “Sampling-based algorithms for optimal motion planning,” *The International Journal of Robotics Research*, vol. 30, no. 7, pp. 846–894, 2011.
- [46] O. Arslan and P. Tsiotras, “Use of relaxation methods in sampling-based algorithms for optimal motion planning,” in *IEEE International Conference on Robotics and Automation*, Karlsruhe, Germany, 2013, pp. 2421–2428.
- [47] M. P. Vitus, Z. Zhou, and C. J. Tomlin, “Stochastic control with uncertain parameters via chance constrained control,” *IEEE Transactions on Automatic Control*, vol. 61, no. 10, pp. 2892–2905, 2016.

- [48] B. Luders, M. Kothari, and J. How, “Chance constrained RRT for probabilistic robustness to environmental uncertainty,” in *AIAA Guidance, Navigation, and Control Conference*, Toronto, Canada, 2010, p. 8160.
- [49] B. D. Luders, S. Karaman, and J. P. How, “Robust sampling-based motion planning with asymptotic optimality guarantees,” in *AIAA Guidance, Navigation, and Control Conference*, Boston, MA, 2013, p. 5097.
- [50] S. C. Pinto and R. J. Afonso, “Risk constrained navigation using MILP-MPC formulation,” *IFAC-PapersOnLine*, vol. 50, no. 1, pp. 3586–3591, 2017.
- [51] M. Ono, M. Pavone, Y. Kuwata, and J. Balaram, “Chance-constrained dynamic programming with application to risk-aware robotic space exploration,” *Autonomous Robots*, vol. 39, no. 4, pp. 555–571, 2015.
- [52] A. Richards, T. Schouwenaars, J. P. How, and E. Feron, “Spacecraft trajectory planning with avoidance constraints using mixed-integer linear programming,” *Journal of Guidance, Control, and Dynamics*, vol. 25, no. 4, pp. 755–764, 2002.
- [53] S. Patil, J. Van Den Berg, and R. Alterovitz, “Estimating probability of collision for safe motion planning under Gaussian motion and sensing uncertainty,” in *International Conference on Robotics and Automation*, St. Paul, MN, 2012, pp. 3238–3244.
- [54] D. Lenz, T. Kessler, and A. Knoll, “Stochastic model predictive controller with chance constraints for comfortable and safe driving behavior of autonomous vehicles,” in *IEEE Intelligent Vehicles Symposium*, Seoul, South Korea, 2015, pp. 292–297.
- [55] Y. Kuwata, J. Teo, S. Karaman, G. Fiore, E. Frazzoli, and J. How, “Motion planning in complex environments using closed-loop prediction,” in *AIAA Guidance, Navigation and Control Conference*, Honolulu, HI, 2008, p. 7166.
- [56] O. Arslan, K. Berntorp, and P. Tsotras, “Sampling-based algorithms for optimal motion planning using closed-loop prediction,” in *IEEE International Conference on Robotics and Automation*, IEEE, Singapore, 2017, pp. 4991–4996.
- [57] J. Van Den Berg, P. Abbeel, and K. Goldberg, “LQG-MP: Optimized path planning for robots with motion uncertainty and imperfect state information,” *The International Journal of Robotics Research*, vol. 30, no. 7, pp. 895–913, 2011.
- [58] A. Bry and N. Roy, “Rapidly-exploring random belief trees for motion planning under uncertainty,” in *IEEE International Conference on Robotics and Automation*, Shanghai, China, 2011, pp. 723–730.

- [59] M. P. Vitus and C. J. Tomlin, “Closed-loop belief space planning for linear, Gaussian systems,” in *IEEE International Conference on Robotics and Automation*, Shanghai, China, 2011, pp. 2152–2159.
- [60] A.-A. Agha-Mohammadi, S. Chakravorty, and N. M. Amato, “FIRM: Sampling-based feedback motion-planning under motion uncertainty and imperfect measurements,” *The International Journal of Robotics Research*, vol. 33, no. 2, pp. 268–304, 2014.
- [61] T. Schouwenaars, B. De Moor, E. Feron, and J. How, “Mixed integer programming for multi-vehicle path planning,” in *European Control Conference*, Porto, Portugal, 2001, pp. 2603–2608.
- [62] D. Mellinger, A. Kushleyev, and V. Kumar, “Mixed-integer quadratic program trajectory generation for heterogeneous quadrotor teams,” in *IEEE International Conference on Robotics and Automation*, 2012, pp. 477–483.
- [63] R. Deits and R. Tedrake, “Efficient mixed-integer planning for UAVs in cluttered environments,” in *IEEE International Conference on Robotics and Automation*, Seattle, WA, 2015, pp. 42–49.
- [64] M. P. Vitus, S. L. Waslander, and C. J. Tomlin, “Locally optimal decomposition for autonomous obstacle avoidance with the tunnel-MILP algorithm,” in *IEEE Conference on Decision and Control*, Cancun, Mexico, 2008, pp. 540–545.
- [65] R. Deits and R. Tedrake, “Footstep planning on uneven terrain with mixed-integer convex optimization,” in *IEEE/RAS International Conference on Humanoid Robots*, Madrid, Spain, 2014, pp. 279–286.
- [66] K. Okamoto, M. Goldshtein, and P. Tsiotras, “Optimal covariance control for stochastic systems under chance constraints,” *IEEE Control Systems Letters*, vol. 2, no. 2, pp. 266–271, 2018.
- [67] J. Ridderhof and P. Tsiotras, “Minimum-fuel powered descent in the presence of random disturbances,” in *AIAA Guidance, Navigation, and Control Conference*, San Diego, CA, 2019.
- [68] J. A. Paulson, E. A. Buehler, R. D. Braatz, and A. Mesbah, “Stochastic model predictive control with joint chance constraints,” *International Journal of Control*, pp. 1–14, 2017.
- [69] P. Hokayem, E. Cinquemani, D. Chatterjee, F. Ramponi, and J. Lygeros, “Stochastic receding horizon control with output feedback and bounded controls,” *Automatica*, vol. 48, no. 1, pp. 77–88, 2012.

- [70] K. Okamoto and P. Tsiotras, “Optimal stochastic vehicle path planning using covariance steering,” *IEEE Robotics and Automation Letters*, 2019.
- [71] D. Q. Mayne, “Model predictive control: Recent developments and future promise,” *Automatica*, vol. 50, no. 12, pp. 2967–2986, 2014.
- [72] S. Di Cairano and I. V. Kolmanovsky, “Real-time optimization and model predictive control for aerospace and automotive applications,” in *2018 American Control Conference*, Milwaukee, WI, 2018, pp. 2392–2409.
- [73] U. Eren, A. Prach, B. B. Koçer, S. V. Raković, E. Kayacan, and B. Açıkmeşe, “Model predictive control in aerospace systems: Current state and opportunities,” *Journal of Guidance, Control, and Dynamics*, vol. 40, no. 7, pp. 1541–1566, 2017.
- [74] D. Q. Mayne, J. B. Rawlings, C. V. Rao, and P. O. Scokaert, “Constrained model predictive control: Stability and optimality,” *Automatica*, vol. 36, no. 6, pp. 789–814, 2000.
- [75] A. Bemporad, F. Borrelli, M. Morari, *et al.*, “Model predictive control based on linear programming—the explicit solution,” *IEEE Transactions on Automatic Control*, vol. 47, no. 12, pp. 1974–1985, 2002.
- [76] A. Bemporad, M. Morari, V. Dua, and E. N. Pistikopoulos, “The explicit linear quadratic regulator for constrained systems,” *Automatica*, vol. 38, no. 1, pp. 3–20, 2002.
- [77] T. Besselmann, J. Lofberg, and M. Morari, “Explicit MPC for LPV systems: Stability and optimality,” *IEEE Transactions on Automatic Control*, vol. 57, no. 9, pp. 2322–2332, 2012.
- [78] K. Zhang, J. Sprinkle, and R. G. Sanfelice, “Computationally aware control of autonomous vehicles: A hybrid model predictive control approach,” *Autonomous Robots*, vol. 39, no. 4, pp. 503–517, 2015.
- [79] A. Bemporad and M. Morari, “Robust model predictive control: A survey,” in *Robustness in identification and control*, 1999, pp. 207–226.
- [80] A. Mesbah, “Stochastic model predictive control: An overview and perspectives for future research,” *IEEE Control Systems*, vol. 36, no. 6, pp. 30–44, 2016.
- [81] M. Farina, L. Giulioni, and R. Scattolini, “Stochastic linear model predictive control with chance constraints—a review,” *Journal of Process Control*, vol. 44, pp. 53–67, 2016.

- [82] D. M. Raimondo, D. Limon, M. Lazar, L. Magni, and E. F. ndez Camacho, “Min-max model predictive control of nonlinear systems: A unifying overview on stability,” *European Journal of Control*, vol. 15, no. 1, pp. 5–21, 2009.
- [83] W. Langson, I. Chrysoschoos, S. Raković, and D. Q. Mayne, “Robust model predictive control using tubes,” *Automatica*, vol. 40, no. 1, pp. 125–133, 2004.
- [84] D. Q. Mayne, M. M. Seron, and S. Raković, “Robust model predictive control of constrained linear systems with bounded disturbances,” *Automatica*, vol. 41, no. 2, pp. 219–224, 2005.
- [85] D. Bernardini and A. Bemporad, “Scenario-based model predictive control of stochastic constrained linear systems,” in *IEEE Conference on Decision and Control*, Shanghai, China, 2009, pp. 6333–6338.
- [86] M. Cannon, B. Kouvaritakis, and X. Wu, “Probabilistic constrained MPC for multiplicative and additive stochastic uncertainty,” *IEEE Transactions on Automatic Control*, vol. 54, no. 7, pp. 1626–1632, 2009.
- [87] M. Cannon, B. Kouvaritakis, and D. Ng, “Probabilistic tubes in linear stochastic model predictive control,” *Systems & Control Letters*, vol. 58, no. 10-11, pp. 747–753, 2009.
- [88] M. Cannon, B. Kouvaritakis, S. V. Rakovic, and Q. Cheng, “Stochastic tubes in model predictive control with probabilistic constraints,” *IEEE Transactions on Automatic Control*, vol. 56, no. 1, pp. 194–200, 2011.
- [89] B. Kouvaritakis, M. Cannon, S. V. Raković, and Q. Cheng, “Explicit use of probabilistic distributions in linear predictive control,” *Automatica*, vol. 46, no. 10, pp. 1719–1724, 2010.
- [90] M. Lorenzen, M. A. Müller, and F. Allgöwer, “Stochastic model predictive control without terminal constraints,” *International Journal of Robust and Nonlinear Control*, vol. 29, no. 15, pp. 4987–5001, 2019.
- [91] L. Hewing and M. N. Zeilinger, “Stochastic model predictive control for linear systems using probabilistic reachable sets,” in *IEEE Conference on Decision and Control*, Miami Beach, FL, 2018, pp. 5182–5188.
- [92] A. Carvalho, Y. Gao, S. Lefevre, and F. Borrelli, “Stochastic predictive control of autonomous vehicles in uncertain environments,” in *International Symposium on Advanced Vehicle Control*, Tokyo, Japan, 2014.

- [93] F. Oldewurtel, C. N. Jones, and M. Morari, “A tractable approximation of chance constrained stochastic MPC based on affine disturbance feedback,” in *IEEE Conference on Decision and Control*, Cancún, Mexico, 2008, pp. 4731–4736.
- [94] J. A. Primbs and C. H. Sung, “Stochastic receding horizon control of constrained linear systems with state and control multiplicative noise,” *IEEE Transactions on Automatic Control*, vol. 54, no. 2, pp. 221–230, 2009.
- [95] M. Farina, L. Giulioni, L. Magni, and R. Scattolini, “A probabilistic approach to model predictive control,” in *IEEE 52nd Annual Conference on Decision and Control*, IEEE, Florence, Italy, 2013, pp. 7734–7739.
- [96] —, “An approach to output-feedback mpc of stochastic linear discrete-time systems,” *Automatica*, vol. 55, pp. 140–149, 2015.
- [97] P. J. Goulart, E. C. Kerrigan, and J. M. Maciejowski, “Optimization over state feedback policies for robust control with constraints,” *Automatica*, vol. 42, no. 4, pp. 523–533, 2006.
- [98] P. Hokayem, D. Chatterjee, and J. Lygeros, “On stochastic receding horizon control with bounded control inputs,” in *The Combined IEEE Conference on Decision and Control and Chinese Control Conference*, Shanghai, China, 2009, pp. 6359–6364.
- [99] P. Hokayem, D. Chatterjee, F. Ramponi, G. Chaloulos, and J. Lygeros, “Stable stochastic receding horizon control of linear systems with bounded control inputs,” in *International Symposium on Mathematical Theory of Networks and Systems*, Budapest, Hungary, 2010, pp. 31–36.
- [100] A. T. Schwarm and M. Nikolaou, “Chance-constrained model predictive control,” *AIChE Journal*, vol. 45, no. 8, pp. 1743–1752, 1999.
- [101] M. Ono, “Joint chance-constrained model predictive control with probabilistic resolvability,” in *American Control Conference*, Montréal, Canada, 2012, pp. 435–441.
- [102] Y. Ma, S. Vichik, and F. Borrelli, “Fast stochastic mpc with optimal risk allocation applied to building control systems,” in *IEEE Conference on Decision and Control*, Maui, HI, 2012, pp. 7559–7564.
- [103] J. A. Paulson, S. Streif, and A. Mesbah, “Stability for receding-horizon stochastic model predictive control,” in *American Control Conference*, Chicago, IL, 2015, pp. 937–943.
- [104] F. Borrelli, A. Bemporad, and M. Morari, *Predictive control for linear and hybrid systems*. Cambridge University Press, 2017.

- [105] A. Antoniou and W.-S. Lu, *Practical optimization: algorithms and engineering applications*. Springer Science & Business Media, 2007.
- [106] D. S. Bernstein, *Matrix Mathematics: Theory, Facts, and Formulas*, 2nd. 2009, vol. 41.
- [107] E. Bakolas, “Covariance control for discrete-time stochastic linear systems with incomplete state information,” in *American Control Conference*, Seattle, WA, 2017, pp. 432–437.
- [108] L. Blackmore and M. Ono, “Convex chance constrained predictive control without sampling,” in *AIAA Guidance, Navigation, and Control Conference*, Chicago, IL, 2009, p. 5876.
- [109] A. Prékopa, “Boole-Bonferroni inequalities and linear programming,” *Operations Research*, vol. 36, no. 1, pp. 145–162, 1988.
- [110] M. Ono, L. Blackmore, and B. C. Williams, “Chance constrained finite horizon optimal control with nonconvex constraints,” in *American Control Conference*, Baltimore, MD, 2010, pp. 1145–1152.
- [111] J. Lofberg, “YALMIP: A toolbox for modeling and optimization in MATLAB,” in *IEEE International Symposium on Computer Aided Control Systems Design*, Taipei, Taiwan, 2004, pp. 284–289.
- [112] MOSEK ApS, *The MOSEK Optimization Toolbox for MATLAB Manual. Version 8.1*. 2017.
- [113] R. Deits and R. Tedrake, “Computing large convex regions of obstacle-free space through semidefinite programming,” in *International Workshop on the Algorithmic Foundations of Robotics*, Istanbul, Turkey, 2014, pp. 109–124.
- [114] G. Voronoi, “Nouvelles applications des paramètres continus à la théorie des formes quadratiques. deuxième mémoire. recherches sur les paralléloèdres primitifs,” *Journal für die Reine und Angewandte Mathematik*, vol. 134, pp. 198–287, 1908.
- [115] D. Chatterjee, F. Ramponi, P. Hokayem, and J. Lygeros, “On mean square boundedness of stochastic linear systems with bounded controls,” *Systems & Control Letters*, vol. 61, no. 2, pp. 375–380, 2012.
- [116] M. Herceg, M. Kvasnica, C. Jones, and M. Morari, “Multi-Parametric Toolbox 3.0,” in *European Control Conference*, <http://control.ee.ethz.ch/~mpt>, Zürich, Switzerland, 2013, pp. 502–510.

- [117] M. Farina and R. Scattolini, “Model predictive control of linear systems with multiplicative unbounded uncertainty and chance constraints,” *Automatica*, vol. 70, pp. 258–265, 2016.
- [118] J. Ackermann, *Robust control: Systems with uncertain physical parameters*. Springer, 1993.
- [119] M. Ono and B. C. Williams, “Iterative risk allocation: A new approach to robust model predictive control with a joint chance constraint,” in *IEEE Conference on Decision and Control*, Cancun, Mexico, 2008, pp. 3427–3432.
- [120] M. P. Vitus and C. J. Tomlin, “On feedback design and risk allocation in chance constrained control,” in *IEEE Conference on Decision and Control and European Control Conference*, Orlando, FL, 2011, pp. 734–739.
- [121] —, “Belief space planning for linear, Gaussian systems in uncertain environments,” in *IFAC World Congress*, vol. 44, Milano, Italy, 2011, pp. 5902–5907.
- [122] A. Richards and J. P. How, “Robust variable horizon model predictive control for vehicle maneuvering,” *International Journal of Robust and Nonlinear Control*, vol. 16, no. 7, pp. 333–351, 2006.
- [123] S. G. Lee, Y. Diaz-Mercado, and M. Egerstedt, “Multirobot control using time-varying density functions,” *IEEE Transactions on Robotics*, vol. 31, no. 2, pp. 489–493, 2015.
- [124] Y. Diaz-Mercado, S. G. Lee, and M. Egerstedt, “Distributed dynamic density coverage for human-swarm interactions,” in *American Control Conference*, Chicago, IL, 2015, pp. 353–358.
- [125] D. Pickem, P. Glotfelter, L. Wang, M. Mote, A. Ames, E. Feron, and M. Egerstedt, “The robotarium: A remotely accessible swarm robotics research testbed,” in *IEEE International Conference on Robotics and Automation*, Singapore, 2017, pp. 1699–1706.
- [126] J. A. Primbs, “Portfolio optimization applications of stochastic receding horizon control,” in *American Control Conference*, New York City, NY, 2007, pp. 1811–1816.
- [127] V. Dombrovskii and T. Obyedko, “Model predictive control for constrained systems with serially correlated stochastic parameters and portfolio optimization,” *Automatica*, vol. 54, pp. 325–331, 2015.

- [128] M. Cannon, B. Kouvaritakis, and X. Wu, “Model predictive control for systems with stochastic multiplicative uncertainty and probabilistic constraints,” *Automatica*, vol. 45, no. 1, pp. 167–172, 2009.
- [129] S. Zafeiropoulos and P. Tsiotras, “Design of a lane-tracking driver steering assist system and its interaction with a two-point visual driver model,” in *American Control Conference*, Portland, OR, 2014, pp. 3911–3917.
- [130] L. Saleh, P. Chevrel, F. Claveau, J.-F. Lafay, and F. Mars, “Shared steering control between a driver and an automation: Stability in the presence of driver behavior uncertainty,” *IEEE Transactions on Intelligent Transportation Systems*, vol. 14, no. 2, pp. 974–983, 2013.
- [131] K. Okamoto and P. Tsiotras, “A comparative study of data-driven human driver lateral control models,” in *American Control Conference*, Milwaukee, WI, 2018, pp. 3988–3993.
- [132] A. Gray, Y. Gao, T. Lin, J. K. Hedrick, and F. Borrelli, “Stochastic predictive control for semi-autonomous vehicles with an uncertain driver model,” in *International IEEE Annual Conference on Intelligent Transportation Systems*, The Hague, The Netherlands, 2013, pp. 2329–2334.
- [133] E. Velenis, E. Frazzoli, and P. Tsiotras, “Steady-state cornering equilibria and stabilisation for a vehicle during extreme operating conditions,” *International Journal of Vehicle Autonomous Systems*, vol. 8, no. 2-4, pp. 217–241, 2010.
- [134] A. W. Marshall and I. Olkin, “Multivariate Chebyshev inequalities,” *The Annals of Mathematical Statistics*, pp. 1001–1014, 1960.

VITA

Kazuhide Okamoto was born in Toyama, Japan, and he earned his bachelor's and master's degrees both in Aeronautics and Astronautics from the University of Tokyo, Japan. He is currently a Ph.D. candidate in Aerospace Engineering at the Georgia Institute of Technology in Atlanta, Georgia, where he is researching stochastic optimal control theory for autonomous systems. He is a recipient of the Funai Overseas Scholarship and the Ito Foundation U.S.A.- FUTI Scholarship. During his time at Georgia Tech, he also held research intern positions at Mitsubishi Electric Research Laboratories, Cambridge, Massachusetts, and at Honda Research Institute USA, Mountain View, California.